Orcina Project 1405

Wind Turbine Validation Report

Orcina Ltd.

Daltongate
Ulverston
Cumbria
LA12 7AJ
United Kingdom

E: orcina@orcina.com
T: +44 (0)1229 584 742

Client:	N/A			
Revision History:	**Report No.**	**Issue**	**Report Date**	**Report Status**
	01	01	30/04/2018	Issued
For Orcina:	**Author:**	A. Ross		
	Checked:	G. McKinnon		
Report file:	R1405#01#01 Wind Turbine Validation.docx			

CONTENTS

Appendix A – NREL 5-MW Wind Turbine – Blade Data

Summary

The rapid expansion of the global offshore wind energy sector has seen the requirement to move away from conventional shallow-water / fixed-bottom wind turbine systems, to more complex offshore wind turbine concepts. One of the fastest growing areas of development is floating offshore wind, where offshore wind turbines are mounted upon a floating foundation. Such systems allow for cost-effective development of offshore wind farms in deeper and farther-reaching waters.

With this continued growth, comprehensive dynamic analysis is critical to the design, engineering and construction of floating offshore wind turbine systems. Turbine modelling capabilities were introduced in OrcaFlex v10.3, which is the world's leading package for the dynamic analysis of offshore marine systems. The turbine model object adds to the expansive list of technical capabilities of the software.

The purpose of this document is to summarise validation of the OrcaFlex turbine model object against documented studies, currently available within industry. The validation study considers the National Renewable Energy Laboratory (NREL) offshore 5-MW baseline wind turbine; which is recognised as an industry-standard reference turbine system.

Two separate turbine systems have been modelled and subjected to detailed analysis in OrcaFlex:

(1) A land-based wind turbine system.
(2) A floating wind turbine system – based on the OC3 Hywind system.

Analysis of the land-based scenario was considered to facilitate basic validation of the turbine response determined via OrcaFlex. Detailed analysis of the OC3 Hywind system was then considered to help validate the behaviour of a fully-coupled floating wind turbine system in OrcaFlex.

From the developed OrcaFlex models, a range of critical results were extracted for comparison against documented results from other wind turbine simulation tools; namely FAST, MSC.ADAMS, Bladed and HAWC2. Validation was then achieved by comparing the OrcaFlex results to those from the considered simulation tools.

The OrcaFlex turbine object is composite in nature and includes functionality to model the generator, gearbox, hub, blades and associated control systems. The turbine blade construction is represented by beam elements that are very similar in nature to the long-established model used for OrcaFlex line objects. As such, the blade structural model is equipped with the capability to capture all degrees-of-freedom of the turbine blades.

Control system modelling, for generator torque control and blade pitch control, are supported through a Python external function. The controller considered for this study is adapted from a similar baseline control system documented by NREL as part of the OC3 Hywind study. This provided the functionality to model variable rotor speed and/or variable blade-pitch.

Modelling of the supporting infrastructure, such as the tower structure, nacelle and spar platform (for the OC3 Hywind model), was achieved through various modelling features already available as part of the OrcaFlex software package.

Overall, the turbine rotor and generator responses, calculated via OrcaFlex, were generally found to agree very closely with the analogous results from the other analysis codes. This applies to both the land-based and OC3 Hywind systems. In order to demonstrate this agreement, a series of charts are included for reference in Section 5 of this report.

When assessing the response of the turbine blades, some key differences were observed between the OrcaFlex and FAST models of the land-based system. This was pin-pointed to differences in the considered blade structural models. The blade structural model adopted as part of FAST accounts for bending stiffness of the turbine blades only; thus, ignoring the axial and torsional degrees-of-freedom for the turbine blades. Conversely, the OrcaFlex model of the system accounts for the axial and torsional degrees-of-freedom, by default.

As a result, for any dynamic load cases that considered the influence of blade pitch, key differences were then observed in the blade structural response predicted between OrcaFlex and FAST. The OrcaFlex turbine model was then simplified to account for this key difference and a close agreement was established between the two analysis codes. Although this simplification did not impact the response of the turbine rotor and generator, it did impact the deflection experienced by the turbine blades, as well as the deflection experienced by the tower. After making this adjustment to the blade structural properties in the OrcaFlex model, the results were generally found to agree with the FAST results. Again, in order to visualise this behaviour, a series of charts are available for reference in Section 5.

For the OC3 Hywind system, the OrcaFlex results were shown to correspond most consistently with the FAST and ADAMS results, submitted by NREL as part of the OC3 study [4]. The spar platform motions (surge, pitch, heave and yaw) generally agreed very well amongst the codes. The exception to this was Bladed, which predicted noticeably different platform motion characteristics. At the time of the OC3 study, it is known that the floating modelling capabilities of the Bladed software were in a stage of early development; which may have contributed to the differences seen in the results.

The mooring tension results determined via OrcaFlex were shown to correspond well with the other analysis codes. It should be noted that no fairlead tension results were available from Bladed, which were not submitted as part of the OC3 study. OrcaFlex modelling of the mooring lines was simplified considerably in order to calibrate the OrcaFlex model with the limited capabilities of the other OC3 analysis codes. Despite these simplifications it is important to note that long-existing OrcaFlex capabilities can facilitate accurate modelling of complex mooring arrangements; such as multi-section mooring lines with varying physical properties, rigging components, crowfoot arrangements and clump weight attachments.

Naturally, some minor and unavoidable discrepancies exist between the results extracted from each analysis code. Without direct access to the analysis models, it is difficult to pin-point specific root causes of the observed disparities. However, it is possible that a number of inherent factors may have contributed; such as the considered aerodynamic induction model, tower interference modelling, hub & tip loss, blade/tower structural models, model discretisation, interpretation of data, general numerical stability in the dynamic simulations and potential deficiencies in earlier versions of the considered analysis codes.

Overall, the wide-range of features available from OrcaFlex have been shown to accurately capture the aerodynamic and hydrodynamic loading on the considered turbine systems. Close agreement was generally observed between the OrcaFlex results, and those available from a range of other simulation tools – particularly with respect to the calculated turbine rotor response.

Further details on the conclusions drawn from this study are contained in Section 2 and the assumed input data & adopted modelling processes are detailed in Section 3 and 4, respectively.

1. Introduction

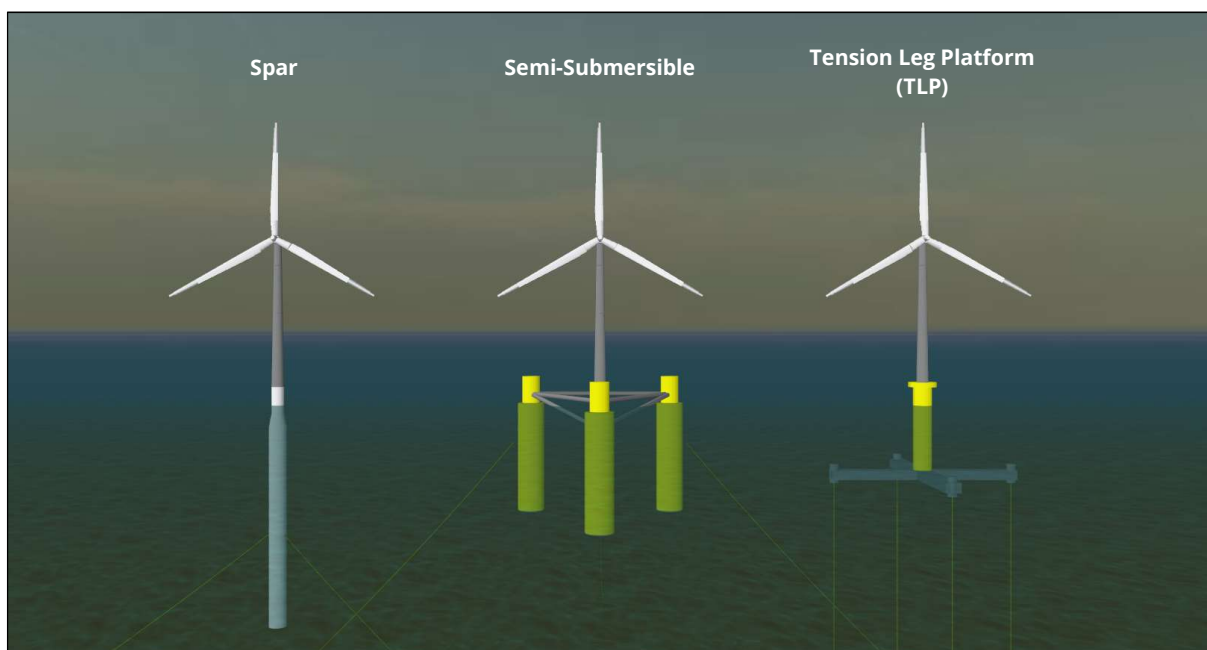## 1.1. OrcaFlex Wind Turbine Object

Turbines are a type of model object introduced in OrcaFlex version 10.3. The turbine object facilitates modelling of horizontal axis wind turbines (HAWTs) which, in turn, promotes modelling of the global dynamic response of floating offshore wind turbine systems.

The turbine object, in conjunction with existing OrcaFlex modelling capabilities, allows the global response of floating wind turbine systems to be captured. Such systems feature strong coupling between aerodynamic loading, the structural response of the turbine blades and the floating platform response. In the context of floating wind turbines, the OrcaFlex turbine object is intended to serve as a critical modelling component for input to the design and analysis of mooring systems.

The turbine object is composite in nature and includes functionality to model the generator, gearbox, hub, blades and associated control systems. The turbine blades can be modelled as rigid bodies or can be flexible, represented by beam elements that are very similar in nature to OrcaFlex line objects. Aerodynamic loading is captured through an implementation of the blade element momentum (BEM) method adapted from AeroDyn v15.04 [1].

Control system modelling, for generator control and blade pitch control, are supported through user specified external functions. This provides the functionality to model variable speed and/or variable blade-pitch turbine systems. Figure 1 illustrates some typical floating wind turbine concepts modelled in OrcaFlex.

In addition, OrcaFlex v10.3 possesses the capability to model full field wind. This allows for variation of wind velocity, in both space and time, by importing full field wind time histories specified via an external file.

Figure 1 – Floating Wind Turbine Systems Modelled in OrcaFlex

1.2. Document Scope

The purpose of this document is to summarise validation of the OrcaFlex turbine object against documented studies, currently available within industry. The validation study considers the National Renewable Energy Laboratory (NREL) offshore 5-MW baseline wind turbine, developed by Jonkman, et al (2009) [2].

This mock turbine system takes the form of a conventional three-bladed system with variable-speed and variable blade-pitch control capabilities. It is recognised as an industry-standard reference model that is representative of a typical utility-scale, multi-megawatt offshore wind turbine. The same turbine specification has been considered for a number of conceptual studies and research projects; including the OC3, OC4 and OC5 projects.

This document focusses on the modelling and analysis of two separate systems, which are replicated and analysed using OrcaFlex v10.3:

(1) A land-based wind turbine scenario that considers the NREL 5-MW wind turbine, using the appropriate input design data – as documented in [2] – hereafter referred to as the 'land-based' system.
(2) A floating wind turbine scenario that considers the same NREL 5-MW wind turbine atop the OC3 Phase IV Hywind (spar buoy) concept – as documented in [3] and [4] – hereafter referred to as the 'OC3 Hywind' system.

For the land-based system, a range of critical results are extracted for comparison against analogous results documented by NREL in [2]. The results reported by NREL utilise their proprietary FAST (v6) aeroelastic simulator code along with a number of external modules designed to assist modelling and processing of coupled nonlinear aero-servo-elastic simulations in the time domain [2,5]. Analysis of this scenario is considered to facilitate basic validation of the turbine response determined via OrcaFlex.

For the OC3 Hywind system, a range of critical results are extracted for comparison against results documented as part of the offshore code comparison collaboration (OC3) study. The OC3 project was performed by means of technical exchange amongst industry, academic and research organisations located world-wide; with the primary aim of enhancing the accuracy and reliability of the predictive capability of the various analysis codes. The OC3 study is documented by NREL in [4] and considers a series of benchmark models and simulations that allow for comparison between the considered wind turbine analysis codes.

The OC3 Hywind model discussed in this report, is based entirely on the benchmark model considered for Phase IV of the OC3 study. Analysis of this scenario is considered to facilitate validation of the turbine response, as determined via OrcaFlex for a fully-coupled floating system.

The input data and assumptions, considered as part of this validation study, are detailed within this document; along with pertinent results and conclusions.

1.3. Abbreviations

Abbreviation	Description
6D	Six-dimensional
ActuatorGamma	Damping Ratio (Blade Pitch Actuator)
ActuatorOmega	Natural Angular Frequency (Blade Pitch Actuator)
ADAMS	Automatic Dynamic Analysis of Mechanical Systems
AeroCent	Fraction of chord from the leading edge to the trailing edge, where it is assumed that pitch axis passes through the aerofoil section at 25% chord
AeroRef	Fraction of chord from leading edge to aerodynamic reference point
Arclength	Distance along blade-pitch axis from root (0.0m) to tip (61.5m)
BEM	Blade Element Momentum
BlFract	Fractional distance along blade-pitch axis from root (0.0) to tip (1.0)
BlPitch	Blade Pitch Angle
BMassDen	Blade section mass per unit length
DNV GL	Det Norske Veritas Germanischer Lloyd
DOF	Degree of Freedom
DOWEC	Dutch Offshore Wind Energy Converter (project name)
DTU	Technical University of Denmark
DU	Delft University
EAStff	Blade section axial stiffness
EdgcgOf	Edgewise CM offset value – distance along chordline from blade-pitch axis to CM of blade section (positive value is towards trailing edge)
EdgStff	Blade section edgewise stiffness
Fair1Ten	Fairlead 1 Tension
Fair2Ten	Fairlead 2 Tension
FAST	Fatigue, Aerodynamics, Structures and Turbulence
FlpStff	Blade section flapwise stiffness
GenPower	Generator Power
GenSpeed	Generator Speed
GenTorq	Generator Torque
GH	Garrad Hassan & Partners Limited
GJStff	Blade section torsional stiffness
GL	Ground Level
HAWC2	Horizontal Axis Wind turbine simulation Code 2nd Generation
HAWT	Horizontal Axis Wind Turbine
IEA	International Energy Agency
IP	In-Plane
IPDefl1	Blade 1 Tip In-plane Deflection
JONSWAP	Joint North Sea Wave Project
MSC	MSC Software Corporation
N/A	Not Applicable
NACA	National Advisory Committee for Aeronautics
NREL	National Renewable Energy Laboratory
OC3	Offshore Code Comparison Collaboration
OC4	Offshore Code Comparison Collaboration Continuation

Abbreviation	Description
OC5	Offshore Code Comparison Collaboration Continuation, with Correlation
OD	Outer Diameter
OOP	Out-of-Plane
OoPDefl1	Blade 1 Tip Out-of-plane Deflection
PHATAS	Program for Horizontal Axis wind Turbine Analysis and Simulation
PI	Proportional–Integral (Controller)
PitchAxis	Fraction of chord from leading edge to pitch axis
PtfmSurge	Platform Surge
PtfmPitch	Platform Pitch
PtfmHeave	Platform Heave
PtfmYaw	Platform Yaw
Radius	Distance along blade-pitch axis relative to rotor centre
RotPower	Rotor Power
RotSpeed	Rotor Speed
RotThrust	Rotor thrust
RotTorq	Rotor Torque
Rpm	Revolutions per Minute
StrcTwst	Blade structural twist angle
SWL	Still Water Level
TLP	Tension Leg Platform
TSR	Tip Speed Ratio
TTDspFA	Tower Top – Fore-aft Deflection
TTDspSS	Tower Top – Side-to-side Deflection
WT	Wall Thickness
YawBrFxp	Tower Top – Fore-aft Shear Force

Table 1 – List of Abbreviations

1.4. Symbols

Symbol	Description
A	Drag Area
C_a	Added Mass Coefficient
$C_{a\text{-}axial}$	Axial Added Mass Coefficient (spar buoy)
$C_{a\text{-}normal}$	Normal Added Mass Coefficient (spar buoy)
C_D	Drag Coefficient (aerofoil)
$C_{D\text{-}axial}$	Axial Drag Coefficient (spar buoy)
$C_{D\text{-}normal}$	Normal Drag Coefficient (spar buoy)
C_L	Lift Coefficient (aerofoil)
C_M	Mass Coefficient (aerofoil)
CM	Centre of Mass
$C_{m\text{-}axial}$	Axial Inertia Coefficient (spar buoy)
$C_{m\text{-}normal}$	Normal Inertia Coefficient (spar buoy)
f	Fluid Force
H	Wave Height (Airy Waves)
H_S	Significant Wave Height
T	Wave Period (Airy Waves)
T_P	Peak Wave Period
Rz	Constraint Rotational DOF (about z-axis)
v_r	Fluid Velocity Relative to Body
α	Angle of Attack
a_f	Fluid Acceleration Relative to Earth
a_r	Fluid Acceleration Relative to Body
Δ	Mass of Displaced Fluid
ρ	Fluid Density
$\sigma 1$	Longitudinal wind speed standard deviation
ω	Individual wave frequency

Table 2 – List of Symbols

1.5. Units

Unit	Description
%	Percent
deg (°)	Degrees
GPa	Gigapascal
Hz	Hertz
kg	Kilogram
kN	Kilonewton
kW	Kilowatt
m	Meter
MW	Megawatt
rad	Radian
s	Second
te	Metric Tonne

Table 3 – List of Units

1.6. References

No.	Document Number	Title
1.	–	AeroDyn v15 User's Guide and Theory Manual NREL (2017)
2.	NREL/TP-500-38060	Definition of a 5-MW Reference Wind Turbine for Offshore System Development (2009)
3.	NREL/TP-500-47535	Definition of the Floating System for Phase IV of OC3 (2010)
4.	NREL/TP-5000-48191	Offshore Code Comparison Collaboration (OC3) for IEA Task 23 Offshore Wind Technology and Development (2010)
5.	NREL/EL-500-38230	FAST User's Guide (2005)
6.	DOWEC-F1W2-HJK-01-046/9	Aero-elastic modelling of the DOWEC 6 MW pre-design in PHATAS (2003)
7.	–	BeamDyn User's Guide and Theory Manual (2016)

Table 4 – List of References

2. Summary and Conclusions

2.1. Land-Based System

2.1.1. Summary

For the land-based system, a range of critical results have been extracted from OrcaFlex for comparison against analogous FAST results, as documented by NREL in [2]. Analysis of this scenario was considered to facilitate basic verification of the turbine response.

In order to consider the steady state response of the land-based system, the operational wind speed range of the turbine (3–25m/s) was considered in increments of 1m/s. A separate dynamic load case was then created for each uniform wind speed increment; amounting to a total of 23 separate load cases.

To ensure consistency between the OrcaFlex and FAST models of the system, wind loading on the tower is excluded from the land-based model. Despite this simplification, it is important to note that OrcaFlex possesses the capability to model aerodynamic loading on the tower. Note, that the effects of tower influence (on the turbine inflow) and blade-to-tower interaction are not considered as part of the OrcaFlex model of the OC3 Hywind system.

The input data considered for the land-based turbine system is summarised in Section 3 and a full summary of results is contained in Section 5.1.

Figure 2 – OrcaFlex Model of the NREL 5-MW Land-Based System

2.1.2. Conclusions

The following conclusions have been drawn from the OrcaFlex analysis of the land-based system:

- Overall, the turbine rotor response (speed, torque, power, thrust) and the blade tip speed ratio (TSR), calculated via OrcaFlex, were found to correspond very well with the analogous FAST results. The same is true for the observed generator speed and torque response from the system.
- When assessing the output generator power, the results indicated a marked difference between the OrcaFlex and FAST results above the rated turbine wind speed (11.4m/s). This difference was attributed to a mechanical-to-electrical conversion loss, considered as part of the FAST model [2]; which represents a generator efficiency of 94.4%. By default, this efficiency is not accounted for as part of the OrcaFlex model of the system. When applying this efficiency to the OrcaFlex calculations, the results were found to correspond very well with the FAST results (<2% error).
- Above the rated wind speed, where the blade pitch controller is active, a noticeable difference was observed between the analysis codes when assessing the blade pitch response. Further investigation determined that the blade structural model adopted as part of FAST model accounts for the bending stiffness of the turbine blades and not the axial and torsional degrees-of-freedom [5].
- The blade structural model utilised by OrcaFlex is similar in outline to the long-established model used by line objects. As such, the model accounts for the axial and torsional degrees-of-freedom, by default. The OrcaFlex turbine model was adjusted to artificially eliminate the blade torsional and axial degrees-of-freedom. This was achieved by assigning an arbitrarily large stiffness to the torsional and axial stiffness properties of the blades; thus, aligning it with the corresponding FAST model. The blade pitch results extracted from the adjusted OrcaFlex model then demonstrated close agreement with the blade pitch response determined via FAST.
- This same discrepancy in the structural model of the turbine blades was also found to impact the blade tip deflection and tower top deflection results. When considering the adjustment to the blade structural properties in the OrcaFlex model, the results were generally found to correspond very well with the FAST results.
- Over the considered suite of results, the most noticeable difference in results was observed for the blade tip in-plane deflection. It is thought that general numerical instability, evident in the FAST calculations, may be contributing to these differences. Despite this, the observed trend in results is shown to correspond reasonably well between the codes.

2.2. OC3 Hywind System

2.2.1. Summary

For the OC3 Hywind system, a range of critical results were extracted from OrcaFlex for comparison against analogous results, documented by NREL, for the OC3 study in [4]. Of the ten analysis codes considered as part of the OC3 study, the results from four codes (FAST, MSC. ADAMS, GH Bladed and Risø-DTU HAWC2) were specifically selected for comparison against the OrcaFlex response of the system.

Figure 3 – OrcaFlex Model of the OC3 Hywind System

The decision to consider this reduced set of codes was primarily based on the availability of the raw results corresponding to each code. Furthermore, the considered codes use Morison's equation as the basis for the hydrodynamics calculations; which is the same approach adopted within the OrcaFlex model of the system (see Section 4.4.2).

The analysis considered load case 5.1 (as defined by NREL in [4]); which was deemed suitable to assess the steady-state dynamic behaviour of the OC3 Hywind system, as modelled in OrcaFlex. For the considered load case, Airy waves, assigned a height of H=6m and period T=10s, were applied in the simulation environment along with a uni-directional steady-state wind speed of 8m/s. No current was considered as part of this load case definition.

As with the land-based model, wind loading on the tower is excluded from the OC3 Hywind model. This approach was taken to ensure consistency between OrcaFlex and the OC3 analysis codes. Note, that the effects of tower shadow, tower influence (on the turbine inflow) and blade-to-tower interaction are not considered as part of the OrcaFlex model of the OC3 Hywind system.

The input data considered for the OC3 Hywind system is summarised in Section 3 and a full summary of results is contained in Section 5.2.

2.2.2. Conclusions

The following conclusions have been drawn from the OrcaFlex analysis of the OC3 Hywind system:

- Overall, the turbine rotor response (speed and power), calculated via OrcaFlex, was found to correspond very well with the analogous results from the other codes. The same is true for the observed generator power response from the system, which accounts for a generator efficiency of 94.4%.

- The blade tip out-of-plane deflection results indicated very close agreement between the codes. It was found that the FAST and GH Bladed models of the system considered only blade bending; whereas the ADAMS and HAWC2 models considered axial, torsion and shear DOFs as part of the blade structural model. The latter is akin to the blade model adopted by OrcaFlex.

- The differences between the blade structural models were observed to have little impact on the blade response. This may be attributed to the turbine operational regime for the considered wind speed of 8m/s (Region 1 of the associated power curve – see Section 3.4, Figure 14). In this region, the rotor torque controller is active meaning that the turbine blades are not required to pitch. From the blade response determined for the land-based turbine, the influence of blade pitch has been shown to expose differences in the adopted blade structural modelling approach.

- For the tower top response (fore-aft shear force and deflection), close agreement was observed between the codes. The exception to this was GH Bladed, which predicted slightly lower mean values. The tower top deflection and shear force, predicted by OrcaFlex, was shown to correspond particularly well with the FAST and ADAMS codes.

- The calculated fairlead tension results, for mooring lines 1 and 2, once again showed close agreement between the analysis codes. The results determined via OrcaFlex were shown to correspond particularly well with the NREL codes. It should be noted that no fairlead tension results were available from GH Bladed, which were not submitted as part of the OC3 study [4].

- The modelling of the OC3 Hywind mooring lines were simplified considerably in order to calibrate the OrcaFlex model with the limited capabilities of the OC3 analysis codes. It is important to note that OrcaFlex possesses the capability to model multi-section mooring lines (with varying physical properties), rigging components and other complex configurations e.g. crowfoot arrangements and clump weight attachments.

- Generally, the spar platform motion responses (surge, pitch, heave and yaw) predicted by GH Bladed were noticeably different when compared to the other codes. This is thought to have directly impacted the lower observed tower top fore-aft shear force and deflection results, discussed above. At the time of the OC3 study, it is known that the floating modelling capabilities of GH Bladed were in a stage of early development; which may have contributed to the differences in the results.

- The mean spar platform surge response, determined via OrcaFlex, showed very close agreement with the NREL codes. The surge predicted by HAWC2 was markedly lower than the surge predicted by OrcaFlex. It is possible that the difference was caused by the position at which the spar platform motions were extracted from the HAWC2 model; which was thought to be at the platform base. Additional checks, performed in OrcaFlex, considered extraction of the spar surge response from the platform base and a significant improvement was then seen in the correlation between the OrcaFlex and HAWC2 results.

- With the exception of GH Bladed, the mean spar platform pitch and heave response, determined via OrcaFlex, showed close agreement with the other codes. Particularly close agreement was observed between OrcaFlex and the NREL codes.

- Within the OrcaFlex simulation of the system, the considered main shaft tilt of 5° was observed to cause some of the rotor torque to act about the yaw axis of the floating system. This resulted in a non-zero mean yaw response from the system. Similar behaviour was observed in the analysis codes considered as part of the OC3 Phase IV study [4].
- The mean yaw response of the platform was relatively consistent between the analysis codes. The oscillations observed in the yaw responses from each code are believed to be caused by a combination of platform pitch motion, in conjunction with rotor inertia. As a result, the observed yaw responses are shown to differ slightly between the codes. Inherent differences in the approach taken to augment the mooring yaw spring stiffness may be also be contributing to the minor inconsistencies observed between the results.

2.3. Further Considerations

The turbine object adds to the already expansive and long-established technical capabilities of OrcaFlex; thus, allowing for the global response of fixed and floating wind turbine systems to be captured efficiently and accurately. The wide-range of features available from OrcaFlex allow for the aerodynamic & hydrodynamic loading on the turbine system to be captured, along with the dynamic response of the turbine system, and supporting infrastructure.

The OC3 Hywind system was selected based on the availability of extensive results from a number of different analysis codes. This was taken as an opportunity to compare the results from OrcaFlex with a variety of codes, active within the industry, at the time of the OC3 study.

The validation study summarised in this document has fundamentally demonstrated close agreement between the OrcaFlex results, and those available from the selected analysis codes – particularly with respect to the calculated turbine response of the considered land-based and floating systems. For the OC3 Hywind system, the results calculated via OrcaFlex were found to correspond most consistently with the FAST and ADAMS results submitted by NREL as part of the OC3 study [4].

As has been highlighted in the previous sub-sections, minor differences exist between the results extracted from each analysis code. Although it is difficult to pin-point the exact source(s) of these disparities, without direct access to the analysis models, a number of contributing factors may exist. Such factors could include the considered aerodynamic induction model, tower interference modelling, hub & tip loss, blade/tower structural models, model discretisation, interpretation of data, general numerical stability in the dynamic simulations and potential deficiencies in earlier versions of the considered analysis codes [4].

It is important to highlight that the results from the OC3 study were gathered in 2009 and it is highly likely that further developments have been made to the various analysis codes since then. For example, the capabilities of FAST (now known as 'OpenFAST') are known to have advanced since the findings from the OC3 study were published. Furthermore, it is safe to assume that the capabilities of GH Bladed (presently known as 'Bladed' and belonging to DNV GL), as well as HAWC2, have also advanced.

In order to assimilate the OrcaFlex models, with those considered by the other analysis codes, it was necessary to suppress certain OrcaFlex modelling capabilities e.g. the considered blade DOFs, mooring system representation and aerodynamic loading on the tower were altered to account for the limited capabilities of the other codes. Despite these simplifications, the underlying aero- and hydrodynamic physical theories, implemented as part of each analysis code, are fundamentally equivalent. Therefore, it is expected that developments made to the various analysis codes, since 2009, should not significantly impact the findings summarised in this report.

3. Design Basis

3.1. 5MW Baseline Wind Turbine Properties

The National Renewable Energy Laboratory (NREL) offshore 5-MW baseline wind turbine takes the form of a conventional upwind three-bladed system with variable-speed and variable blade-pitch control capabilities. The appropriate input design data for the land-based wind turbine is sourced from NREL document *NREL/TP-500-38060 – Definition of a 5-MW Reference Wind Turbine for Offshore System Development* [2].

A basic summary of the considered system is illustrated and tabulated below in Figure 4 and Table 5, respectively.

Property	Value(s)
Rating	5-MW
Blade Quantity	3
Control System(s)	Variable Speed, Variable Blade Pitch
Drivetrain	High Speed, Multiple-Stage Gearbox
Rotor Diameter	126 m
Hub Diameter	3 m
Cut-in, Rated, Cut-out Wind Speed	3 m/s, 11.4 m/s, 25 m/s
Main Shaft Tilt	5 °
Rotor Mass	110.00 te
Nacelle Mass	240.00 te
Tower Mass	347.46 te

Table 5 – Wind Turbine Data Overview [2]
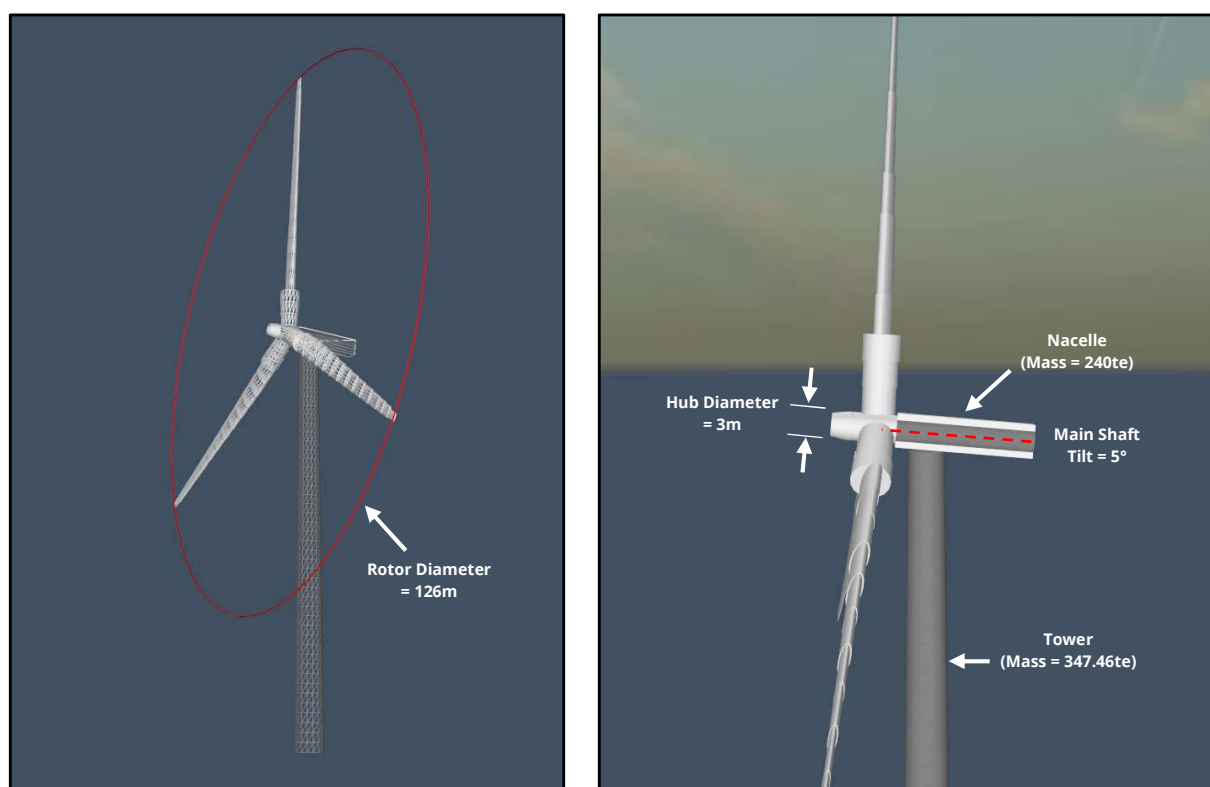
Figure 4 – Wind Turbine System

3.2. Turbine Blades

3.2.1. Blade Structural Properties

A summary of the blade structural properties is given below. Figure 5 illustrates the presented data in further detail.

Property	Value
Blade Material	Glass fibre
Blade Length (Root to Tip)	61.5m
Overall Blade Mass	17.740 te
Radial CM (relative to Blade Root)	20.475 m
Blade Pre-cone Angle	2.5 °

Table 6 – Blade Structural Properties [2]
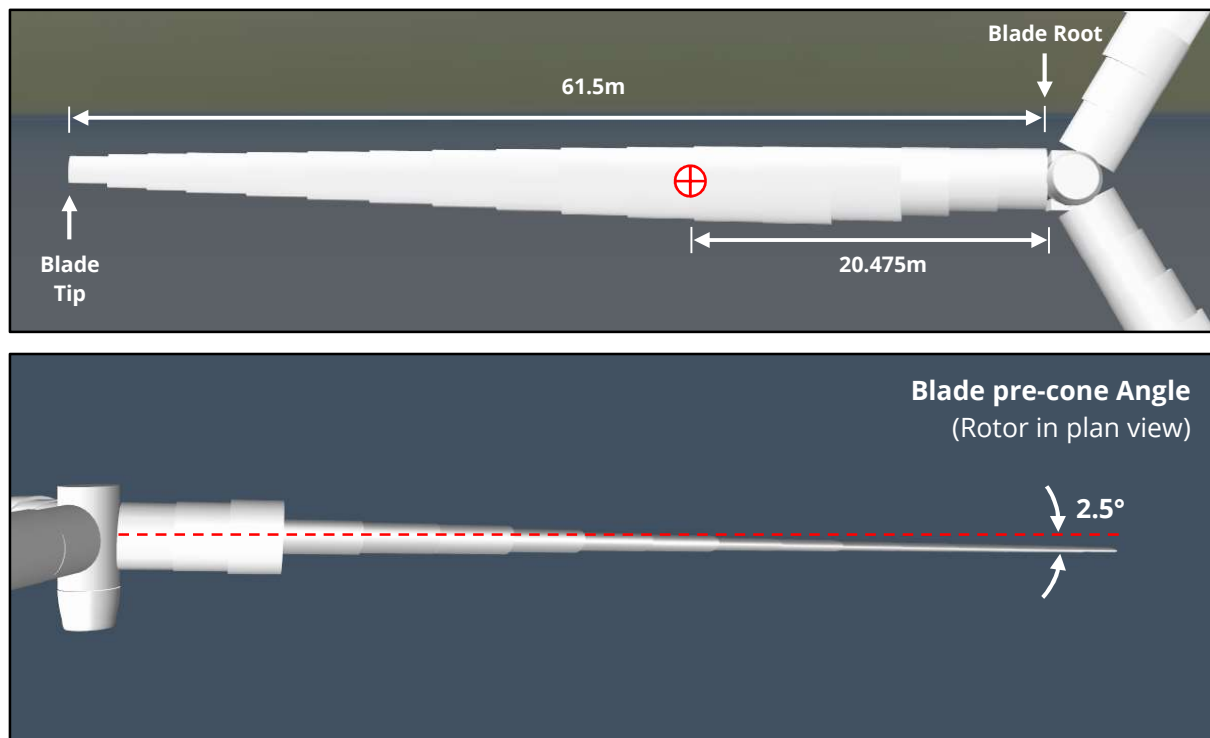
Figure 5 – Turbine Blade

3.2.2. Blade Aerodynamic Properties

The distributed aerodynamic properties of the turbine blades are listed in Table 7. In addition, Figure 6 illustrates the terminology relevant to the presented data.

The blade root consists of 2 different cylinder types; designated 'Cylinder1' and 'Cylinder 2' with drag coefficients (C_D) of 0.50 and 0.35, respectively. The remainder of each blade comprises 6 unique aerofoils, as summarised in the table below. Each aerofoil has specific coefficients of lift (C_L), drag (C_D), and moment (C_M) assigned to it. These coefficients define the aerodynamic loads applied to the wing for each given incidence angle. For further details related to the lift, drag and moment coefficients, assigned to each aerofoil, please refer to Appendix A.

Node	Node Arc length [m]	Structural Twist Angle [°]	Chord Length [m]	Thickness [%]	Aerofoil Type
1	1.367	13.308	3.542	100.00	Cylinder1
2	4.100	13.308	3.854	100.00	Cylinder1
3	6.833	13.308	4.167	100.00	Cylinder2
4	10.250	13.308	4.557	40.50	DU40_A17
5	14.350	11.488	4.652	35.09	DU35_A17
6	18.450	10.162	4.458	35.09	DU35_A17
7	22.550	9.009	4.249	30.00	DU30_A17
8	26.650	7.795	4.007	25.00	DU25_A17
9	30.750	6.549	3.748	25.00	DU25_A17
10	34.850	5.359	3.502	21.00	DU21_A17
11	38.950	4.188	3.256	21.00	DU21_A17
12	43.050	3.144	3.010	18.00	NACA64_A17
13	47.150	2.319	2.764	18.00	NACA64_A17
14	51.250	1.526	2.518	18.00	NACA64_A17
15	54.667	0.863	2.313	18.00	NACA64_A17
16	57.400	0.370	2.086	18.00	NACA64_A17
17	60.133	0.106	1.419	18.00	NACA64_A17

Note:
Node arc lengths are measured relative to the blade root.

Table 7 – Blade Aerodynamic Properties [2,6]
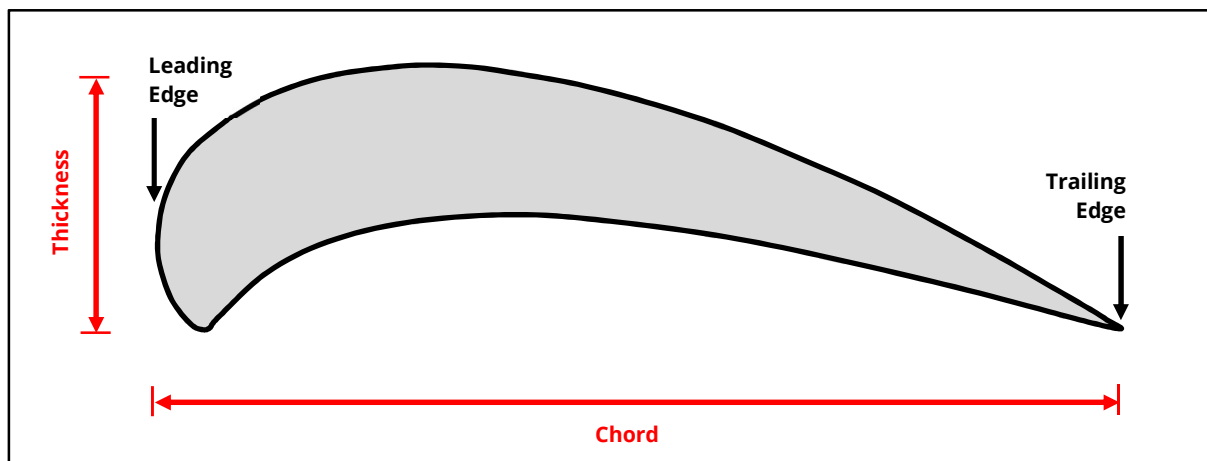
Figure 6 – Aerofoil Terminology

The node arc lengths are directed along the blade-pitch axis from the blade root.

Note that the 'DU' in each aerofoil name refers to Delft University and 'NACA' refers to the National Advisory Committee for Aeronautics. The number immediately following the 'DU' in each aerofoil designation corresponds to the thickness of the aerofoil, as a percentage of chord length.

### 3.2.3.   Rotor and Nacelle Properties

The rotor hub serves as an interface between the turbine blades and the main shaft; which feeds into the nacelle. The nacelle is mounted on top of the tower and houses numerous components necessary for power generation. Such components include the generator, gearbox and drivetrain assemblies (see Figure 7 and Figure 9).

Physical properties, relevant to modelling of the hub and nacelle, are summarised in Table 8. Note that for calculation of the nacelle inertia properties, the structure is assumed to be prismatic and box-shaped. This is considered to be a reasonable assumption when considering the structural nature of nacelle structures, in general.

Further data summarising the geometry of the considered set up is shown in Table 9 and Figure 8.

Property	Value
Hub Mass	56.78 te
Hub Inertia (about Main Shaft)	115.926 te.m^2
Nacelle Mass	240.00 te
Nacelle Dimensions (l x b x h)	14.285 x 2.286 x 3.500 m
Nacelle Drag Areas (x ,y ,z)	8.0, 50.0, 32.7 m^2
Nacelle Inertia (about x, y, z axis)	350.02, 5409.97, 2607.89 te.m^2
Drag Coefficient (C_D) (along x, y, z)	1.0, 1.2, 1.2

Table 8 – Hub and Nacelle Physical Properties [2]
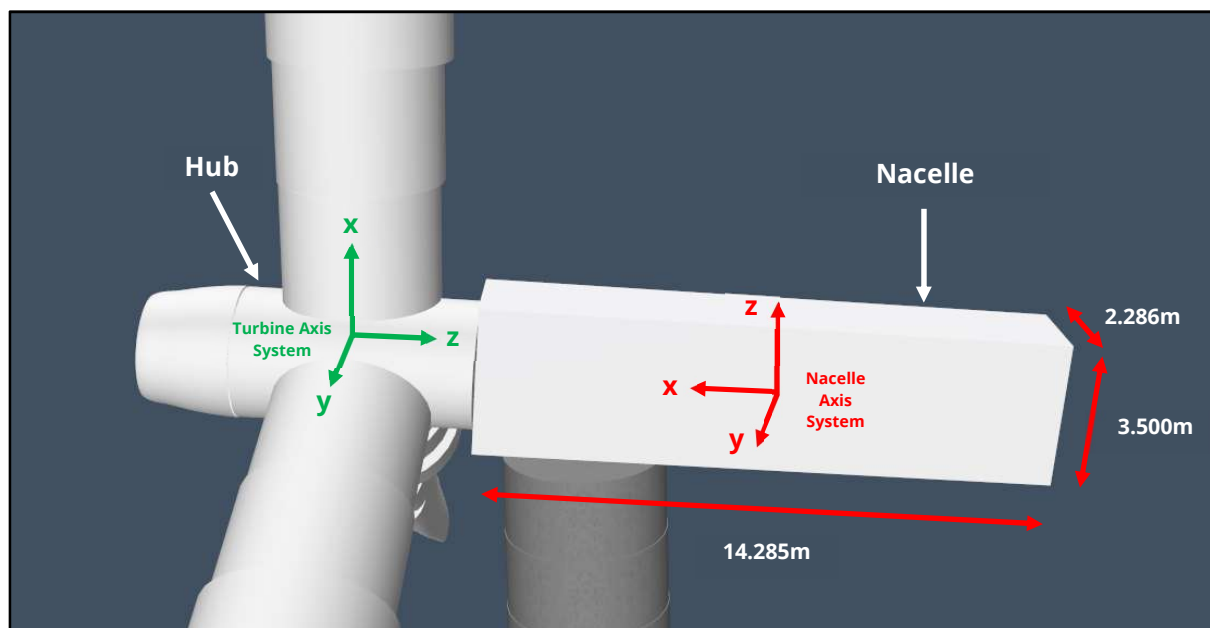
Figure 7 – Hub and Nacelle

Dimension	Property	Value
A	Vertical Offset – Yaw Bearing to Main Shaft (along yaw axis)	1.963 m
B	Hub Centre Horizontal Offset from Yaw Axis (over-hang)	5.000 m
C	Hub Centre Offset from Yaw Axis (along main shaft)	5.019 m
D	Hub Centre Offset from Rotor Bearing (along main shaft)	1.912 m
E	Nacelle CM Horizontal Offset (downwind of yaw axis)	1.900 m
F	Nacelle CM Vertical Offset (from yaw bearing)	1.750 m
G	Tilt – Main Shaft and Nacelle	5.000 °
H	Hub Diameter	3.000 m

Table 9 – Hub and Nacelle Geometric Data [2]

Note that the hub CM is located at the hub centre at an elevation of 90m above GL. The yaw bearing, which is coincident with the top of the tower (see Section 3.2.5), is located at an elevation of 87.6m above ground level.
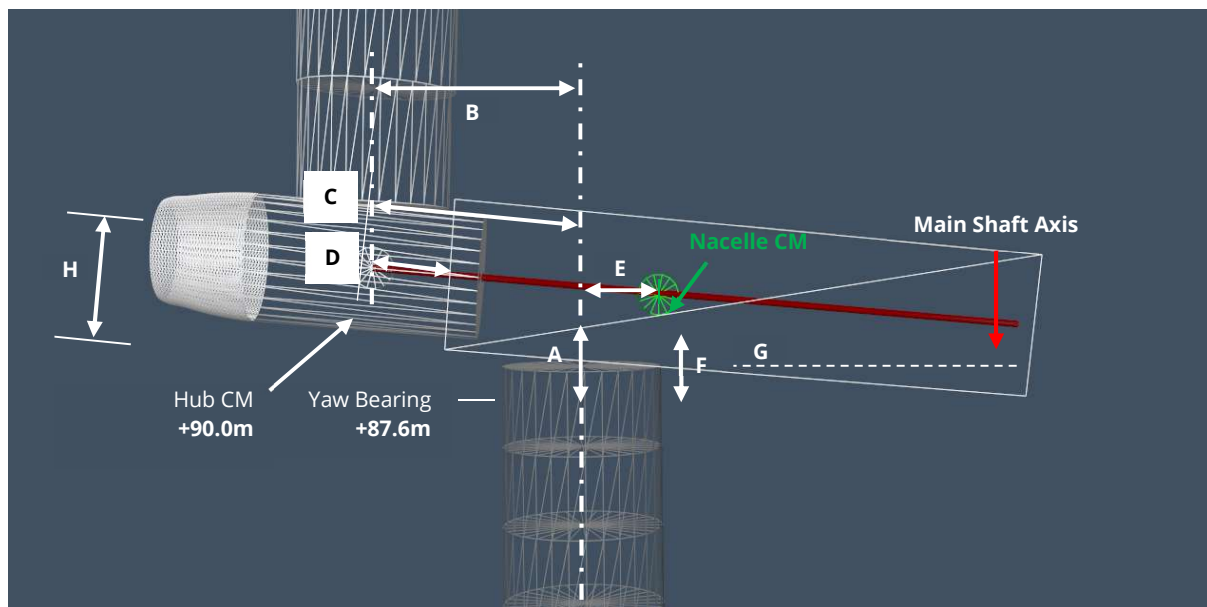
Figure 8 – Hub and Nacelle Geometry

3.2.4. Drivetrain Properties

The gearbox is modelled as a typical multiple-stage gearbox with a ratio of 97:1. The drivetrain properties applicable to OrcaFlex modelling of the wind turbine are summarised in the table below. No frictional losses are considered and no mechanical-to-electrical conversion losses are accounted for. A simplified illustration of the drivetrain assembly is shown in Figure 9.

Property	Value
Gearbox Ratio	97:1
Rated Rotor Speed	12.1 rpm
Rated Generator Speed	1173.7 rpm
Generator Inertia about High-Speed Shaft	0.534 te.m^2

Table 10 – Drivetrain Properties [2]
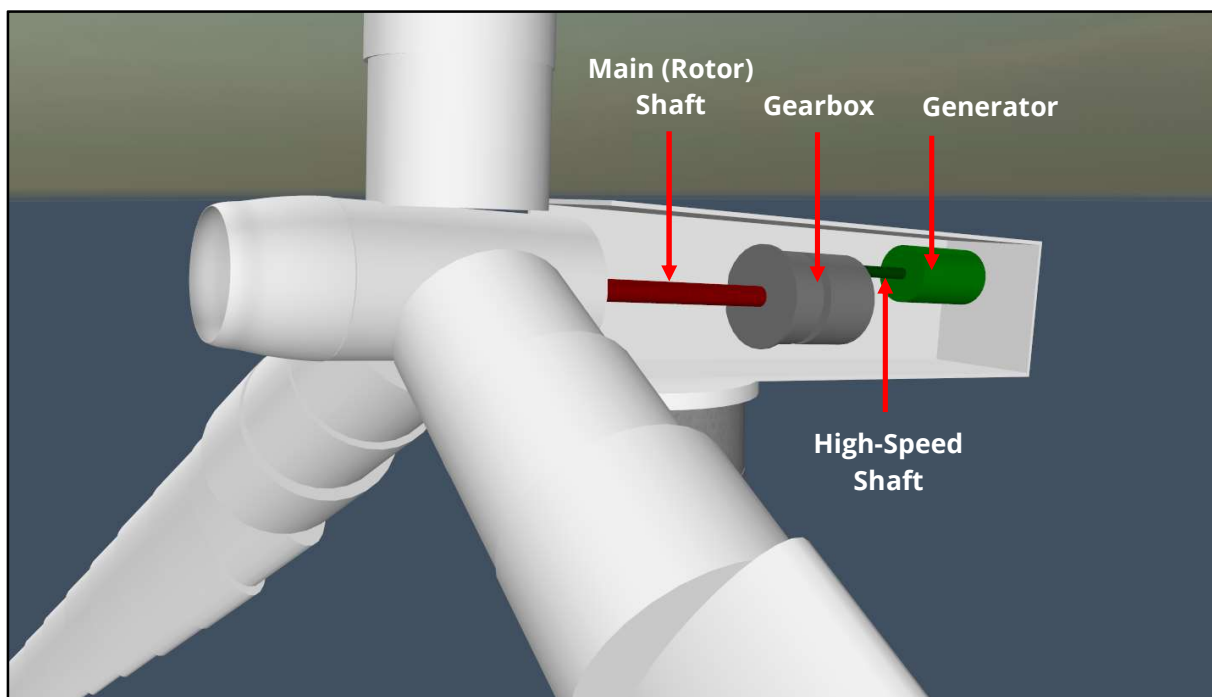
Figure 9 – Turbine Drivetrain

3.2.5. Land-Based Tower Properties

The tower for the land-based system is assumed to be of a conical tubular steel construction. Pertinent geometric details are summarised in Table 11, and illustrated in Figure 10. Both the radius and wall thickness of the tower are assumed to be linearly tapered from the tower base to the tower top. The top of the tower is referred to as the yaw bearing, which is positioned at an elevation of 87.6m above ground level (GL).

Property	Value
Length	87.6 m
Base Elevation (relative to GL)	0.00 m
Base Outer Diameter	6.000 m
Base Wall Thickness	0.035 m
Top Elevation (relative to GL)	+87.6 m
Top Outer Diameter	3.870 m
Top Wall Thickness	0.025 m

Table 11 – Land-Based Tower Geometric Properties [2]
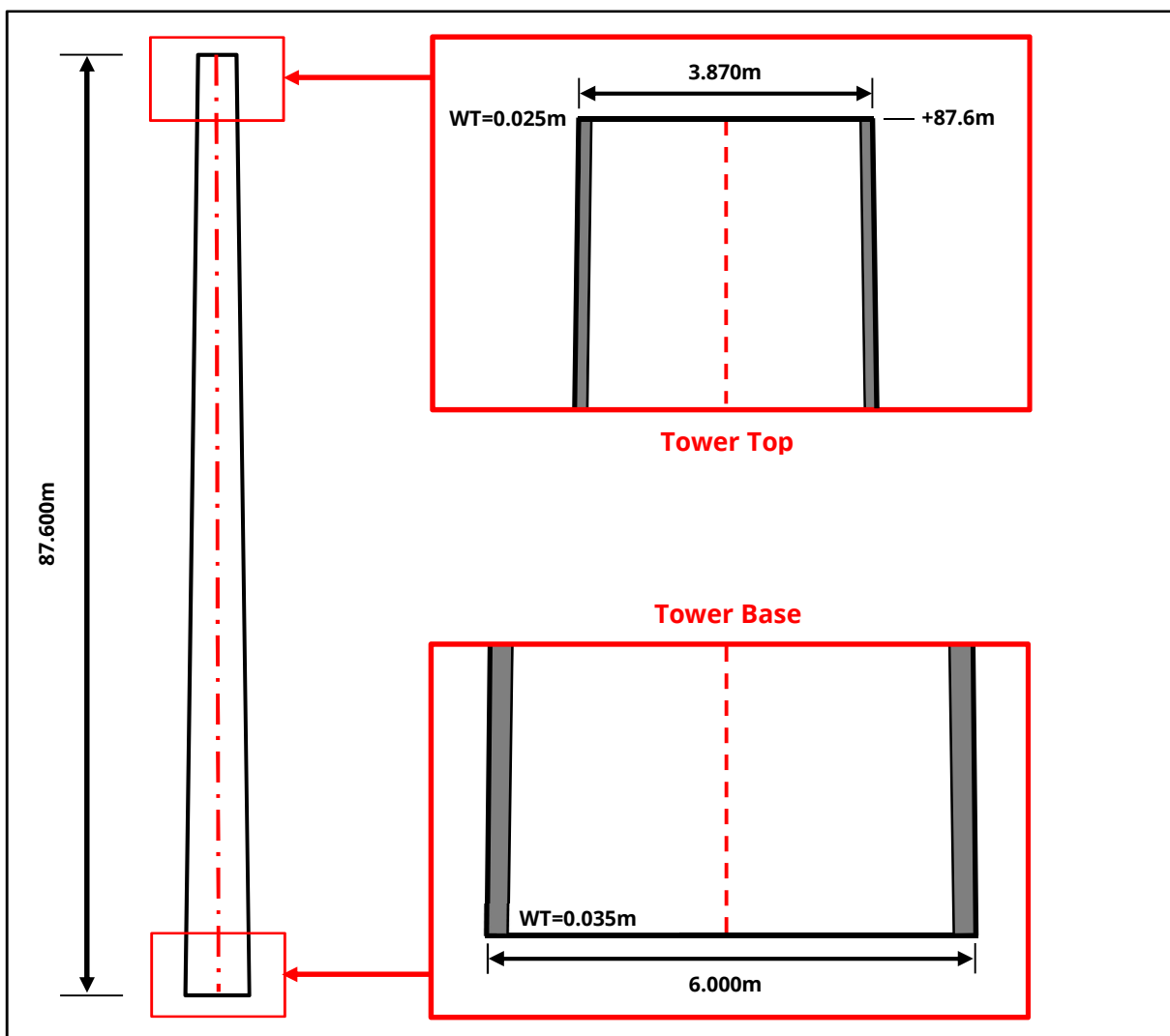
Figure 10 – Land-Based Tower Geometry

The considered tower physical properties are listed below. Note that an effective steel density of 8.50te/m^3 is considered (as opposed to a standard steel density of 7.85te/m^3). This approach is taken to account for the weight of ancillary tower components; such as bolts, welds, flanges, paint coating, etc.

Property	Value
Overall Integrated Mass	347.46 te
CM Location (above GL)	38.148 m
Material	Steel
Material Effective Density	8.50 te/m^3
Material Young's Modulus	210 GPa
Material Shear Modulus	80.8 GPa
Poisson Ratio	0.30
Added Mass Coefficient (C_a)	1.00
Drag Coefficient (C_D)	1.20

Table 12 – Land-Based Tower Physical Properties [2]

3.3. OC3 Hywind Properties

3.3.1. OC3 Hywind Tower Properties

It is important to highlight that the geometric properties of the OC3 Hywind tower differ slightly to the corresponding properties of the land-based tower. The considered geometric details for the OC3 Hywind tower are summarised in Table 13.

As the base of the tower is coincident with the top of the spar platform, which is located at an elevation of 10m above SWL (see Section 3.3.2), the OC3-Hywind tower is 10m shorter than the land-based tower; making it **77.6m** in length. Furthermore, the base of the tower is **6.5m** in diameter, with a wall thickness of **0.027m**; whereas the land-based equivalent has a base diameter of 6m, with a wall thickness of 0.035m. Additionally, the top of the tower has a wall thickness of **0.019m**; in comparison to the land-based tower-top wall thickness of 0.025m.

In a similar approach to modelling of the land-based tower, both the radius and wall thickness are assumed to be linearly tapered from the tower base to the tower top. With the above changes, the tower has an overall mass of **249.72te**.

The above approach is consistent with the approach adopted by NREL [3], which was taken to ensure the top of the tower is positioned at an elevation of 87.6m above the still water level (SWL).

Property	Value
Length	77.6 m
Base Elevation (relative to SWL)	+10.00 m
Base Outer Diameter	6.500 m
Base Wall Thickness	0.027 m
Top Elevation (relative to SWL)	+87.6 m
Top Outer Diameter	3.870 m
Top Wall Thickness	0.019 m

Table 13 – OC3 Hywind Tower Geometric Properties [3]

The considered tower physical properties are listed below. Note that an effective steel density of 8.50te/m^3 is considered (as opposed to a standard steel density of 7.85te/m^3). This approach is taken to account for the weight of ancillary tower components; such as bolts, welds, flanges, paint coating, etc.

Property	Value
Overall Integrated Mass	249.718 te
CM Location (above SWL)	43.318 m
Material	Steel
Material Effective Density	8.50 te/m^3
Material Young's Modulus	210 GPa
Material Shear Modulus	80.8 GPa
Poisson Ratio	0.30
Added Mass Coefficient (C_a)	1.00
Drag Coefficient (C_D)	1.20

Table 14 – OC3 Hywind Tower Physical Properties [3]
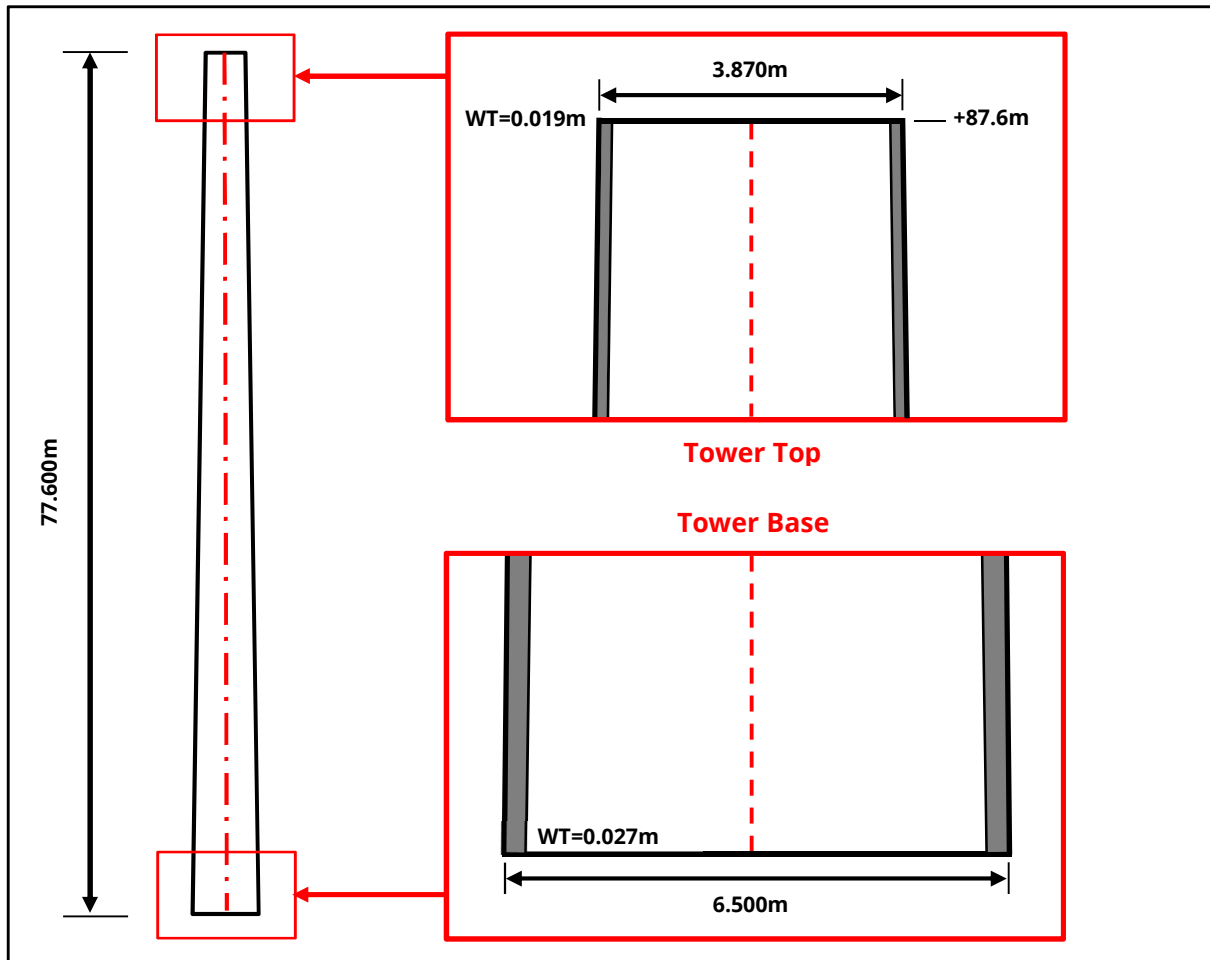
Figure 11 – OC3 Hywind Tower Geometry [3]

3.3.2. Spar Platform Properties

The geometry of the spar platform comprises three main sections, as summarised in Figure 12 and Table 15. In its static position, the spar has a draft of 120m; meaning that the top of the spar, upon which the tower is mounted, extends to an elevation of 10m above the SWL [3].
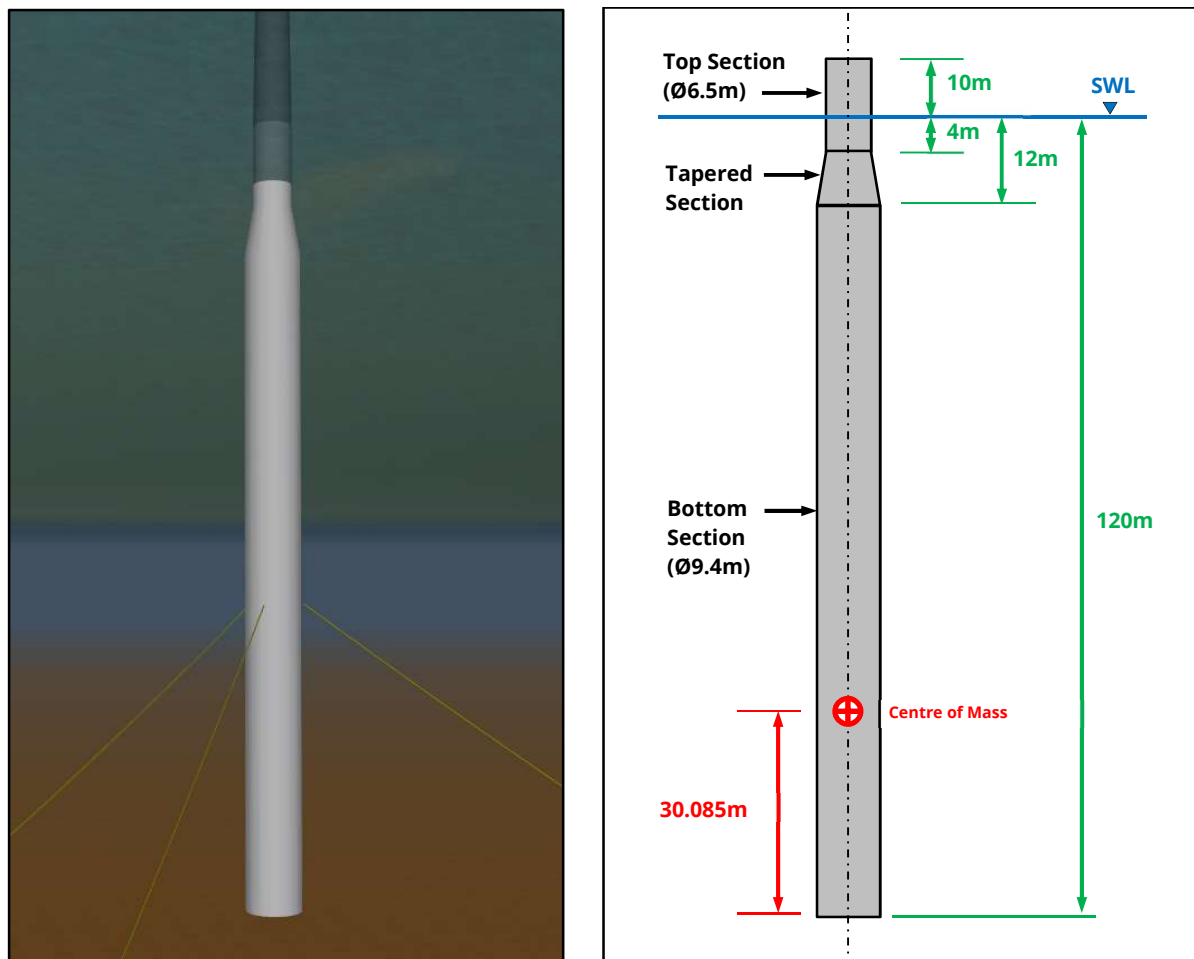
Figure 12 – Spar Platform Geometry (Static Position) [3]

Property	Value
Overall Length	130 m
Total Draft	120 m
Elevation to Platform Top	+10 m
Top Section OD / Length	6.5 / 14 m
Tapered Section Length	8 m
Bottom Section OD / Length	9.4 / 108 m

Note:
Values are given relative to the static position of the spar platform.

Table 15 – Spar Platform Geometric Properties [3]

The spar platform has an overall mass of 7,466.33te and the centre of mass (CM) of the structure is located approximately 30.1m above the base of the platform (as shown in Figure 12). To remain consistent with the approach adopted by NREL in [3], the axial hydrodynamic coefficients of drag, added mass and inertia of the spar platform are all assigned zero values.

A summary of the spar platform's structural and geometric properties is provided in Table 16. The hydrodynamic coefficients considered for the spar platform are summarised in Table 17.

Property	Value
Overall Mass	7,466.33 te
Seawater Displacement	8029.21 te
Roll, Pitch, Yaw Inertia	4,229,230; 4,229,230; 164,230 te.m^2
Centre of Mass (rel. to Platform Base)	30.085 m

Note:
All values are given relative to the static position of the spar platform.

Table 16 – Spar Platform Structural Properties [3]

Property	Value
Normal Drag Coefficient ($C_{D-normal}$)	0.60
Normal Added Mass Coefficient ($C_{a-normal}$)	0.97
Normal Inertia Coefficient ($C_{m-normal}$)	1.97 (= 1 + $C_{a-normal}$)
Axial Drag Coefficient ($C_{D-axial}$)	0.00
Axial Added Mass Coefficient ($C_{a-axial}$)	0.00
Axial Inertia Coefficient ($C_{m-axial}$)	1.00 (= 1 + $C_{a-axial}$)

Note:
An axial inertia coefficient ($C_{m-axial}$) of 1 is considered to ensure Froude-Krylov forces are captured in the corresponding OrcaFlex model (see Section 4.4.2).

Table 17 – Spar Platform Hydrodynamic Properties [3]

3.3.3. Mooring Properties

The OC3 Hywind system is moored to the seabed by means of three separate mooring lines. Realistically, each mooring line would comprise multiple sections with varying structural properties, along with some form of clump weight arrangement. However, in order to simplify the modelling process, each mooring line is generalised as a single line, with associated physical properties taken from [3] (see Table 18).

Property	Value
Quantity of Mooring Lines	3
Length (Unstretched)	902.2 m
Effective Diameter	0.090 m
Unit Weight – In Air / Submerged	77.707 / 71.162 kg/m
Axial Stiffness	384.243 MN
Mooring Line-to-Seabed Friction Coefficient	0.50 (assumed)

Table 18 – Mooring Line Physical Properties [3]
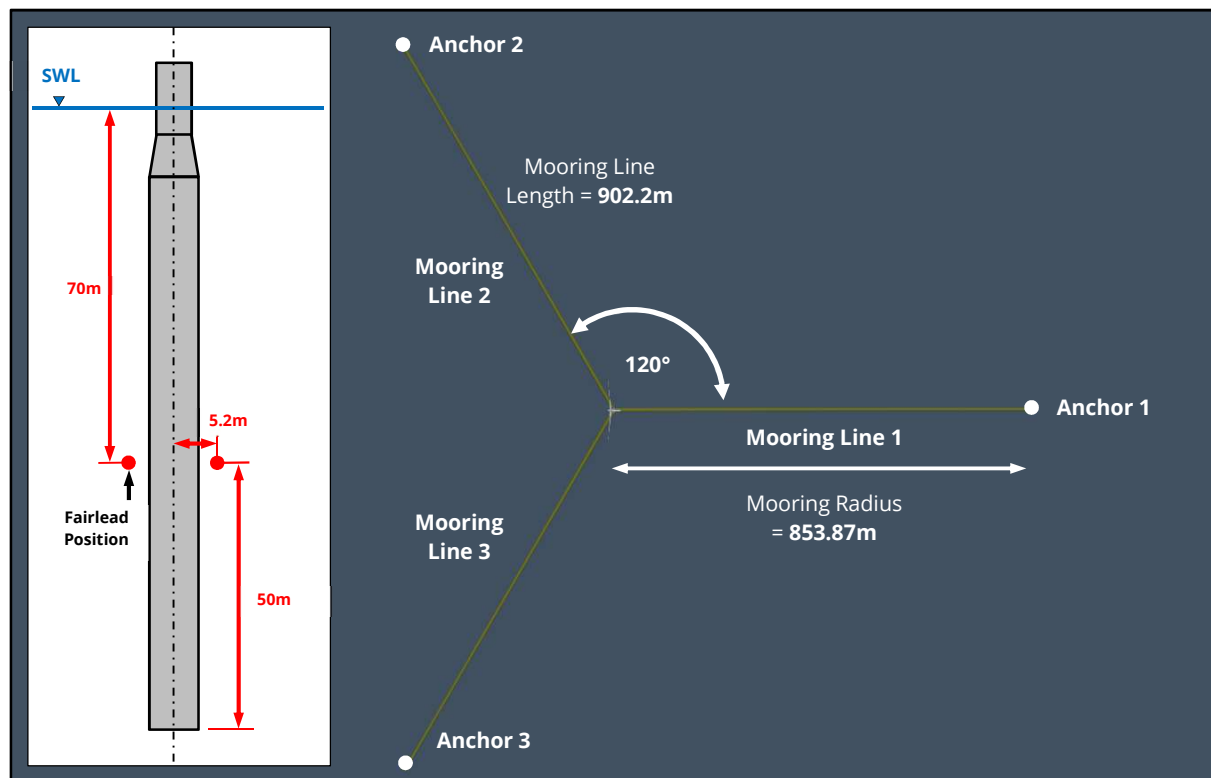
Figure 13 – Mooring Geometry [3]

The connection point for each mooring line on the spar platform (referred to as the fairlead) is positioned at a depth of 70m below SWL, relative to the static position of the spar platform. Each fairlead is positioned at a radius of 5.2m from the spar centreline. At the considered water depth of 320m, the anchor point for each radius is fixed to the seabed at a radius of 853.87m from the spar centreline. The spar fairleads, mooring lines and anchor locations are positioned evenly around the platform, in azimuth increments of 120°.

The mooring line connection properties are listed in Table 19, and illustrated as part of Figure 13.

Property	Value
Angle between Adjacent Lines	120 °
Water Depth	320 m
Fairlead Depth	70 m
Anchor Radius (rel. to Spar Centre)	853.87 m
Fairlead Radius (rel. to Spar Centre)	5.2 m

Note:
Fairlead depth is given relative to the static position of the spar platform.

Table 19 – Mooring Line Connection Properties [3]

Lastly, it is important to note that, to remain consistent with the approach adopted by NREL in [3,4], the mooring bend stiffness is neglected along with hydrodynamic drag and added mass effects. This approach has particular relevance to the mooring line representation adopted in OrcaFlex. Further details related to the mooring line modelling process can be found in Section 4.5.

3.4. Control System Overview

The NREL 5-MW offshore wind turbine is a variable-speed, variable blade-pitch system. Such turbine systems require two distinct control systems during operation: a generator torque controller and a blade pitch controller. The control systems generally work independently of each other, within the necessary windspeed range.

As detailed in Table 5, the system is designed to operate within a wind speed range of **3–25m/s**. The influence of the operational wind speed range on the power output of the wind turbine is shown in Figure 14. The lower-bound wind speed is referred to as the 'cut-in' speed. Around the cut-in speed, the generator is used as a motor (via the generator torque controller) to help the wind overcome the turbine inertia and allow the blades to start turning. For turbine operation between the 'cut-in' speed and the 'rated' speed (Region 1 in Figure 14), the blade pitch is fixed and the generator torque controller is used to maximise power capture.

At the 'rated' wind speed (11.4m/s in this case), the turbine is able to generate electricity at its maximum (or rated) capacity. At this point, the generation of electricity is no longer achieved via generator torque control and the control system switches to regulation of blade pitch. Above the rated wind speed, the control system turns the blades in/out of the wind to alter the aerodynamic forces experienced by the rotor i.e. by controlling blade pitch to ensure the generated power remains constant, as dictated by the wind turbine rating (see Region 3 in Figure 14).

The upper-bound wind speed is referred to as the 'cut-out' speed. At this point, the turbine shuts down to avoid damage to the system. In such wind conditions, the blade-pitch controller will work to increase the angle of attack of the blades i.e. the flat side of the blade is angled further into the wind. This process is known as 'stalling'. Furthermore, a brake system (contained within the nacelle housing) is available to assist the rotor hub in coming to a controlled stop. Note that modelling of wind turbine dynamic stall and brake effects were not available as part of OrcaFlex, at the time of writing.
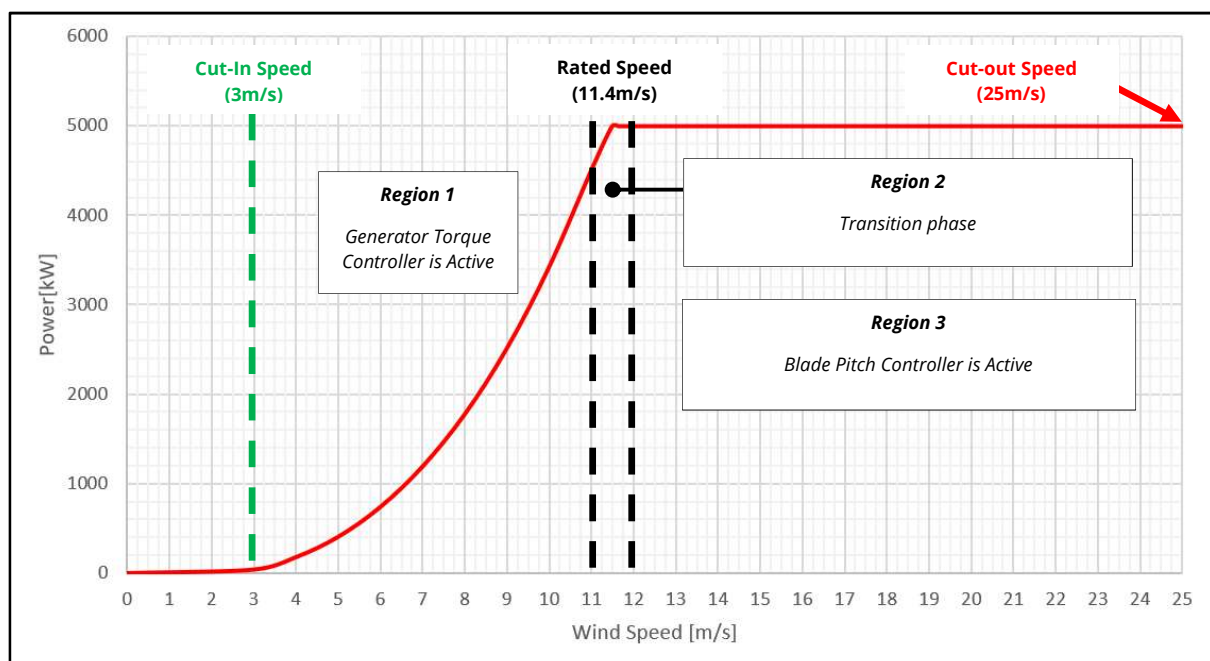
Figure 14 – NREL 5-MW Turbine – Power vs Wind Speed Curve

3.5. Environmental Data

The environmental properties listed in Table 20 are considered as part of the OrcaFlex analysis process.

Property	Value
Air Density	1.225 kg/m^3
Air Kinematic Viscosity	15x10^{-6} m^2/s
Seawater Density	1025 kg/m^3
Seawater Kinematic Viscosity	1.35x10^{-6} m^2/s

Table 20 – Environmental Properties [2]

4. System Modelling

The modelled setup for the land-based and OC3 Hywind turbine systems are illustrated in Figure 15. Further details relating to critical aspects of the modelling process are summarised in the following sub-sections.
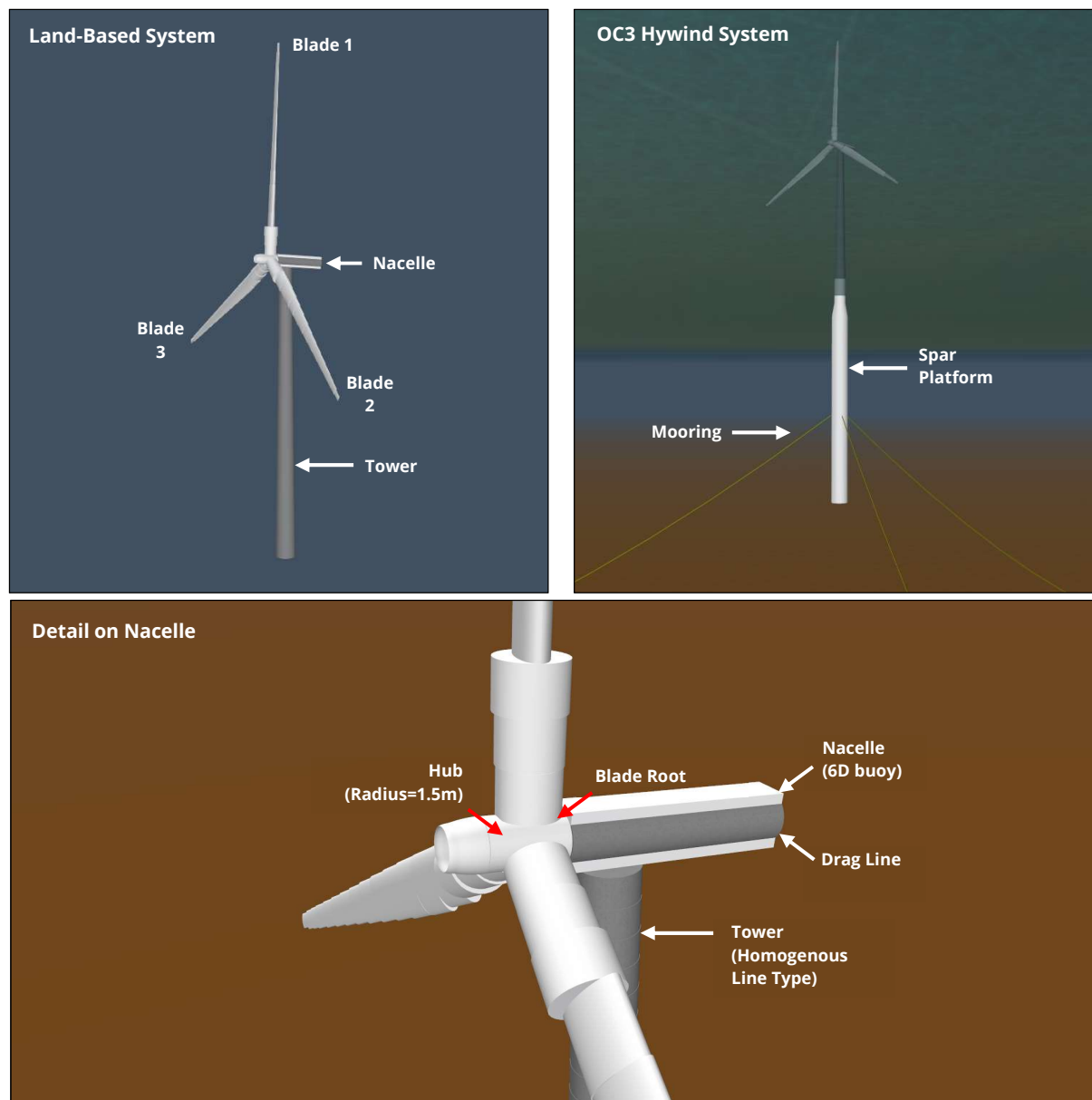
Figure 15 – Wind Turbine System Modelling

4.1. Turbine Modelling

4.1.1. Generator and Hub

Based on the input data specified in Section 3.2.4, the generator gear ratio is set to 97; which represents the number of turns the generator shaft makes when the main rotor shaft turns once. The generator inertia is set to 0.534te.m^2.

The rotor hub radius of 1.5m is assigned to the turbine object; which represents the offset of the blade root from the turbine reference origin. Furthermore, the axial and transverse moments of inertia about the main shaft are specified, based on information detailed in Section 3.2.3. The hub centre of mass is positioned at the geometric centre of the rotor.

4.1.2. Blade Construction

In OrcaFlex, turbine blades are represented by a structural model similar in outline to that used by lines, with massless segments connecting nodes at which inertia is lumped, ordered from end A to end B.

The blade extends from the root at end A to the tip at end B. Each blade comprises 17 single-element sections (see Table 21 and Figure 16). To better capture the structure response at the blade root and tip, a segment length of 2.733m is considered for the 3 inner-most and outer-most blade sections. This is illustrated in Figure 16 and aligns with the approach adopted by NREL in [2].

The blade fitting angles are set to 2.5° and 0° for the pre-cone angle and initial pitch, respectively. The blade degrees-of-freedom (DOFs) are set to 'free', which includes the six DOFs of each node (three translational and three rotational) within the calculation process. This setting means the nodes can rotate and translate relative to each other, allowing blade flexibility to be modelled and aero-elastic coupling effects to be captured.

Section No.	Section Length [m]	Cumulative Length [m]	Number of Segments	Wing Type
1	2.733	2.733	1	Cylinder1
2	2.733	5.467	1	Cylinder1
3	2.733	8.200	1	Cylinder2
4	4.100	12.300	1	DU40
5	4.100	16.400	1	DU35
6	4.100	20.500	1	DU35
7	4.100	24.600	1	DU30
8	4.100	28.700	1	DU25
9	4.100	32.800	1	DU25
10	4.100	36.900	1	DU21
11	4.100	41.000	1	DU21
12	4.100	45.100	1	NACA64
13	4.100	49.200	1	NACA64
14	4.100	53.300	1	NACA64
15	2.733	56.033	1	NACA64
16	2.733	58.767	1	NACA64
17	2.733	61.500	1	NACA64

Table 21 – Modelled Blade Construction [2]
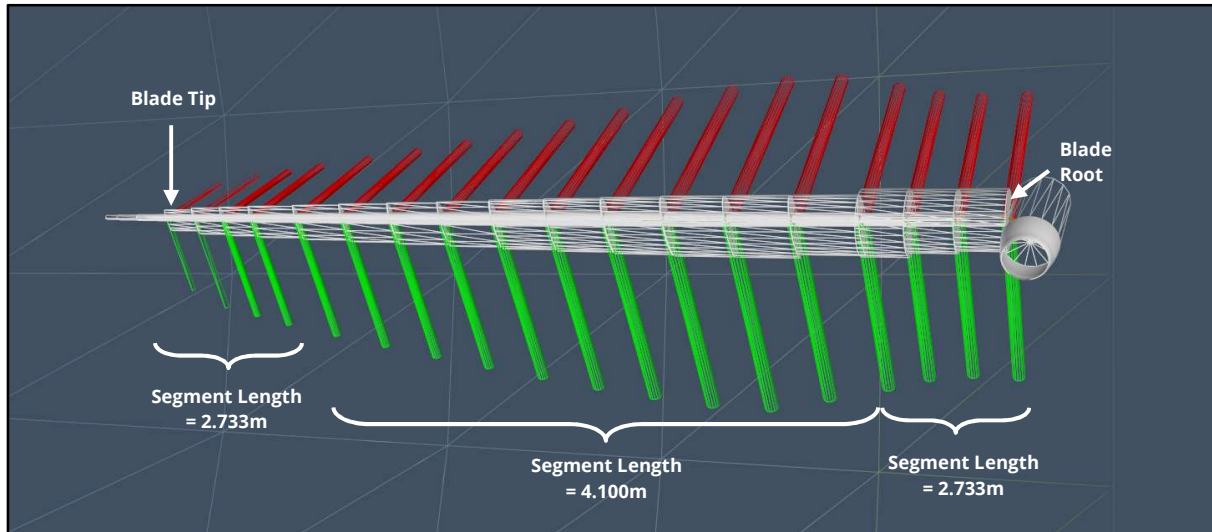
Figure 16 – Blade with Node Axes Visible

4.1.3. Blade Wing Types

A series of wing types are used to model the aerofoil associated to each blade section. The properties of each wing type are represented by a table of lift (C_L), drag (C_D), and moment (C_M) coefficients as a function of the incidence angle of the flow relative to the wing. These coefficients define the aerodynamic loads applied to the wing for each given incidence angle (or angle of attack) (α); which is in the range -180° ≤ α ≤ 180°.

Figure 17 shows an example of the wing type data form for the DU40 aerofoil, along with the corresponding graph displaying the coefficient curves. For further details related to the lift, drag and moment coefficient curves, assigned to each aerofoil, please refer to Appendix A.
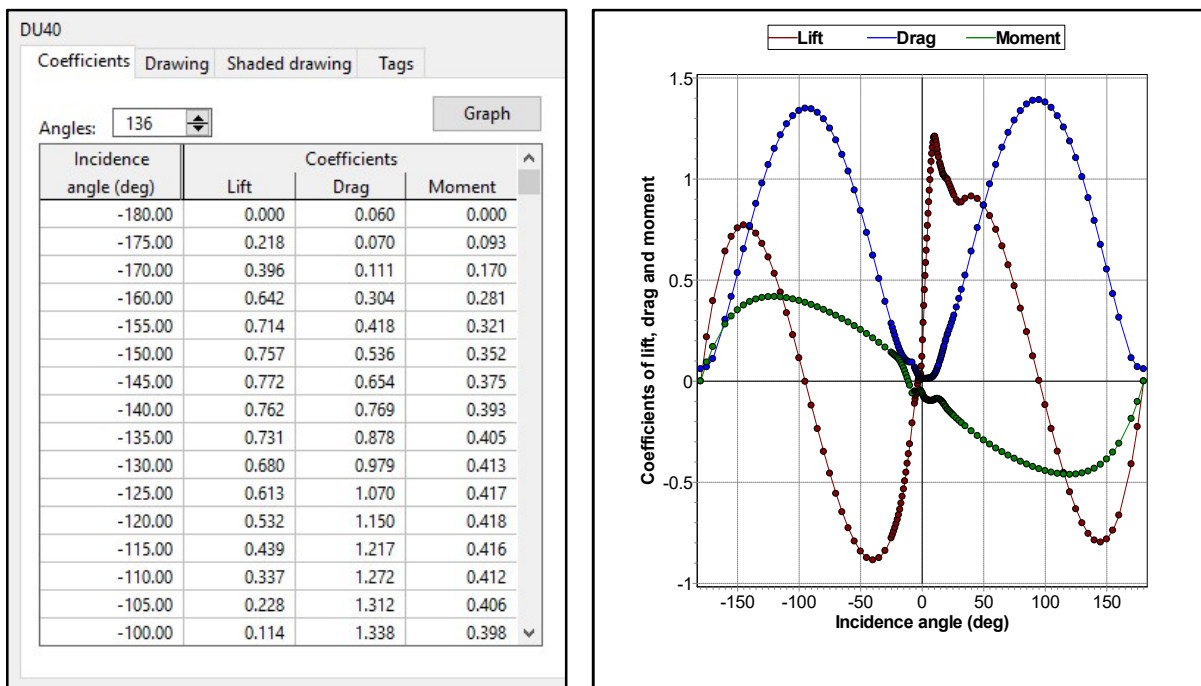
Figure 17 – 'Wing Type' Data Form (DU40)

4.1.4. Blade Geometry, Inertia and Structure

Definition of the blade geometry, inertia and structural properties is achieved from the raw data supplied in [2] (see also Appendix A.1 of this document).

The arc lengths selected for modelling of the blade properties represent the mid-segment points along each blade. This is rationalised by the fact that OrcaFlex calculates external aerodynamic loading at the *mid-segment* frames on each blade – at the specified aerodynamic centre – as shown in Figure 18. Furthermore, the blade geometry, inertia and structure properties are interpolated at the same mid-segment points, and they are the points at which moments / curvatures are reported.

Corresponding blade properties, for the selected arc length values, are then determined via linear interpolation of the available raw data.

It should be noted that the mass per unit length values, reported within the raw data, have been increased by a factor of 4.5%. This corresponds with the approach summarised by NREL in [2]; which results in an overall blade mass of 17,740kg.
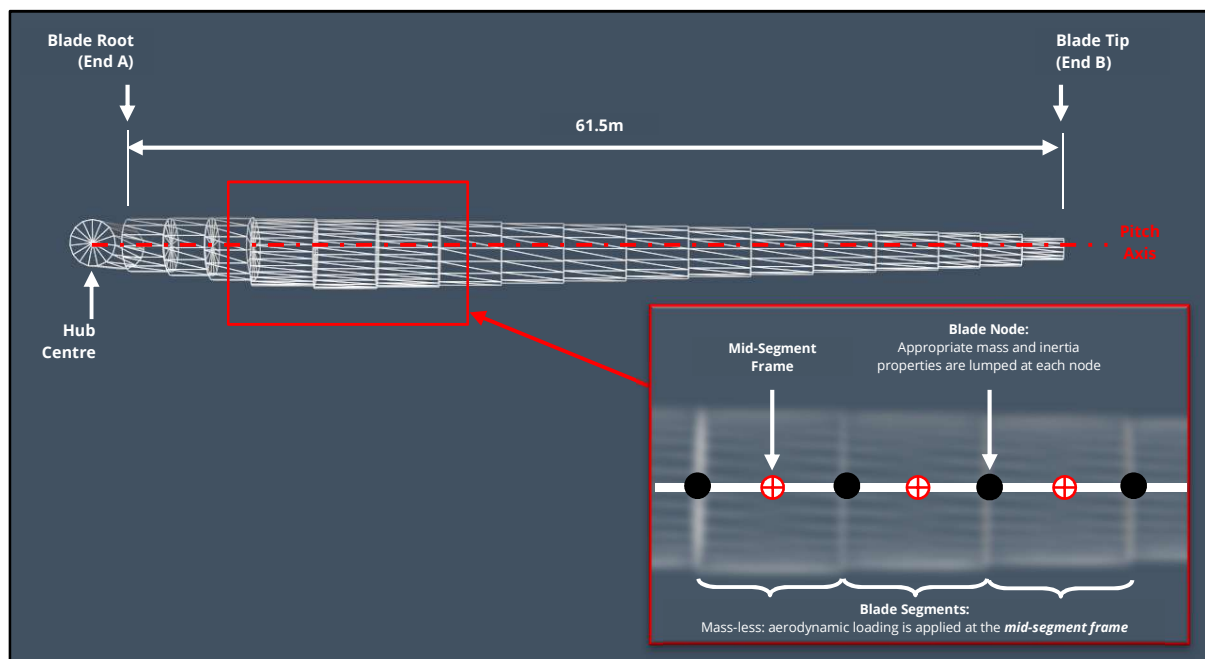
Figure 18 – Blade Structural Model

4.1.5. Blade Tip Deflection

In order to calculate the deflection at each blade tip, three 'reference' 6D buoys are attached to the turbine object at the necessary points. This provides a useful frame of reference, against which the in-plane and out-of-plane deflection of each blade tip can be determined (see Figure 19).

Each reference 6D buoy is set with negligible properties and is positioned along the blade pitch axis (with a pre-cone angle of 2.5°), at the nominal (un-deflected) position of the blade tip. This assigns a negligible mass to the buoy and sets all other lumped buoy properties to zero.

Blade tip deflection is extracted by means of a User Defined Result, which uses a dedicated Python script to determine the blade tip out-of-plane and in-plane deflections.
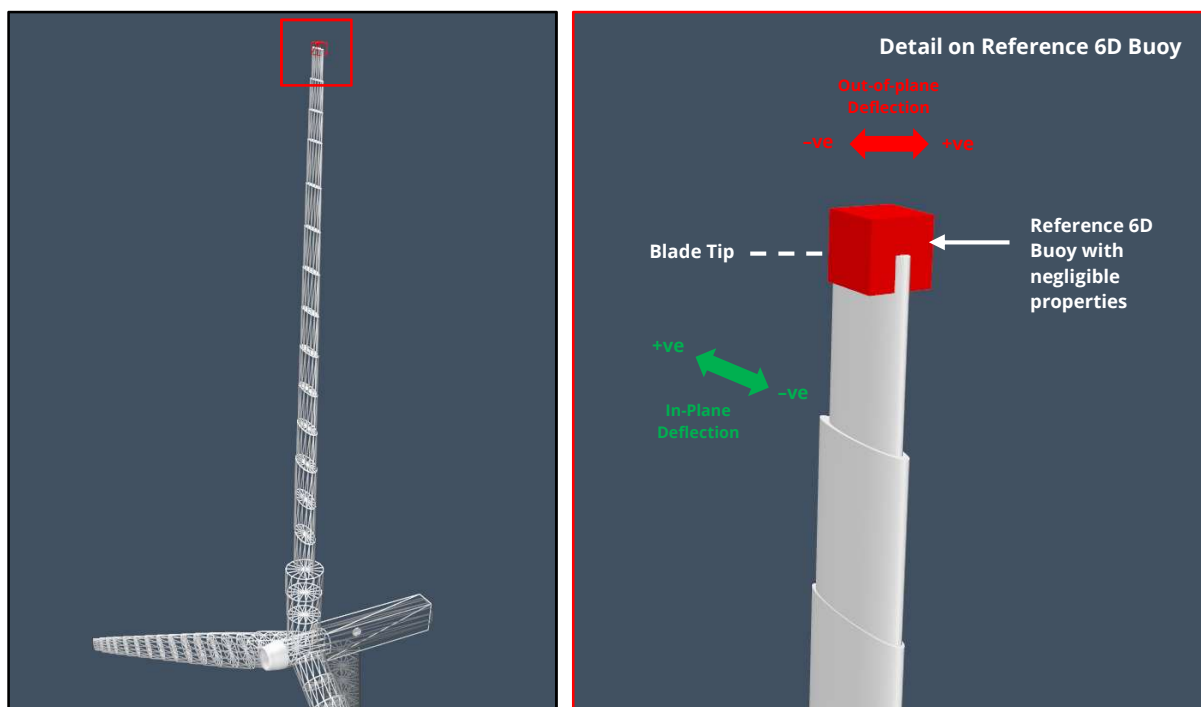
Figure 19 – Reference 6D Buoy for Blade Tip Deflection Calculation

It should be noted that, at the time of writing, blade tip deflection results could only be facilitated using the supplementary modelling technique described above. In subsequent versions of the software (10.4 onwards) direct calculation of blade tip deflection results will be available in OrcaFlex; thus, negating any requirement for supplementary 6D buoys and/or user defined results.

4.2. Nacelle Modelling

The nacelle is modelled as a 'lumped' 6D buoy with appropriate mass, CM and inertia properties assigned to it (see Section 3.2.3). As OrcaFlex cannot presently capture aerodynamic effects on a 6D buoy, a mass-less drag line is attached to the nacelle with suitable drag and added mass coefficients incorporated (see Figure 15).

Within the developed turbine system model, the nacelle serves as a connection point for both the turbine and tower objects.

4.3. Tower Modelling

4.3.1. Tower Line Type

In order to model the wall thickness variation of the conical tower construction, both the land-based and OC3 Hywind tower structures are represented by a line object, with a 'homogeneous pipe' line type assigned to it. Utilisation of this category allows for modelling of the appropriate variable outer/inner diameter profiles, as well as the associated tower physical properties, as documented in Sections 3.2.5 and 3.3.1.

To remain consistent with the other analysis codes, against which the OrcaFlex models are assessed, wind loading on the tower is excluded from the land-based and OC3 Hywind models. Despite this, it is important to note that OrcaFlex does possess the capability to model wind loading on line objects.

4.3.2. Tower Deflection

In order to calculate the deflection at the top of the tower, an additional 'reference' 6D buoy is attached to the tower line object at the necessary location. Again, this provides a useful frame of reference, against which the fore-aft and side-to-side deflection of the tower can be determined (see Figure 20).

Tower deflections are measured at the tower top (End A) and are relative to the centreline of the undeflected tower. Note that positive fore-aft deflection is measured down-wind of the tower, and positive side-to-side deflection is measured towards the starboard side of the floating system (see Figure 20).

To facilitate measurement of the necessary deflections, a reference 6D buoy, set with negligible properties, is positioned at the nominal (un-deflected) position of the tower top. The tower top deflection is extracted via the same User Defined Result script used for calculation of the blade tip deflections.
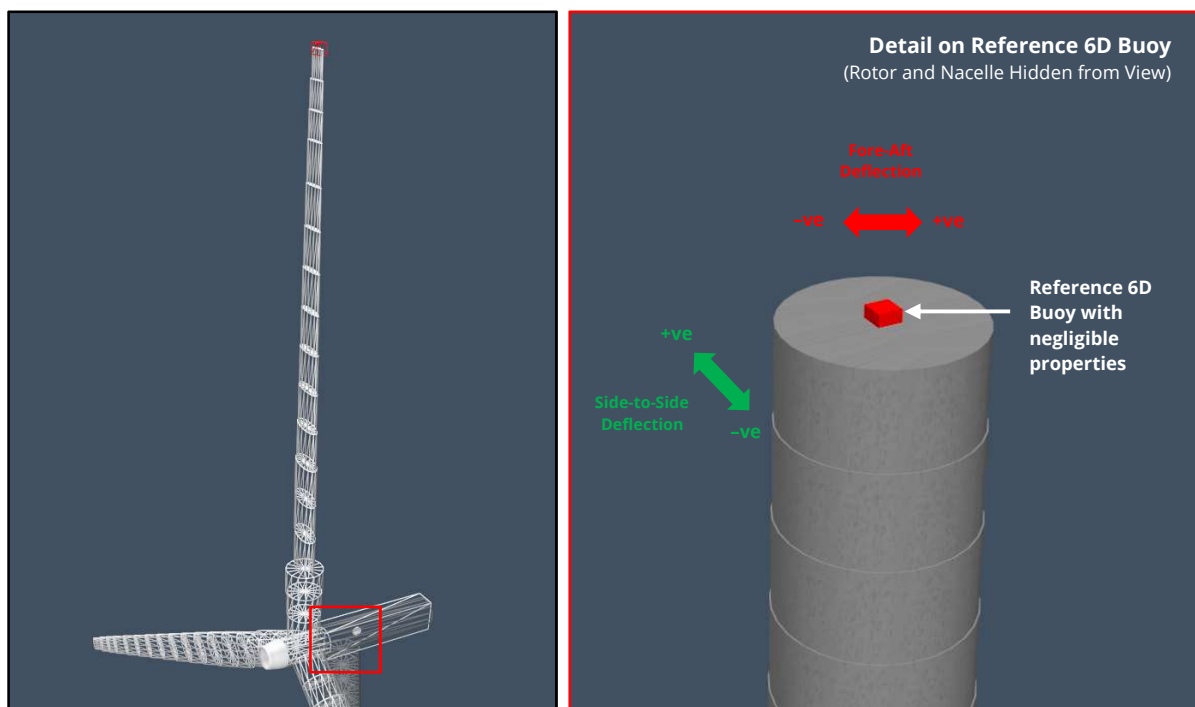
Figure 20 – Reference 6D Buoy for Tower Top Deflection Calculation

4.4. Spar Platform Modelling

4.4.1. Spar Structural Model

The spar platform is classified as a slender axisymmetric surface-piercing buoy which is modelled using the 'spar' category of 6D buoy, offered by OrcaFlex. In this capacity the spar platform is a rigid body, having 6 degrees-of-freedom, with the appropriate mass, CM, inertia, geometric & hydrodynamic properties assigned to it (see Section 3.3.2).

The spar construction is split into a total of 40 discrete cylinders, as defined on the *geometry* page of the 6D buoy data form. In order to accurately capture changes to buoyancy and hydrodynamic loading on the surface-piercing spar buoy, a fine discretisation of 1m is assigned to the top section, tapered section and the top 8m of the bottom section. For the remainder of the bottom section, a discretisation of 10m is considered.
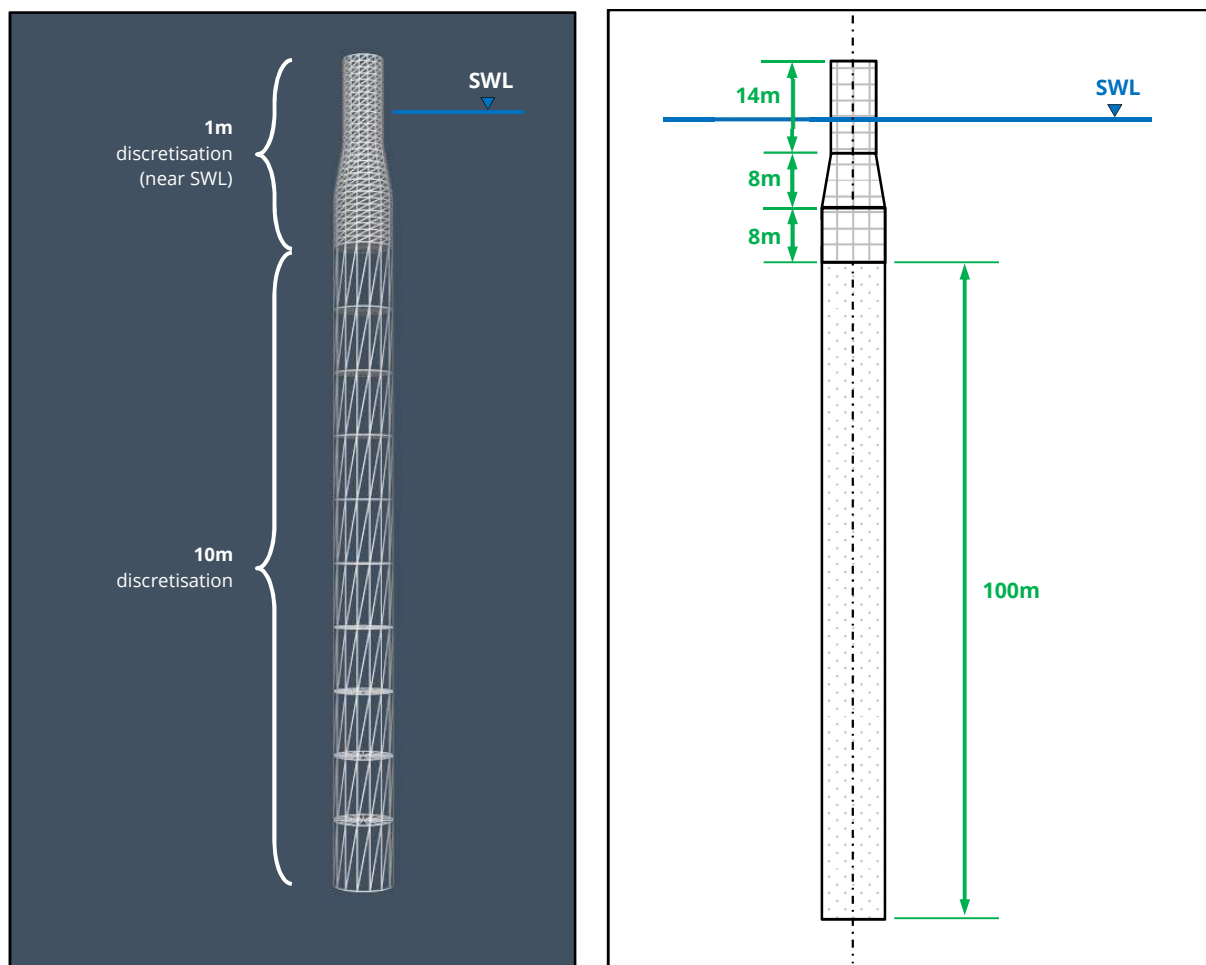
Figure 21 – Spar Platform Discretisation

4.4.2. Spar Hydrodynamic Model

Generally, analysis codes capable of modelling the OC3 Hywind system can model the influence of hydrodynamics using one of two possible methods: Morison's equation or potential-flow theory. Either model is deemed acceptable for simulating the hydrodynamic loading imparted on the spar platform, with the proviso that diffraction effects and the influence of radiation damping are both negligible – as is assumed for the OC3 Hywind analysis summarised in this report [4].

For the OrcaFlex model of the OC3 Hywind system, Morison's equation is considered. When considering the standard form of Morison's equation, the relationship must be expanded to account for the influence of hydrostatics and axial (heave) forces which are encountered by the spar platform due to wave excitation [4]. Within OrcaFlex, such effects are captured by default using the extended form of Morison's equation:

$$\boldsymbol{f} = \left(\boldsymbol{\Delta a_f} + \boldsymbol{C_a \Delta a_r}\right) + \tfrac{1}{2}\boldsymbol{\rho C_D A v_r |v_r|} \tag{4.1}$$

$$\underbrace{\left(\boldsymbol{\Delta a_f} + \boldsymbol{C_a \Delta a_r}\right)}_{\text{Inertia Force}} \underbrace{\tfrac{1}{2}\boldsymbol{\rho C_D A v_r |v_r|}}_{\text{Drag Force}}$$

Where:

f is the fluid force
Δ is the mass of fluid displaced by the body
a_f is the fluid acceleration relative to earth
C_a is the added mass coefficient for the body
a_r is the fluid acceleration relative to the body
ρ is the density of water
v_r is the fluid velocity relative to the body
C_D is the drag coefficient for the body
A is the drag area.

As is highlighted in Equation 4.1, the parenthesised term represents the inertia force, with the remaining term representing the drag force. The inertia force consists of two parts, one proportional to fluid acceleration relative to earth (referred to as the Froude-Krylov component), and one proportional to fluid acceleration relative to the body (referred to as the added mass component). The Froude-Krylov force is the integral over the surface of the body of the hydrostatic pressure in the incident wave, undisturbed by the presence of the body.

To ensure the Froude-Krylov force is modelled appropriately in OrcaFlex, the 6D buoy representing the spar platform is assigned an axial inertia coefficient of $C_{m\text{-axial}}$ = '~'. This setting is equivalent to $1 + C_{a\text{-axial}}$; where $C_{a\text{-axial}}$ = 0. Therefore, $C_{m\text{-axial}}$ = 1 (as summarised in Section 3.3.2, Table 17).

4.5. Mooring Line Modelling

4.5.1. Mooring Line Representation

The mooring lines are modelled in OrcaFlex using the 'general' line type category, which is used to assign the necessary physical properties to each mooring line (see Section 3.3.3 – Table 18). In actual practice, the OC3 Hywind mooring lines would be attached to the spar platform by means of a suitable delta connection (otherwise referred to as a 'crowfoot' arrangement) – as illustrated in Figure 22). The purpose of the delta connection is to provide an element of yaw stiffness to the system.

At the time of writing, precise details of the delta connection were unavailable; therefore, each mooring line is modelled as a single catenary line. This approach is consistent with that adopted by NREL in [3]. The nominal yaw spring stiffness, that would be achieved via the delta connection, is then modelled in OrcaFlex using alternative methods (see Section 4.5.2 for further details).
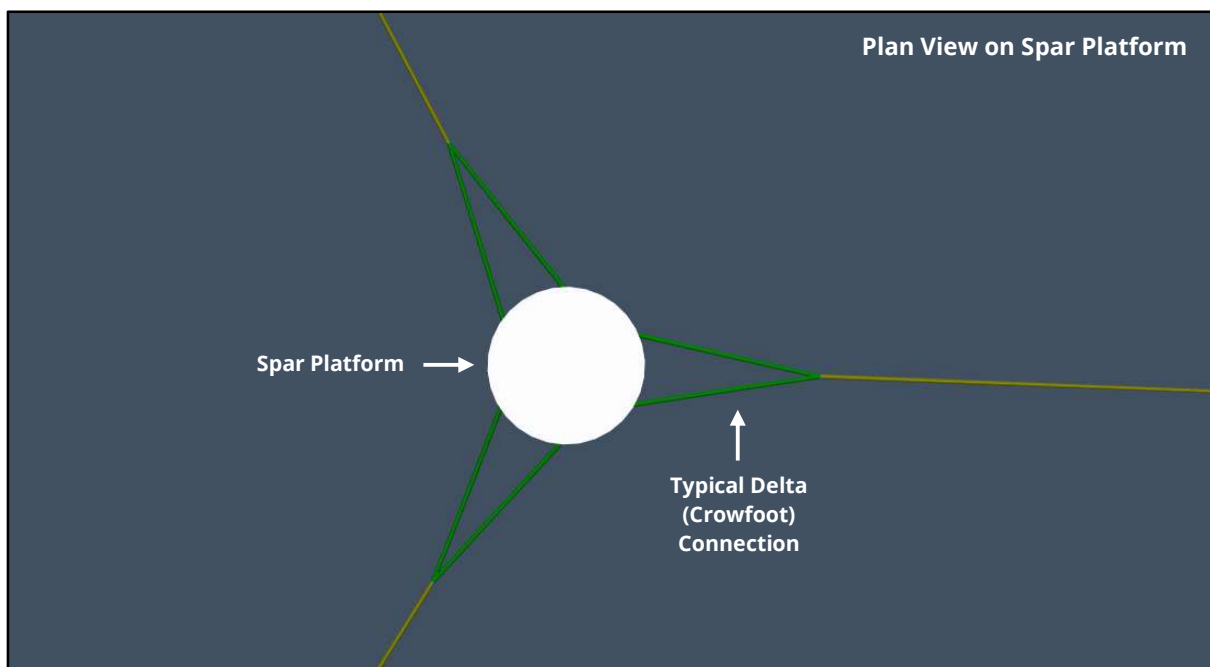
Figure 22 – Typical Delta Connection ('Crowfoot') Arrangement

The single mooring lines are represented in OrcaFlex using the *analytic catenary* method. This method is new to OrcaFlex v10.3, and is offered as an alternative to the default *finite element* representation. For the analytic catenary line representation, the mooring line response is calculated from classical analytic catenary equations. This is different to the usual finite element method where the line is discretised into individual nodes that each carry degrees of freedom.

The analytic catenary equations account for simple properties of a line such as its weight, buoyancy, axial stiffness and axial seabed friction. More complicated effects such as bend stiffness, drag and added mass are ignored. Therefore, the only calculated degrees of freedom in the system are those of the spar platform and the objects connected to it. This simplification means that, at the start of a given simulation, a lookup table is calculated that relates fairlead tension to offset. This table is calculated only once, at the start of the simulation.

This methodology is analogous to the approach summarised by NREL in [3], which considers a force-displacement relationship for each mooring line. This relationship accounts for a total of 500

horizontal displacement steps, corresponding to a horizontal tension range of 0.1kN to 14,098.8kN. These input values are then used to help define the solution grid, for the top end of each mooring line, using the *analytic catenary* representation in OrcaFlex.

Figure 23 displays a comparison between the horizontal tension vs horizontal offset curve calculated by NREL, and the corresponding curve calculated using the *analytic catenary* representation in OrcaFlex. The force-displacement relationships show a near-identical match, thus demonstrating that the analytic catenary representation correlates well with the force-displacement method summarised in [3].
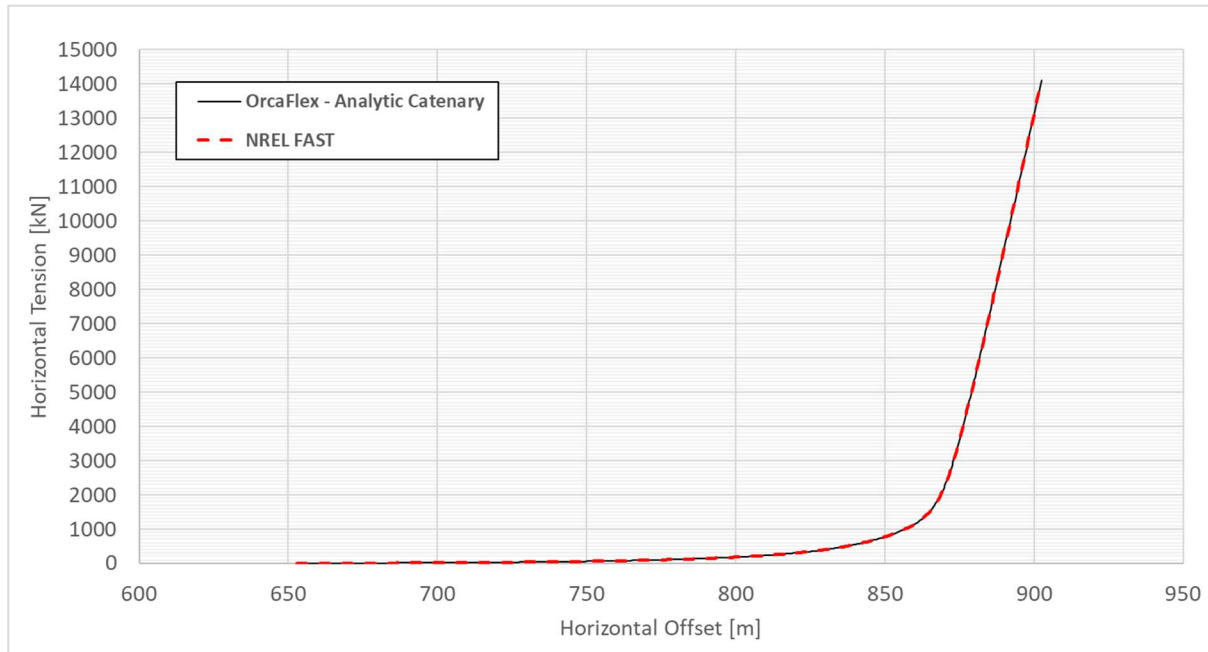
Figure 23 – Load-Displacement Relationship Comparison (NREL vs OrcaFlex)

4.5.2. Mooring Yaw Spring Stiffness

In the absence of specific delta connection data, the nominal yaw spring stiffness is modelled through implementation of a pair of constraint objects; which provide an enhanced means of connecting objects in OrcaFlex. More specifically, they introduce the possibility to fix, or make free, individual degrees-of-freedom (DOFs). For any free DOFs, it is also possible to specify a nominal stiffness value, which is used in this case to introduce the necessary yaw spring stiffness to the system.

From data summarised in [3] and [4], a yaw spring stiffness of 98,340 kNm/rad is specified for the mooring system. This is equal to 1,716.36 kN.m/deg, when considering the default unit convention in OrcaFlex. The connections between the spar platform and the constraint objects are then specifically configured to allow the yaw spring stiffness to be transferred to the floating system.

Within the developed OrcaFlex model, the first constraint (named *fixed_constraint*) is fixed in space, at an x,y,z position of 0,0,–70m. In this location, the constraint is positioned in-line with the central axis of the spar platform, at the same depth as the mooring fairleads (see Figure 24). The constraint is configured to include all DOFs, with the exception of Rz; which represents the rotational DOF of the platform about the z-axis.

The second constraint (named *yaw_constraint*) is connected to the *fixed_constraint* at an x,y,z position of 0,0,0m. The constraint is configured to exclude all DOFs, with the exception of Rz. On the 'stiffness & damping' page of the constraint data form, the required rotational stiffness of 1716.36kN.m/deg is specified.

Lastly, the *spar* 6D buoy is connected to the *yaw_constraint* at an x,y,z position of 0,0, –50m to allow the yaw spring stiffness to be transferred to the floating system.
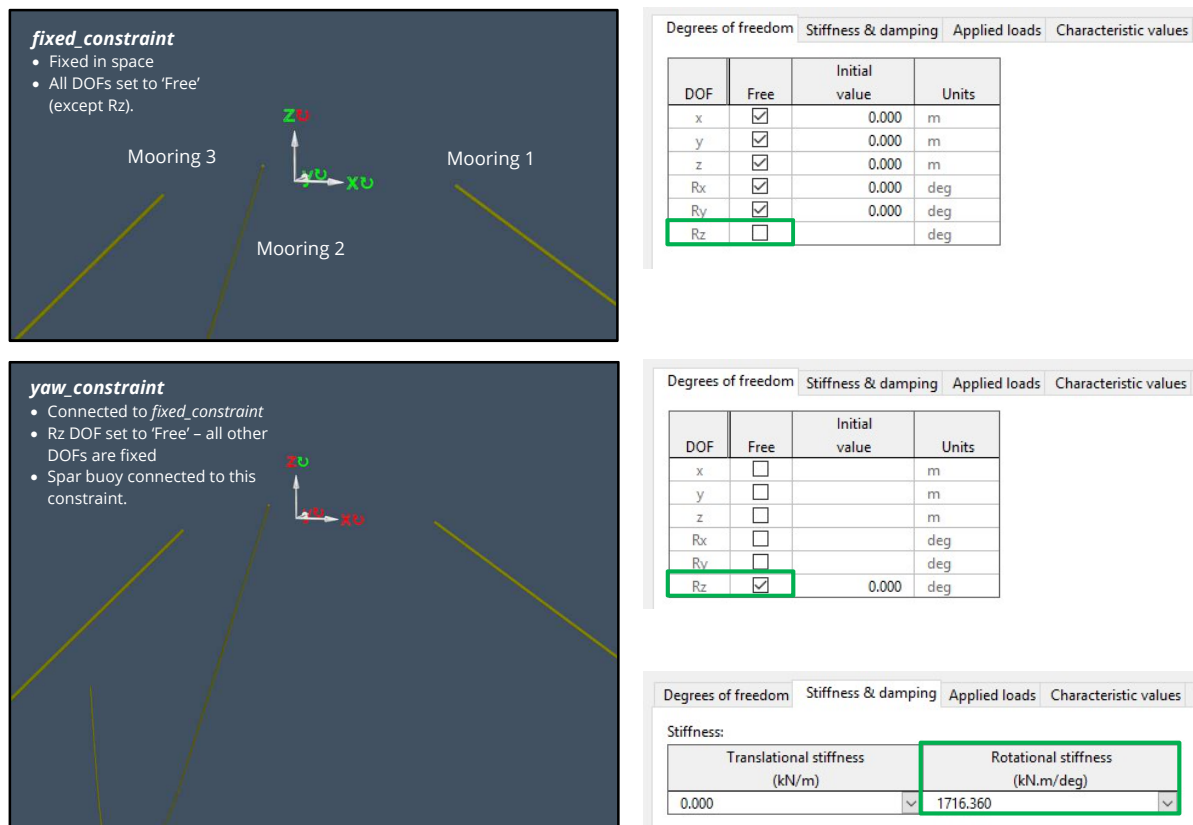
Figure 24 – Yaw Spring Stiffness Constraint Setup (Spar Platform Hidden from View)

4.6. Control System Modelling

The turbine control systems are facilitated by a Python external function; adapted from a similar baseline control system documented as part of [2]. Below the rated wind speed, the external function controls the generator *torque*. Above the rated wind speed, the blade *pitch* is controlled by a proportional-integral (PI) system implemented within the same external function code.

To enhance the functionality of the external function, a series of object tags are assigned to the turbine object; depending on whether the system is land-based or floating (see Figure 25 and Figure 26). The tags are used to pass parameters to the external function. In this capacity, the object tags allow user specification of whether or not the turbine system is floating (via the *FloatingSystem* tag).

The tags also allow specification of whether or not the blade pitch actuator (*UseActuator*) is active. The blade pitch actuator is an optional second order sub-system of the blade pitch controller. The actuator functions to turn a blade pitch angle demand into a physical response about the blade's pitch degree-of-freedom. For the blade pitch actuator system, additional tags are included to specify the natural angular frequency and damping ratio of the second order system; denoted *ActuatorOmega* and *ActuatorGamma*, respectively.

It should be noted that blade pitch actuator dynamics are not considered as part of the other analysis codes considered in [2] and [4]. Therefore, to maintain consistency, the object tags assigned to the OrcaFlex turbine control system consider a very high natural angular frequency of 30Hz (= 188rad/s) and a damping ratio of 2% critical (0.02), respectively. These values are specifically chosen to diminish the influence of blade pitch actuator dynamics [2].

Figure 25 – Turbine Object Tags for External Function (Land-based System)

Figure 26 – Turbine Object Tags for External Function (OC3 Hywind System)

4.7. Environment Modelling

4.7.1. Land-Based System

To consider the steady state response of the land-based system, the operational wind speed range of the turbine (3–25m/s) is considered in increments of 1m/s. A separate dynamic load case is then created for each uniform wind speed increment; amounting to a total of 23 separate load cases.

A 'Time history (speed)' wind type is used to represent the uni-directional steady-state wind applied in the simulation environment. Note, to ensure the model is comparable with the NREL study documented in [2], the influence of aerodynamic loading on the tower and nacelle is disabled.

The duration of each dynamic simulation is set to 500s, with a 50s build-up phase. To minimise the likelihood of any transient behaviour persisting in the overall simulation, the wind speed is linearly ramped from zero to the nominal steady-state speed during the 50s build-up phase.

Suitable results, describing the steady state behaviour of the turbine, are then extracted for comparison against the corresponding FAST results (documented by NREL in [2], Section 9).

4.7.2. OC3 Hywind System

The load cases considered for Phase IV of the OC3 study are listed in Table 22 below [4]. Of the listed cases, load case 5.1 is deemed to sufficiently capture the steady-state dynamic behaviour of the OC3 Hywind system. The justification being that time domain analysis is considered, along with application of wind & waves, with all possible degrees-of-freedom enabled in the modelled system. Additionally, the corresponding load case results (documented in [4], Figure 48) are considered satisfactory to facilitate validation of the results obtained from the analogous OrcaFlex model of the system.
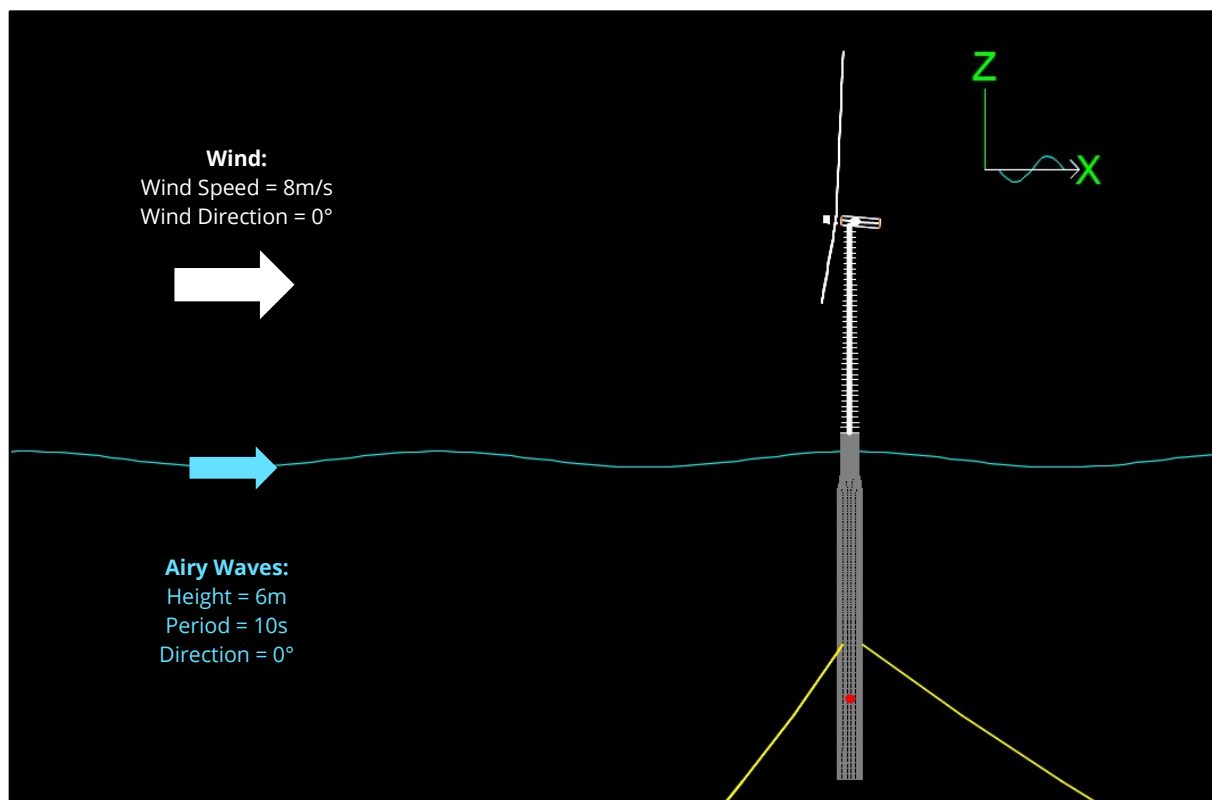
Figure 27 – OC3 Hywind – Modelled Wind & Wave Conditions (Load Case 5.1)

To ensure any transient behaviour is eliminated from the system, and to allow the spar platform motion to settle, the duration of the simulation is set to 1500s with a 50s build-up phase. Airy waves, assigned a height of H=6m and period T=10s, are applied in the simulation environment. During the build-up phase (stage 0), the sea conditions are ramped up from zero in order to avoid the occurrence of sudden transients in the simulation.

A uni-directional steady-state wind is applied in the same direction as the modelled waves and the wind speed is linearly ramped from 0m/s to 8m/s during the build-up phase, using the *Time history (speed)* wind model available in OrcaFlex. A steady uniform wind speed of 8m/s is then considered for the remainder of the simulation. No current is considered as part of this load case definition.

The considered wind and wave conditions are illustrated in Figure 27.

NREL Load Case Number	Enabled DOFs	Wind Conditions	Wave Conditions	Analysis Type
1.2	Platform, tower, drivetrain, blades	None	None	Eigenanalysis
1.3	Platform, tower, drivetrain, blades	None	None	Static
1.4	Platform	None	None	Free-decay time domain
4.1	Platform, tower	None	Regular Airy: H=6m, T=10s	Dynamic time domain
4.2	Platform, tower	None	Irregular Airy: H_S = 6 m, T_P = 10 s, JONSWAP wave spectrum	Frequency domain
5.1	**Platform, tower, drivetrain, blades**	**Steady, uniform, no shear: wind speed = 8m/s**	**Regular Airy: H = 6m, T = 10s**	**Dynamic time domain**
5.2	Platform, tower, drivetrain, blades	Turbulent: wind speed = 11.4m/s, σ1 = 1.981m/s, Mann model	Irregular: H_S = 6m, T_P = 10s JONSWAP wave spectrum	Frequency domain
5.3	Platform, tower, drivetrain, blades	Turbulent: wind speed = 18m/s, σ1 = 2.674 m/s, Mann model	Irregular Airy: H_S = 6m, T_P = 10s, JONSWAP wave spectrum	Frequency domain
5.4	Platform, tower, drivetrain, blades	Steady, uniform, no shear: Wind Speed = 8m/s	Regular Airy: H = 2m, ω = 0.1, 0.2, …, 3.5 rad/s	Time domain for calculation of 'Effective RAOs'

Table 22 – NREL Load Case 5.1 [4]

5. Results Comparisons

5.1. Land-Based System Results

Table 23 summarises the result parameters of interest for the land-based system, along with the corresponding FAST designation, as documented by NREL in [2]. The third column details the results variable(s) required to extract the corresponding results from the OrcaFlex simulations. Note that some results are calculated from a combination of OrcaFlex results variables.

For each result presented in Table 23, a chart is produced that provides a useful visual comparison between the OrcaFlex and FAST results. In each of the charts contained in the following sub-sections, the solid black curve represents the calculated OrcaFlex results, whilst the red-dashed curve represents the corresponding FAST results.

Results Parameter	NREL Result Designation	OrcaFlex Result Variable
Rotor		
Rotor Speed	RotSpeed	Main shaft angular velocity
Rotor Torque	RotTorq	Main shaft torque
Rotor Power	RotPower	Main shaft angular velocity **x** Main shaft torque
Rotor Thrust	RotThrust	Connection Lz force
Generator		
Generator Speed	GenSpeed	Generator angular velocity
Generator Torque	GenTorq	Generator torque
Generator Power	GenPower	Generator power
Blade 1		
Tip-speed Ratio	TSR	Node Angular Velocity (oeEndB) / Wind speed
Pitch Angle	BlPitch	Blade pitch (Blade 1)
Average Tip Out-of-plane Deflection	OoPDefl1	*User Defined Result*
Average Tip In-plane Deflection	IPDefl1	*User Defined Result*
Tower Deflection		
Average Tower Top – Fore-aft Deflection	TTDspFA	*User Defined Result*
Average Tower Top – Side-to-side Deflection	TTDspSS	*User Defined Result*

Note:
Tower deflections are measured at the tower top (End A) and are relative to the centreline of the undeflected tower.

Table 23 – Land-Based System – Result Output Parameters [2]

5.1.1. Rotor Results Comparison

Figure 28 displays the OrcaFlex vs FAST results comparison for the turbine rotor speed and rotor torque response. In addition, Figure 29 shows a comparison of the calculated rotor power and rotor thrust results. The charts display very close agreement between the calculated results.
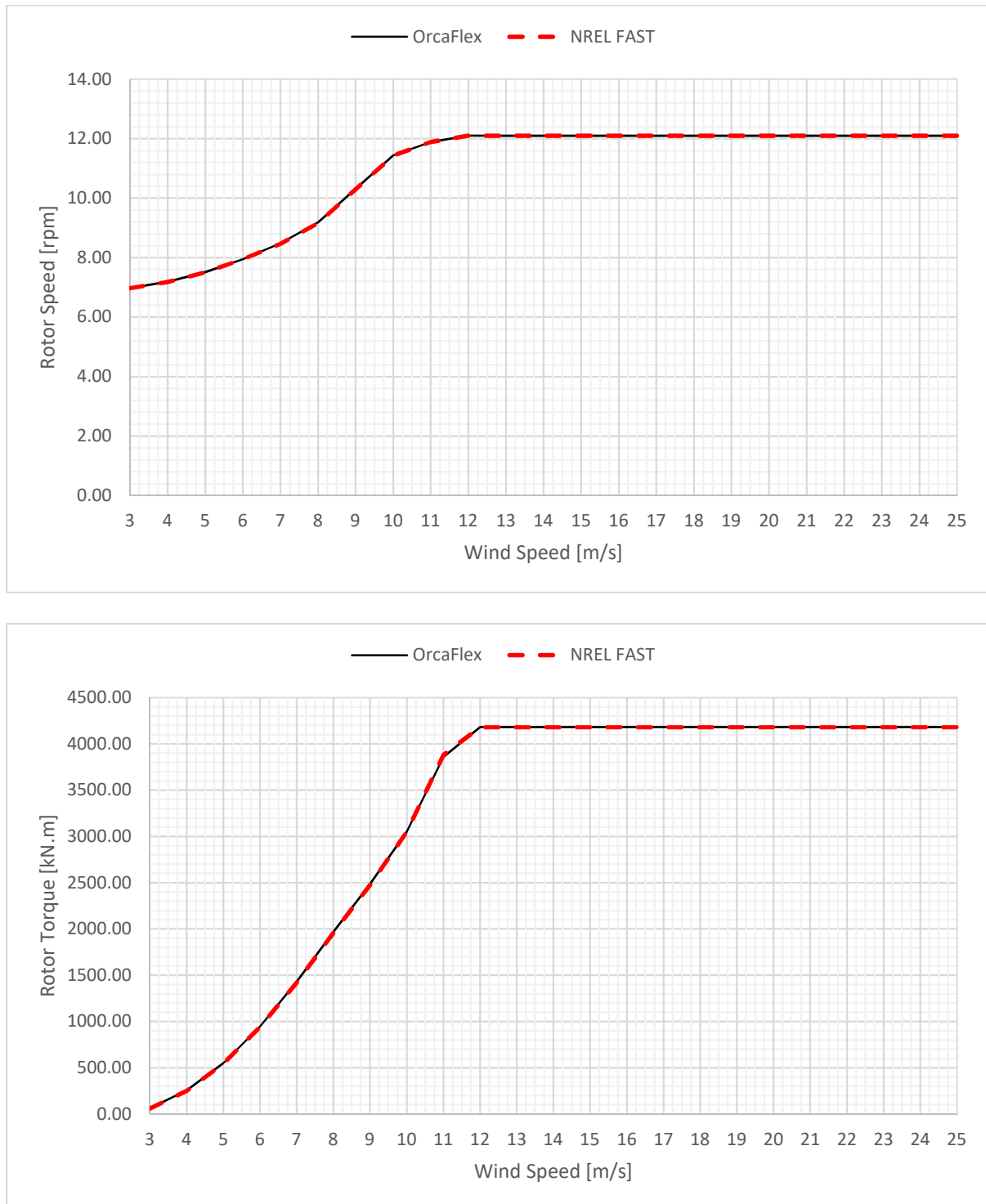
Figure 28 – Rotor Speed & Rotor Torque Results Comparisons
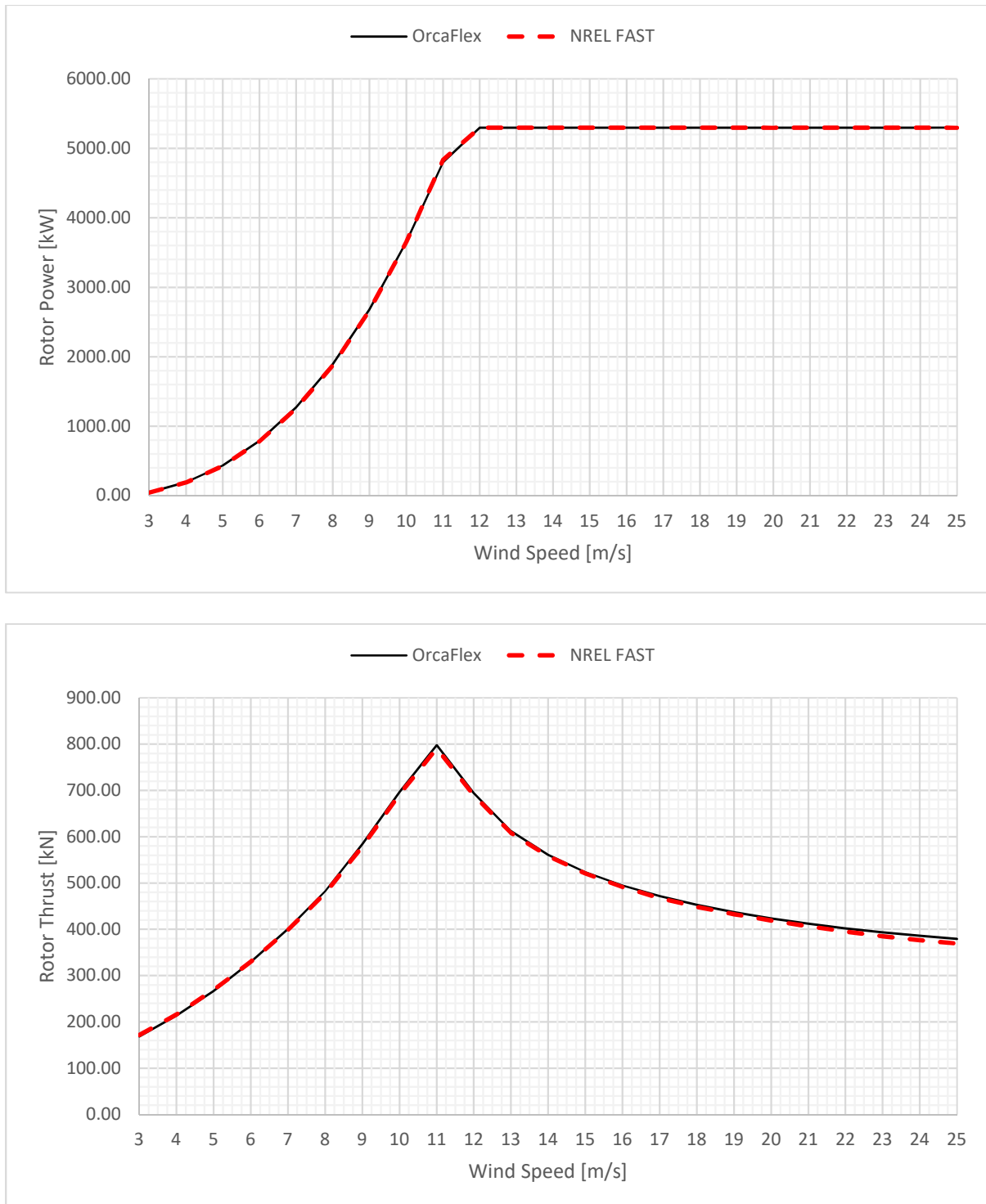
Figure 29 – Rotor Power & Rotor Thrust Results Comparisons

5.1.2. Generator Results Comparison

Figure 30 displays the OrcaFlex vs FAST results comparison for the generator speed and generator torque. Once again, the charts display very close agreement between the results calculated from each analysis code.
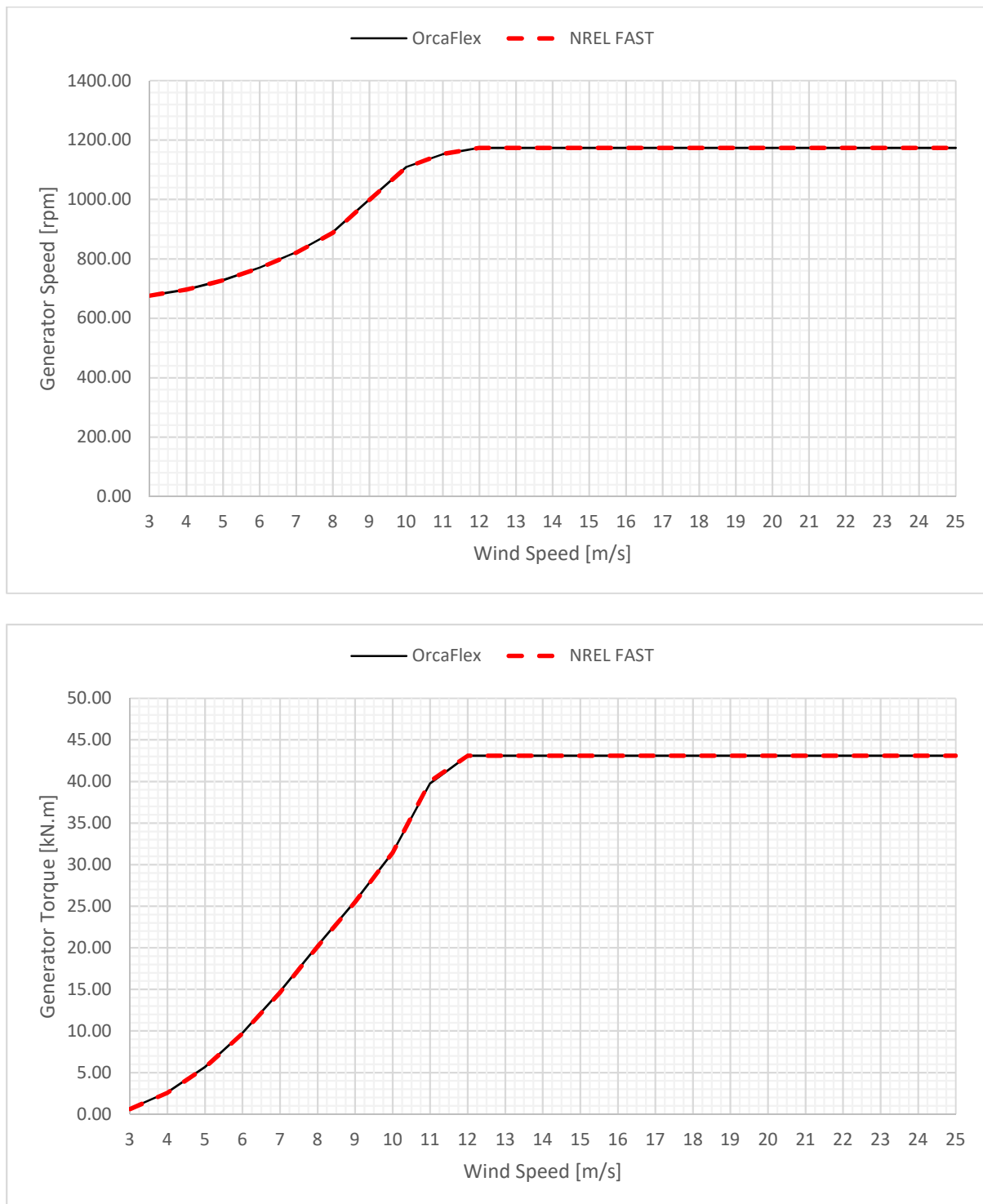
Figure 30 – Generator Speed and Generator Torque Results Comparisons

Figure 31 displays the generator power results comparison. The chart indicates a marked difference between the OrcaFlex and FAST results, with steady-state power outputs (in Region 3) of 5.3MW and 5.0MW, respectively.

This difference is attributed to a mechanical-to-electrical conversion loss, considered in the FAST model [2]; which represents a generator efficiency of 94.4%. When applying this same efficiency to the calculated OrcaFlex results, a close agreement was observed when comparing to the corresponding FAST results. This is displayed in Figure 31, where the adjusted OrcaFlex results are represented by the solid green line.
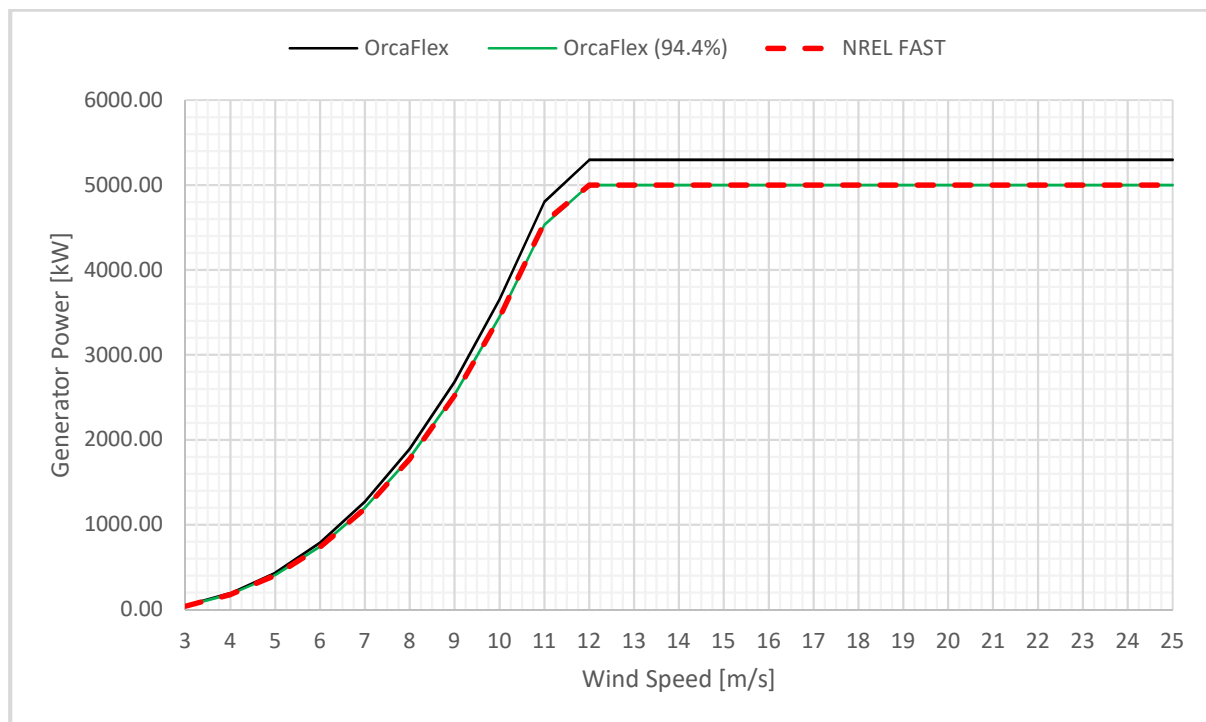
Figure 31 – Generator Power Results Comparison

5.1.3. Blade 1 Results Comparison

Figure 32 displays a noticeable difference between the calculated blade pitch results. Above the rated wind speed, this difference steadily increases with increasing wind speed. The observed differences are believed to be caused by the blade structural model incorporated as part of the FAST version of the land-based turbine. This model only accounts for the bending stiffness of the turbine blades [5], meaning the axial and torsional degrees-of-freedom of the turbine blades are neglected. Conversely, the OrcaFlex turbine object accounts for these degrees-of-freedom, by default.
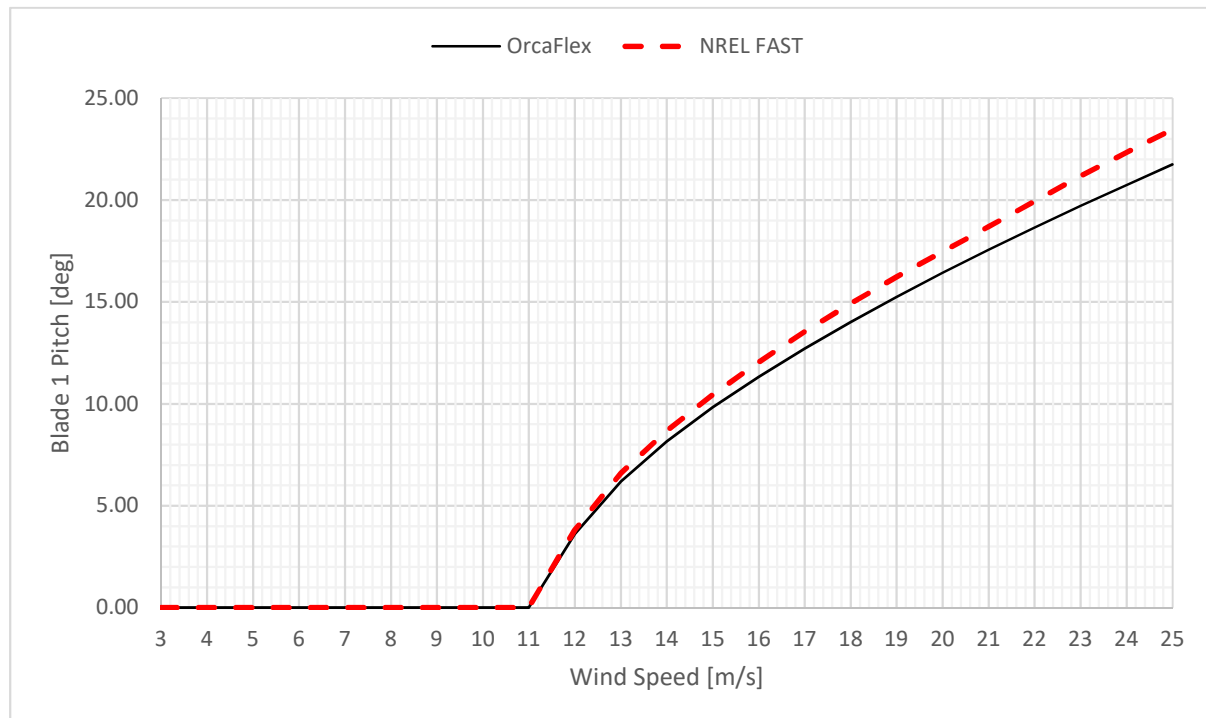
Figure 32 – Blade 1 Pitch Results Comparison

To account for this key difference in modelling approach, the OrcaFlex version of the land-based turbine model was modified to assign an arbitrarily high stiffness value of $1 \times 10^9 kN.m^2$ to both the torsional and axial stiffness properties of the turbine blades. This had the effect of artificially eliminating the blade torsional and axial degrees-of-freedom.

The effect of this modification is shown below in Figure 33, where an additional curve named 'OrcaFlex (Adjusted)' has been added to the chart already presented above in Figure 32. Here, the results obtained through the adjusted OrcaFlex model can be seen to match more closely than those calculated via the 'default' model.

The influence this has on the pitch angle response from blade 1 was found to directly impact the calculated results for the blade tip in-plane & out-of-plane deflections, as well as the tower top fore-aft & side-to-side deflections. These results are discussed in further detail below, and in the following sub-sections. Consequently, each of the corresponding charts contain an additional curve which accounts for the modifications made to the OrcaFlex blade structural properties, as discussed above.

Note, the same modifications were found to have minimal impact on the response of the turbine rotor and generator, already discussed in Sections 5.1.2 and 5.1.1.
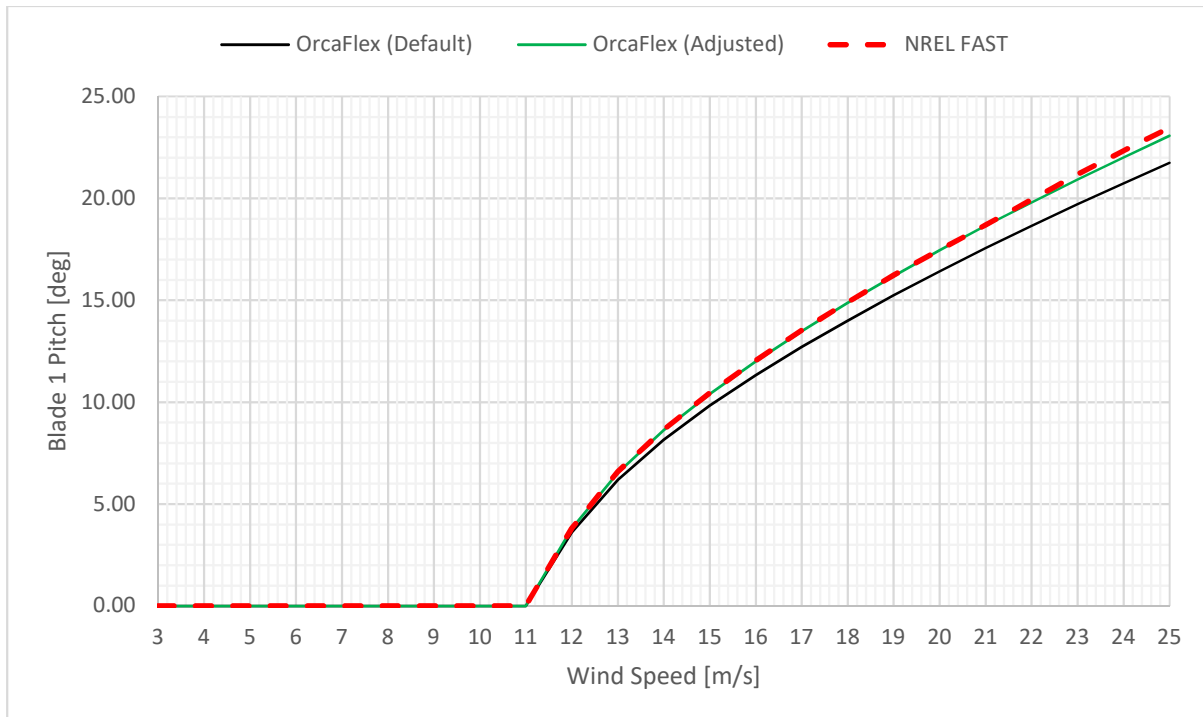
Figure 33 – Blade 1 Pitch Results Comparison (Adjusted)

Figure 34 below displays the OrcaFlex vs FAST results comparison for the average Blade 1 tip *out-of-plane* deflection. Above the rated wind speed of 11.4m/s (Region 3), where the blade pitch controller is active, the 'default' OrcaFlex model indicated a difference between the FAST and OrcaFlex results; which steadily increased with increasing wind speed. Consideration of the adjusted OrcaFlex model resulted in improved agreement between the calculated results.
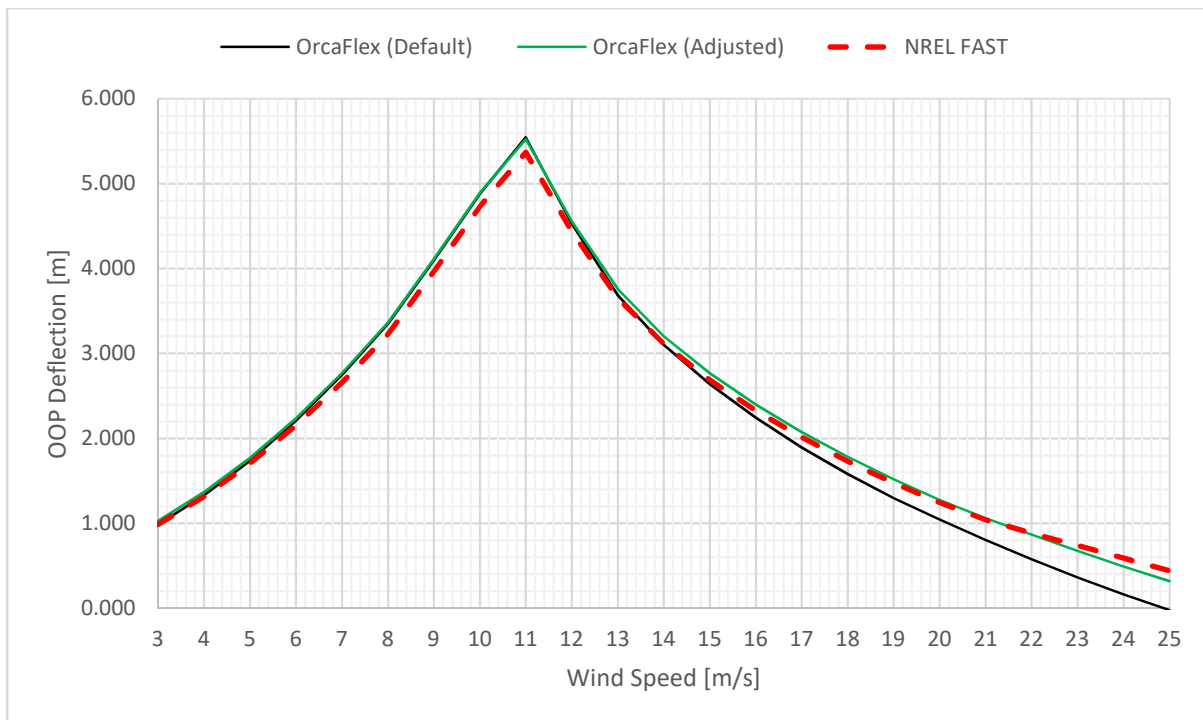
Figure 34 – Average Blade 1 Out-of-Plane Tip Deflection Results Comparison

Figure 35 displays the OrcaFlex vs FAST results comparison for the Blade 1 tip *in-plane* deflection. For the operational wind speed range, the plots display a noticeable difference between the calculated results; particularly above the rated wind speed of 11.4m/s. Once again, consideration of the adjusted OrcaFlex model resulted in closer agreement between the calculated results.

Although the observed trends are very similar, a noticeable difference remains in the numerical results between the two codes. It is thought that general numerical instability in the FAST calculations, evident by the slightly erratic nature of the curve presented in Figure 35, may be contributing to these general differences.

Lastly, the tip speed ratio response indicated very close agreement between the calculated FAST results and both OrcaFlex models covering the default & adjusted cases (see Figure 36). This close correlation between results can be attributed to the TSR behaviour being predominantly dependent on the rotor response, as opposed to the blade pitch response.
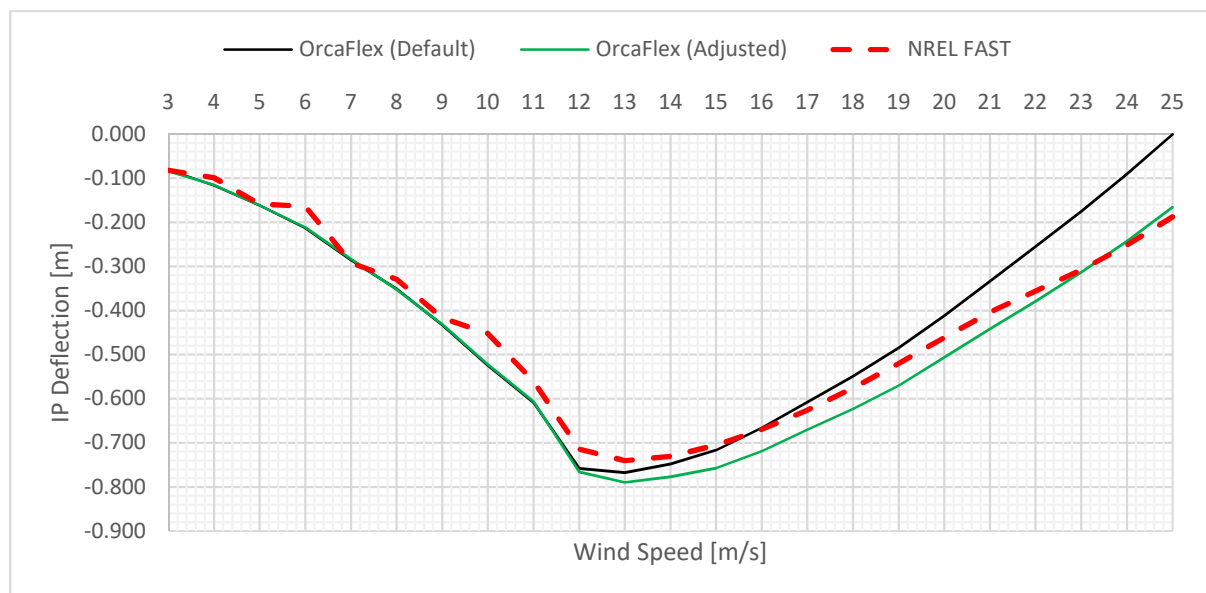
Figure 35 – Average Blade 1 In-Plane Tip Deflection Results Comparison
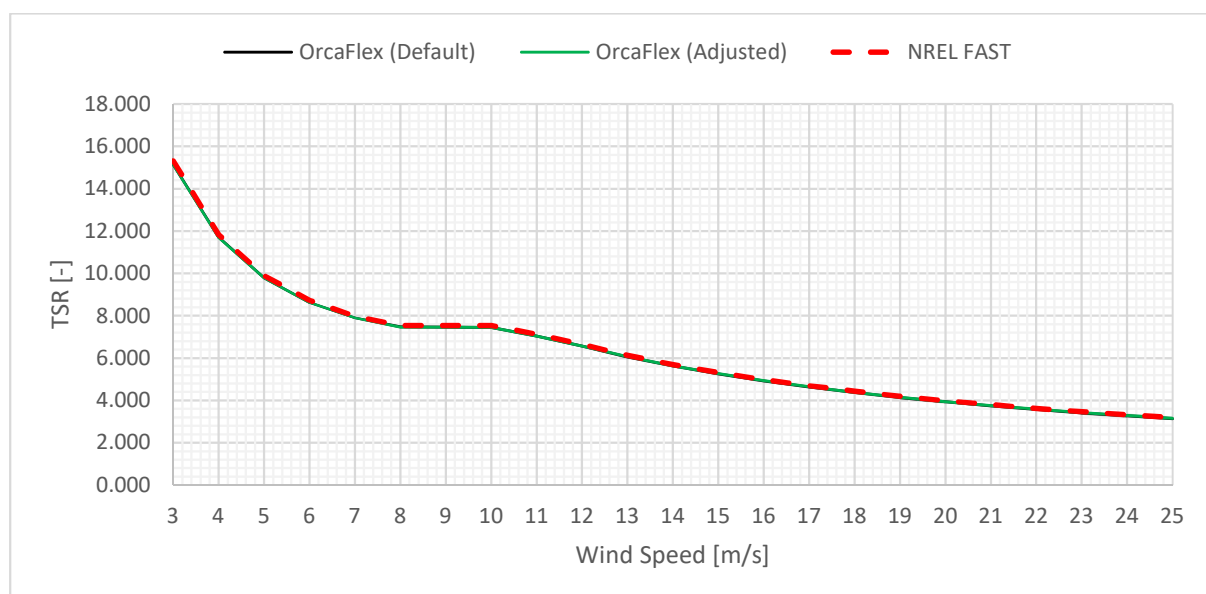
Figure 36 – TSR Results Comparison

5.1.4. Average Tower Top Deflection Results Comparison

Figure 37 and Figure 38 display the OrcaFlex vs FAST results comparison for the tower average fore-aft and side-to-side deflections, respectively. The tower deflection response, in both directions, indicated a minor dependence on the pitch response of the turbine blades. When considering the adjusted OrcaFlex model, a closer agreement between the calculated results was observed.
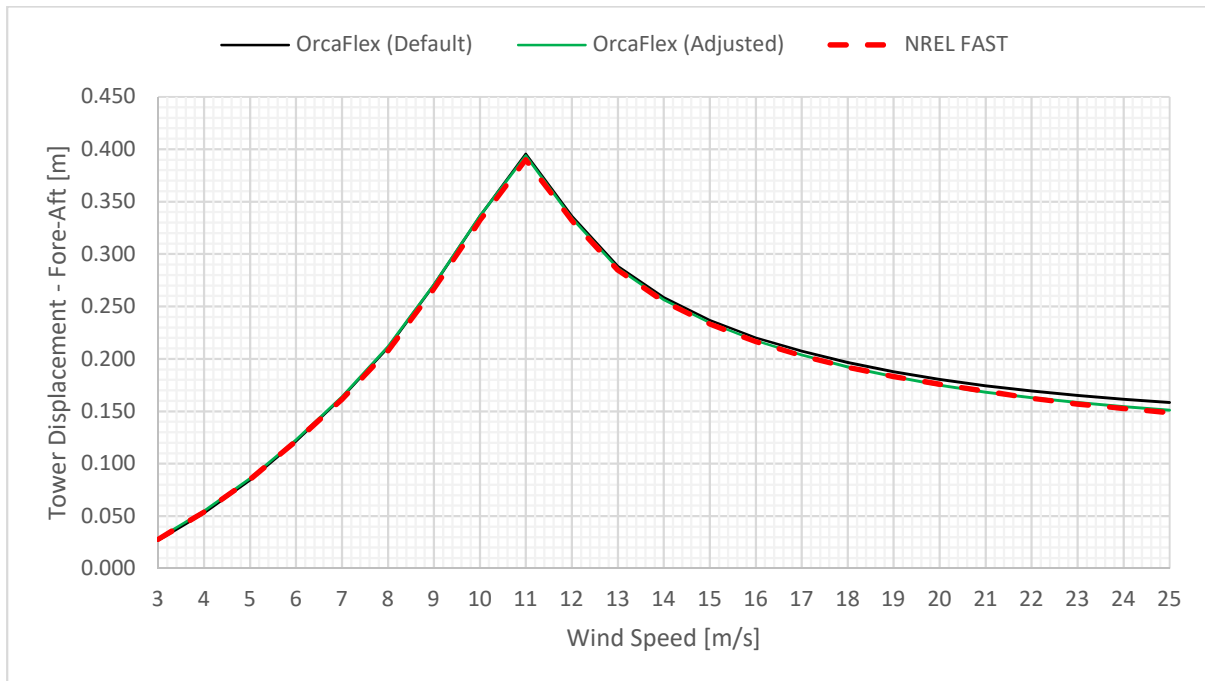
Figure 37 – Average Tower Top Fore-Aft Deflection Results Comparison
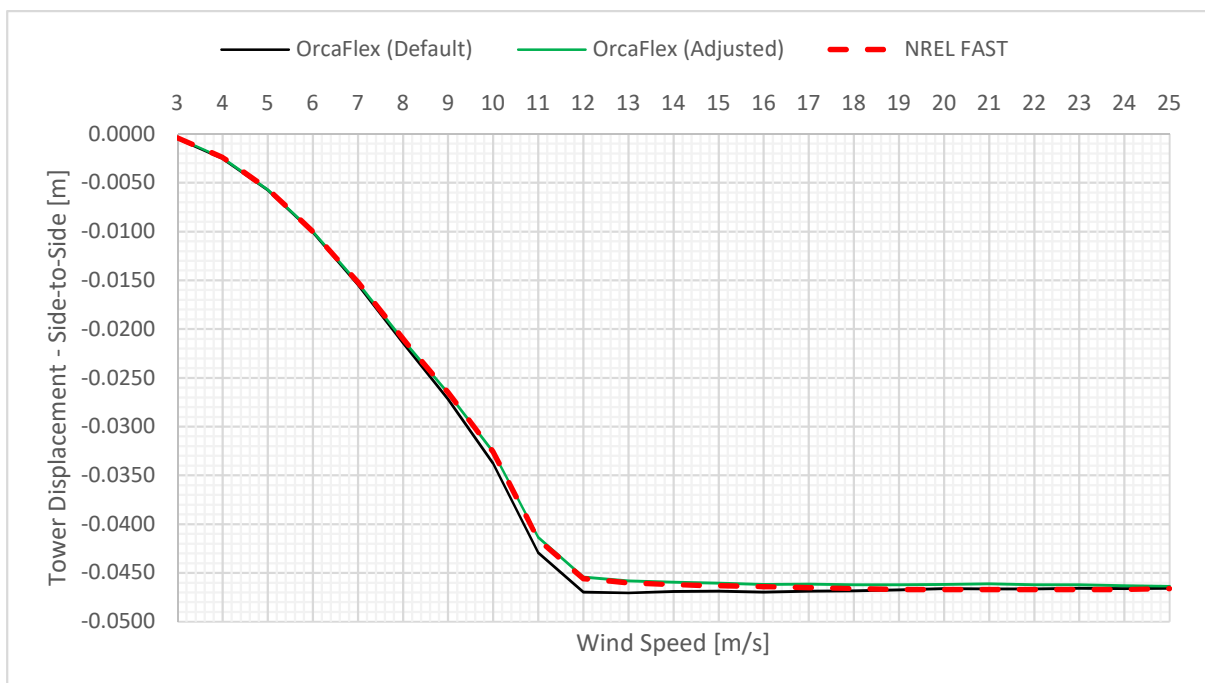
Figure 38 – Average Tower Top Side-to-Side Deflection Results Comparison

5.2. OC3 Hywind System Results

Table 24 summarises the result parameters of interest for the OC3 Hywind system, along with the corresponding results designation, as documented by NREL in [4]. The third column details the results variable(s) required to extract the corresponding results from the OrcaFlex simulation representing load case 5.1 [4].

Results Parameter	NREL Result Designation	OrcaFlex Result Variable
Rotor		
Rotor Speed	RotSpeed	Main shaft angular velocity
Rotor Torque	RotTorq	Main shaft torque
Generator		
Generator Power	GenPower	Generator power
Blade 1		
Tip Out-of-plane Deflection	OoPDefl1	*User Defined Result*
Tower Top		
Tower Top – Fore-aft Shear Force	YawBrFxp	x shear force (end A)
Tower Top – Fore-aft Deflection[†]	TTDspFA	*User Defined Result*
Mooring		
Fairlead 1 Tension	Fair1Ten	Effective tension (end A)
Fairlead 2 Tension	Fair2Ten	Effective tension (end A)
Spar Platform		
Platform Surge[*]	PtfmSurge	X
Platform Pitch[*]	PtfmPitch	Rotation 2
Platform Heave[*]	PtfmHeave	Z
Platform Yaw[*]	PtfmYaw	Rotation 3

Note:
(†) Tower deflections are measured at the tower top (End A) and are relative to the centreline of the undeflected tower.
(*) Spar platform motions are extracted from a fixed x,y,z position of 0,0,120m relative to the platform base (see Figure 44).

Table 24 – OC3 Hywind System – Result Output Parameters [4]

Of the ten analysis codes considered as part of the OC3 study [4], the results from four codes have been specifically selected for comparison against the analogous OrcaFlex results:

(1) FAST (submitted by NREL)
(2) MSC.ADAMS (submitted by NREL)
(3) GH Bladed
(4) Risø-DTU HAWC2.

The decision to consider this reduced set of codes is primarily based on the availability of the raw results corresponding to each code i.e. full results, for all results variables of interest, are available for the considered codes; whereas full results for the neglected codes were generally unavailable, at the time of writing. Furthermore, the considered codes use Morison's equation as the basis for the hydrodynamics calculations; which is the same approach adopted as part of the developed OrcaFlex model of the system.

For each result presented in Table 24, a separate chart is produced that provides a useful visual comparison between the OrcaFlex results and the corresponding results from the considered set of analysis codes. In each chart, a time history of the system response is then checked for the final 20s of the simulation (i.e. two wave passages). This also amounts to three full rotations of the turbine rotor, which is considered sufficient to assess the steady-state response of the system. This approach is consistent with that summarised in [4]. Note that the solid red curve on each chart represents the response calculated via OrcaFlex.

5.2.1. Rotor Results Comparison

Figure 39 displays the results comparison covering both the speed and torque response from the turbine rotor. For all of the considered codes, the charts display close agreement with regard to the response of the turbine rotor.

In comparison to the other codes, the magnitude of the OrcaFlex results was shown to differ by no more than 0.2rpm and 85kN.m for the rotor speed and rotor torque, respectively. In this case, the results obtained via OrcaFlex are shown to correspond particularly well with those of both FAST and ADAMS.
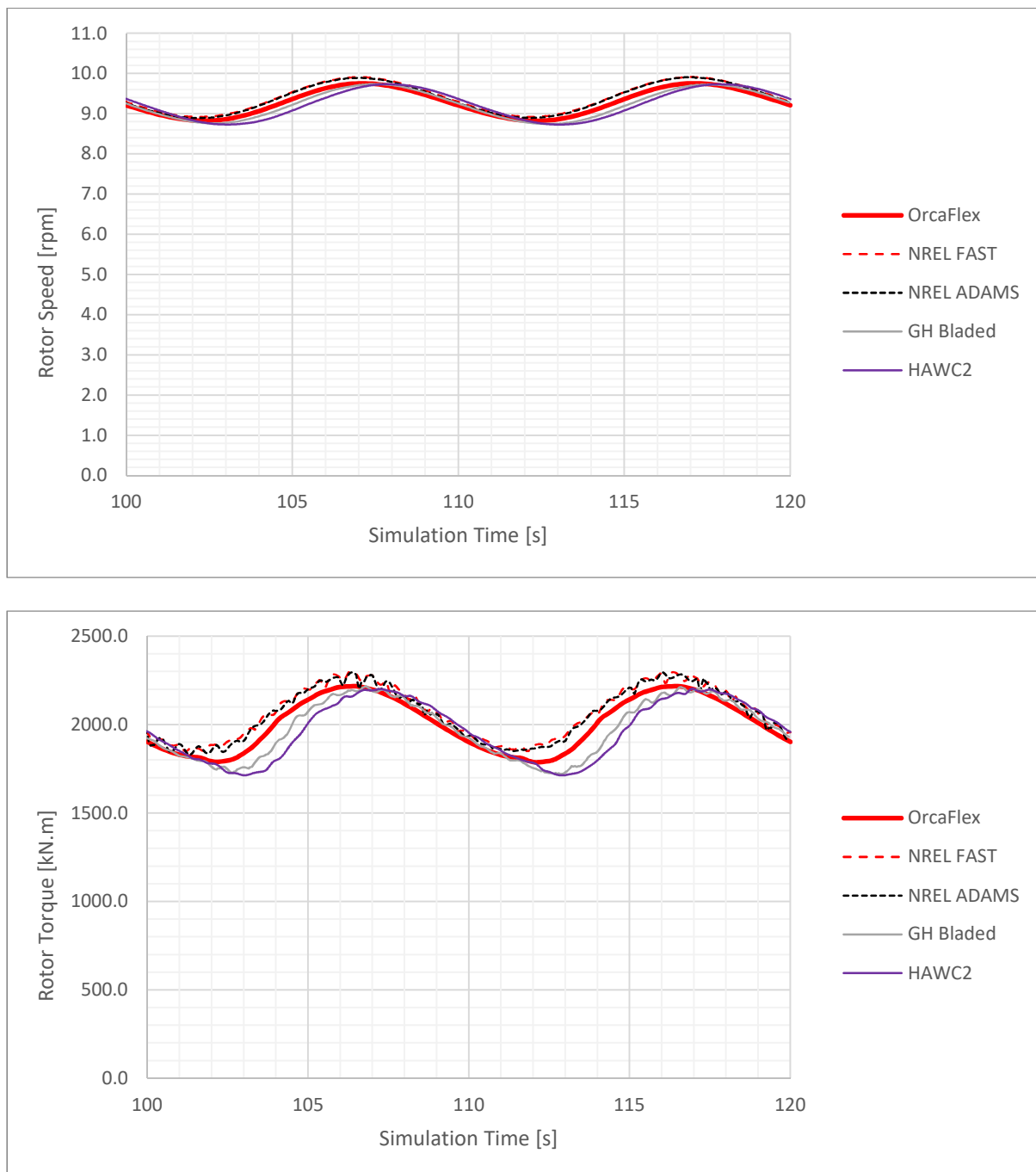
Figure 39 – Rotor Speed and Rotor Torque Results Comparisons

5.2.2. Generator Results Comparison

Figure 40 displays the comparison of results covering the generator power response from the turbine system. All of the presented results account for a generator efficiency of 94.4%. For all of the considered codes, the chart displays relatively close agreement between the amplitude and phase response of the generator.

Generally, the magnitude of the OrcaFlex results were shown to differ by no more than 0.1MW in comparison to the other codes; which represents 2% of the rated turbine power (5MW). The amplitude of the response, calculated via OrcaFlex, is shown to correspond particularly well with the GH Bladed and HAWC2 results, whereas the phase of the response matches more closely to the NREL codes.
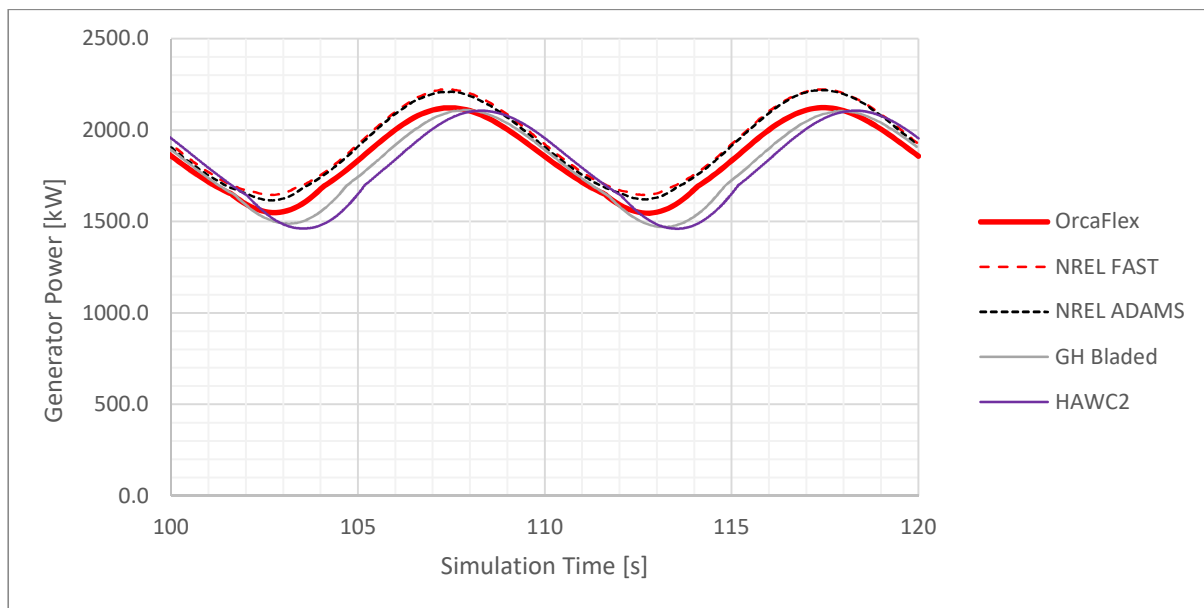
Note:
Results consider a generator efficiency of 94.4%

Figure 40 – Generator Power Results Comparison

5.2.3. Blade Tip Deflection Results Comparison

The blade tip out-of-plane deflection results, determined for Blade 1, are shown in Figure 41. The chart displays very close agreement between the mean blade tip deflection values; where the mean deflection calculated via OrcaFlex (3.39m) was shown to compare well with FAST, ADAMS & GH Bladed; which all reported mean deflection values of 3.30m, 3.21m & 3.29m, respectively. The minor differences observed in the results are attributed to inherent differences in the blade structural model considered as part of each analysis code.

It is worth highlighting that, after further investigation, the FAST and GH Bladed models of the system were found to consider only blade bending. The ADAMS and HAWC2 models considered axial, torsion and shear DOFs as part of the blade structural model; which is akin to the blade model adopted by OrcaFlex.

At the considered wind speed (8m/s), the turbine operates in Region 1 (see Figure 14), where the rotor *torque* controller is active. From the results presented for the land-based turbine, differences in blade tip deflection were only observed above the rated wind speed (Region 3) where the blade *pitch* controller is active. Therefore, the considered blade degrees-of-freedom were found to have little impact on the blade response, in this case.

To demonstrate this further, the blade torsional and axial stiffness properties were once again modified to assign an arbitrarily high stiffness value of $1 \times 10^9 kN.m^2$ to the OC3 Hywind model; thus, artificially eliminating these degrees-of-freedom. Figure 41 includes an additional curve named 'OrcaFlex (Adjusted)', coloured green, which represents the out-of-plane deflection of the blade tip after making this modification. The mean deflection response of the blade tip was 3.40m, which closely agrees with the other codes.

Lastly, it should also be noted that, from information provided in [4], Figure 41 excludes any results from HAWC2, due to an assumed error in the results submitted as part of the OC3 study.
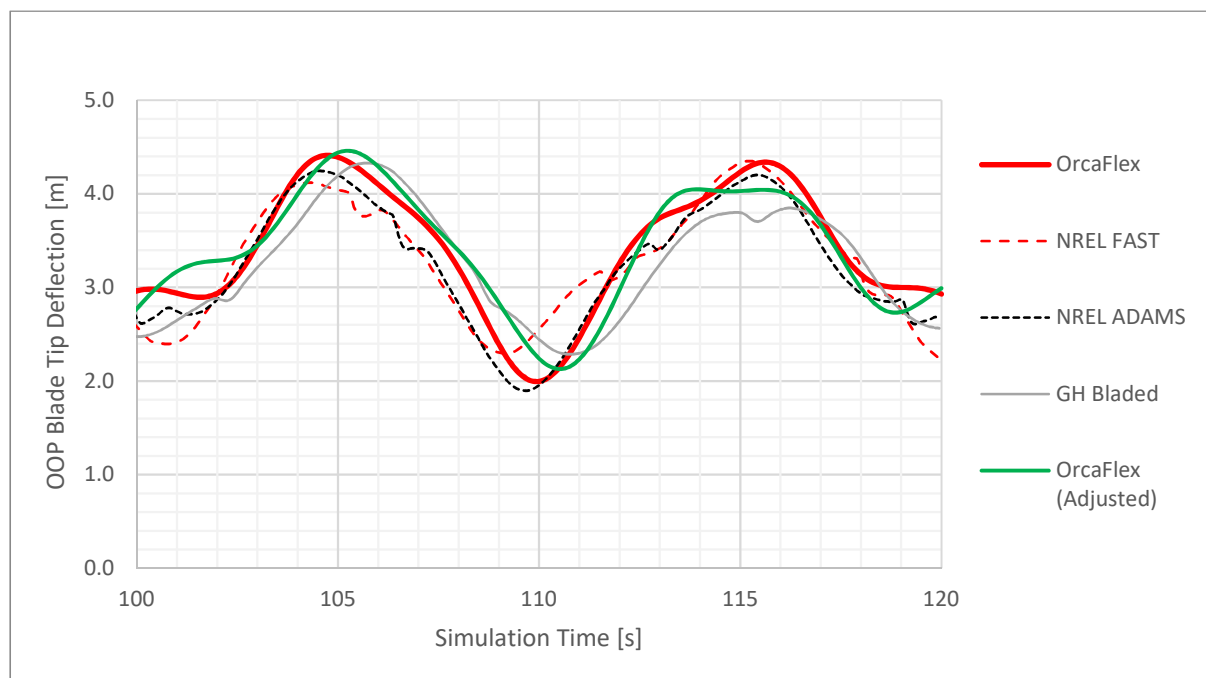
Figure 41 – Blade 1 Out-of-Plane Tip Deflection Results Comparison

5.2.4. Tower Top Results Comparison

Figure 42 displays the tower top shear force and fore-aft deflection results calculated by the various codes. For the tower top shear force, the chart displays relatively close agreement between the mean shear force values; where the mean force calculated via OrcaFlex (559.6kN) is shown to match relatively closely with FAST, ADAMS, and HAWC2; which all report mean shear force values of 577.0kN, 569.9kN and 551.8kN, respectively. The exception to this is GH Bladed, which predicts a slightly lower mean tower shear force of 521.7kN.

A similar trend was observed for the tower top fore-aft deflection, where the mean deflections calculated by the codes are all in relatively close agreement (0.24–0.25m). Again, the exception to this is GH Bladed, which predicted a significantly lower mean tower deflection of 0.10m.

Generally, the tower top deflection and shear force responses predicted by OrcaFlex are shown to correspond particularly well with the NREL codes.
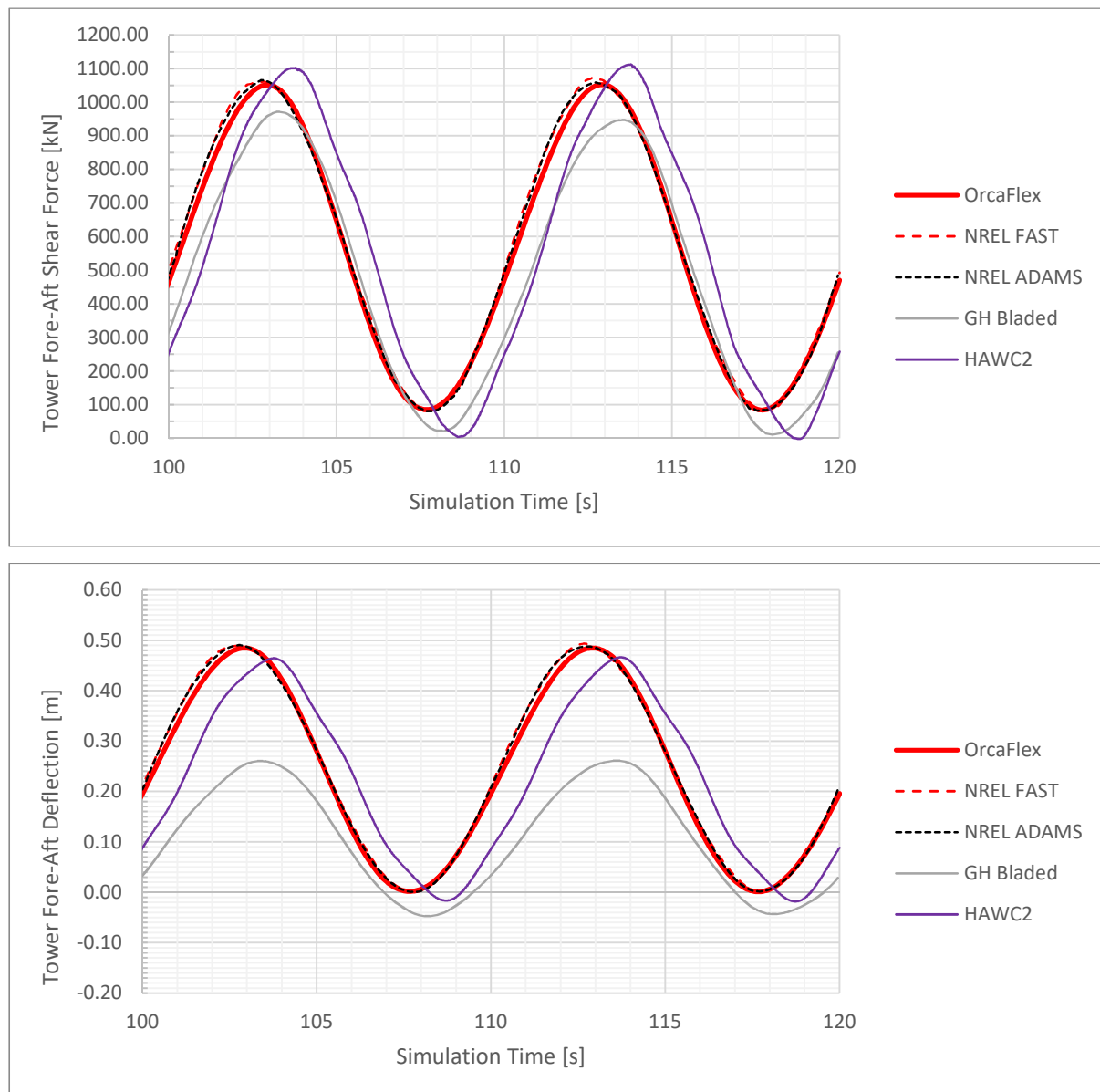
Figure 42 – Tower Top Fore-Aft Deflection and Tower Top Shear Force Results Comparisons

5.2.5. Mooring Results Comparison

Figure 43 compares the calculated fairlead tension results for mooring lines 1 and 2. Overall, the results observed for fairlead 1 show close agreement between the codes; with differences in magnitude observed to be minimal (< 2kN). More specifically, the tension predicted by OrcaFlex corresponds very well with the amplitude and phase response determined via NREL ADAMS.

Although there is close agreement between the results reported at fairlead 1, the mean tension predicted by HAWC2 at fairlead 2 is approximately 7–8kN higher in magnitude than the tension estimated by the OrcaFlex and NREL codes. In this case, the tension predicted by OrcaFlex matches very closely with the results determined via both NREL codes (FAST and ADAMS).

It is worth highlighting that the calculated fairlead tensions demonstrate a logical dependence on the surge motion of the spar platform. When comparing the fairlead tension results against the spar platform surge results (shown in Figure 46), the tension observed at fairlead 1 is shown to decrease and increase as the platform surges forward and aft, respectively. Conversely, the tension at fairlead 2 increases and decreases as a result of the same respective platform surge motions.

Lastly, it should be noted that Figure 43 excludes any results from GH Bladed, which were not submitted as part of the OC3 study [4].
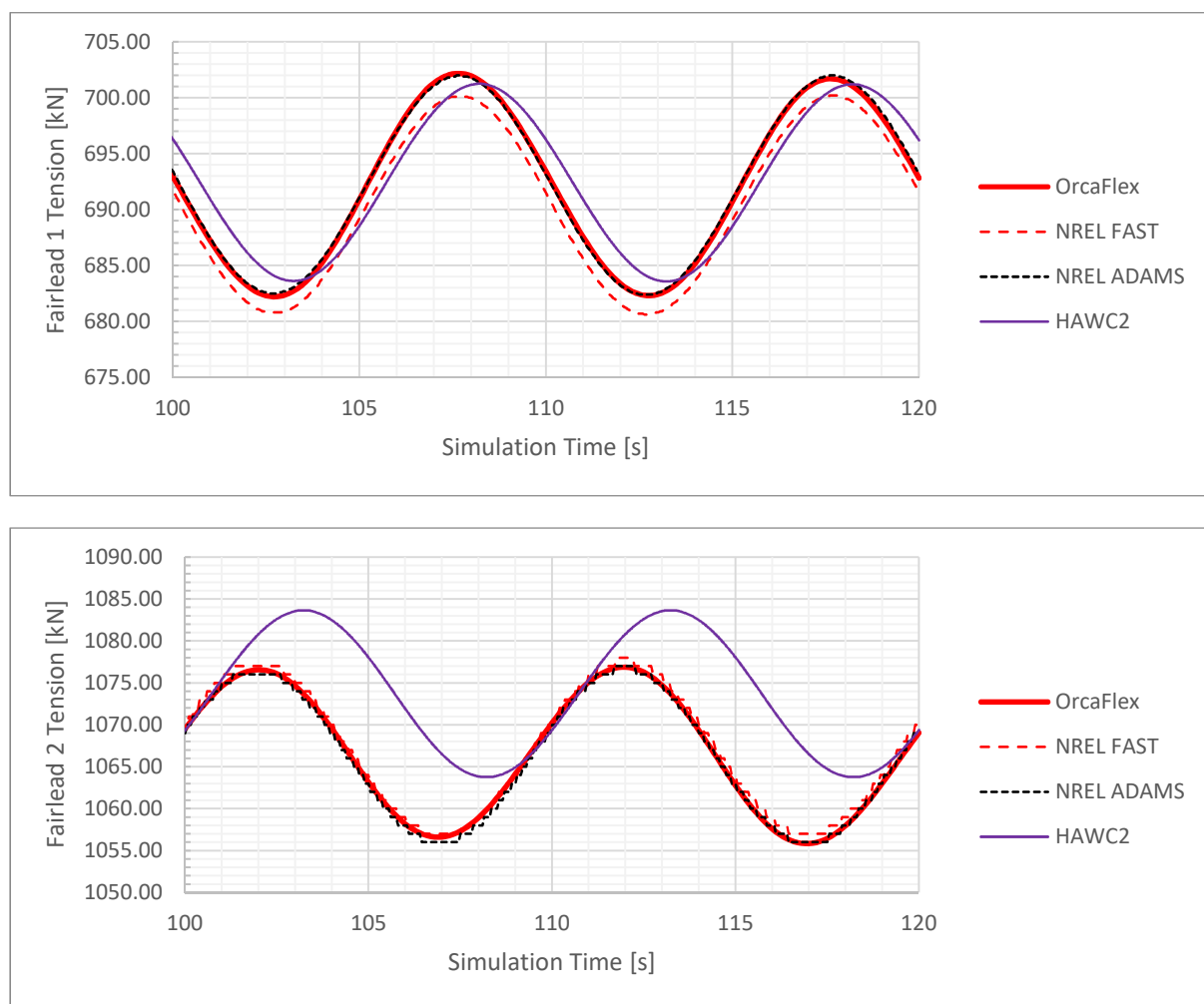
Figure 43 – Fairlead Tension Results Comparisons

5.2.6. Spar Platform Results Comparison

The motions of the spar platform are extracted from the OrcaFlex model at a fixed position on the spar buoy: x,y,z position of 0,0,120m relative to the local axis system (located at the platform base). This represents the point at which the centreline of the spar intersects the still water level when the system is in its undisplaced (static) position. This is illustrated in Figure 44 along with the conventions used to define the positive surge, pitch, heave and yaw motions of the spar platform.
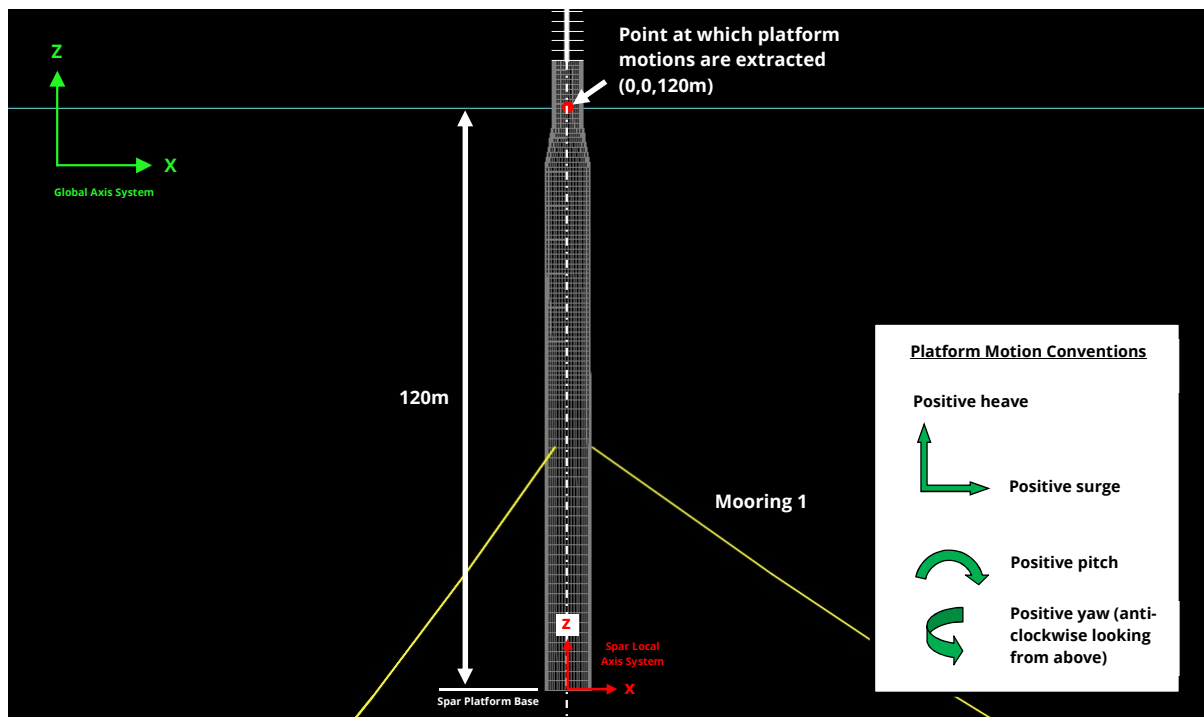
Figure 44 – Position for Platform Motion Extraction

Spar Platform Surge

Within the OrcaFlex simulation of the OC3 Hywind system, the spar platform starts at a global X position of 0m (in its static state). Over the course of the simulation, the influence of environmental loading on the system causes the spar to drift before restraint from the mooring system allows the platform surge to settle to a mean position of X=13.51m. Further illustration of this behaviour is shown in Figure 45 and the behaviour is also evident in the results presented in Figure 46.

Figure 46 displays the surge response of the spar platform, as calculated by the various codes. The mean platform surge response determined via OrcaFlex (13.51m) shows very close agreement with the NREL codes, which estimate mean surge values of 13.54m and 13.37m for the FAST and ADAMS codes, respectively. Furthermore, the phase and amplitude of the oscillations observed in the OrcaFlex results match very well with the NREL codes.

Significant differences were observed in the surge response calculated via GH Bladed and HAWC2. Although the amplitude of the GH Bladed results is similar to OrcaFlex, and the NREL codes, the observed mean surge is significantly lower (7.2m).
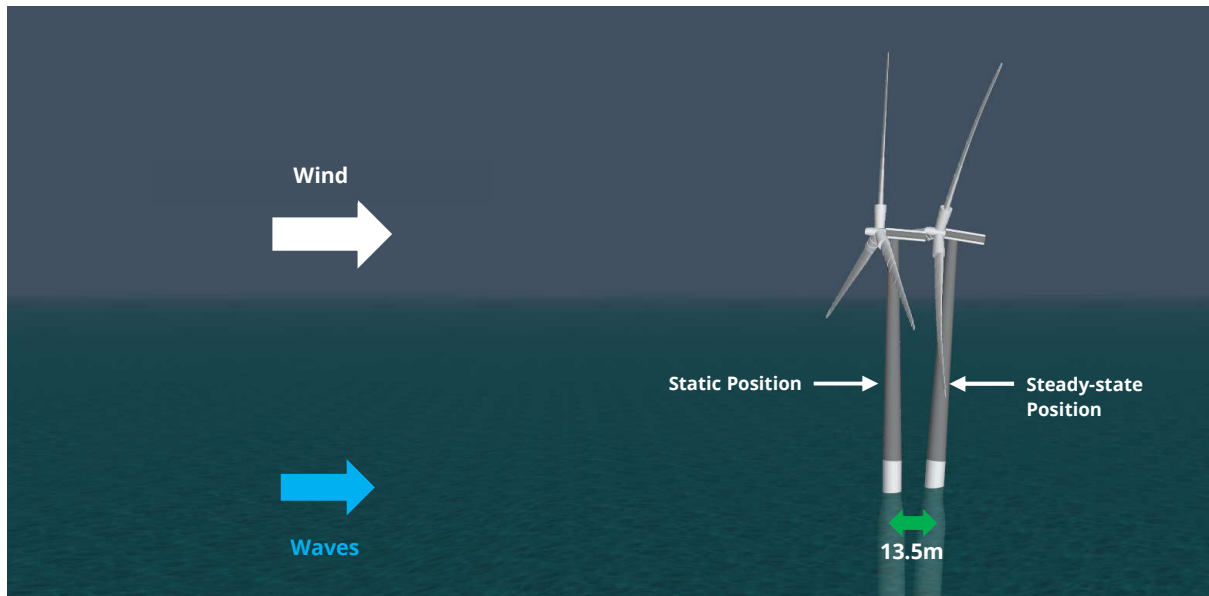
Figure 45 – OC3 Hywind Surge Response in OrcaFlex
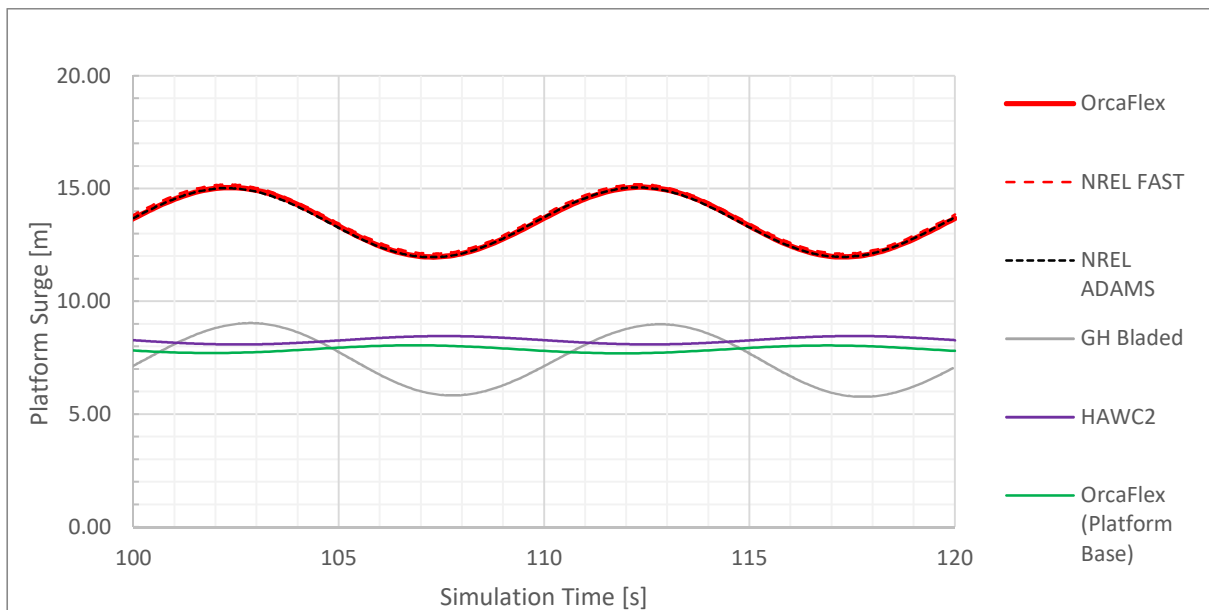
Figure 46 – Spar Platform Surge Results Comparison

The mean surge predicted by HAWC2 is also markedly lower (8.3m). Furthermore, the amplitude of the surge response is significantly lower than the responses predicted by the other codes. This difference may be attributed to the position at which the spar platform motions were extracted from the HAWC2 model. For example, if the motions were extracted from the base of the platform, as opposed to the still water level, this would automatically eliminate any additional surge contribution brought about by pitch-induced lever arm effects.

To illustrate this, an additional curve has been added to Figure 46 (coloured green), which considers the surge response at the *base* of the platform in OrcaFlex i.e. at an x,y,z position of 0,0,0m relative to the local axis system of the spar buoy (see Figure 44). When accounting for this difference, a marked improvement is seen in the correlation between the OrcaFlex and HAWC2 results.

Spar Platform Pitch

Figure 47 displays the pitch response of the spar platform, as calculated by the various codes. The mean pitch response determined via OrcaFlex (2.69°) shows very close agreement with the NREL codes, which estimate mean pitch values of 2.75° & 2.71° for the FAST & ADAMS codes, respectively. Furthermore, the phase and amplitude of the oscillations observed in the OrcaFlex results match very closely with the NREL codes.

A mean platform pitch of 2.59° is observed for the HAWC2 results. Unlike the platform surge response, the pitch response of the rigid-body spar does not depend on the position at which the spar platform motions are extracted. As a result, the response from the HAWC2 results match reasonably well with the OrcaFlex and NREL codes.

Once again, significant differences were observed in the platform response calculated via GH Bladed. Although the amplitude of the GH Bladed results is similar to OrcaFlex, FAST and ADAMS, the observed mean pitch is noticeably lower (1.35°). This response may have directly impacted the lower predicted mean tower top fore-aft shear force and deflection results, discussed in Section 5.2.4.
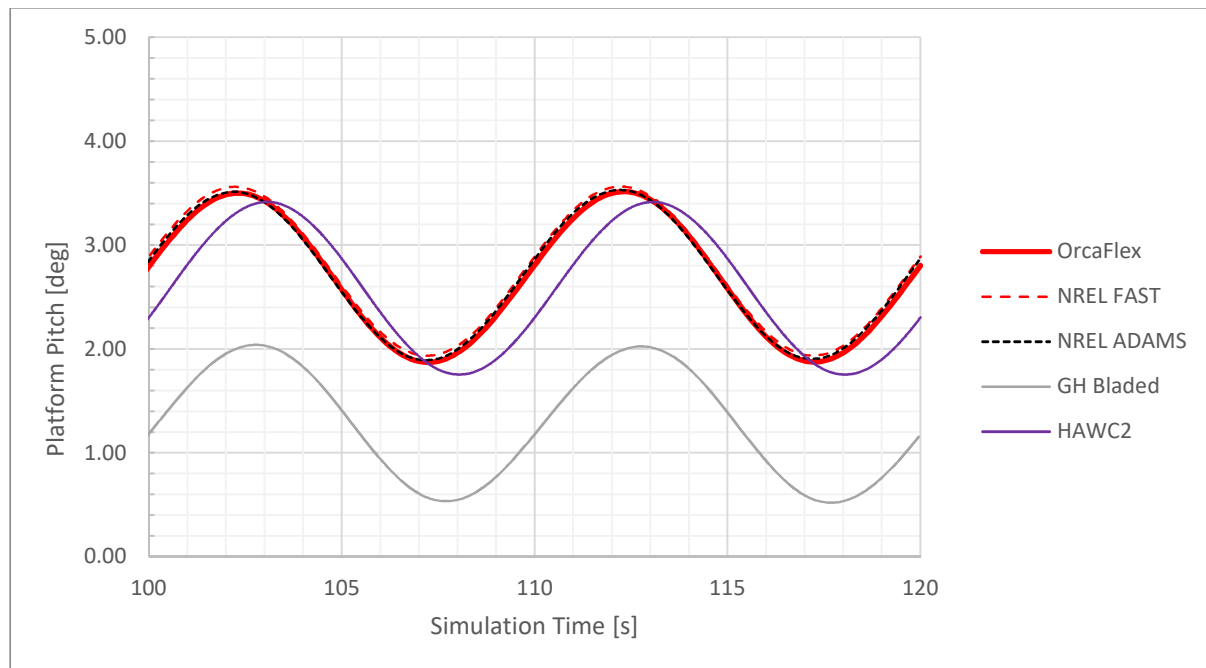
Figure 47 – Spar Platform Pitch Results Comparison

Spar Platform Heave

The calculated heave response of the spar platform, from the various codes, is shown in Figure 48. The mean heave response predicted by OrcaFlex (–0.15m) corresponds particularly well with the HAWC2 mean response (–0.14m). Although the NREL codes predict a slightly lower mean heave (–0.22m), the phase and amplitude of the OrcaFlex results match reasonably well with FAST and ADAMS.

Once again, the platform response determined via GH Bladed was shown to differ from the other codes, with slightly higher heave fluctuations resulting in a reduced mean spar heave response of –0.04m.
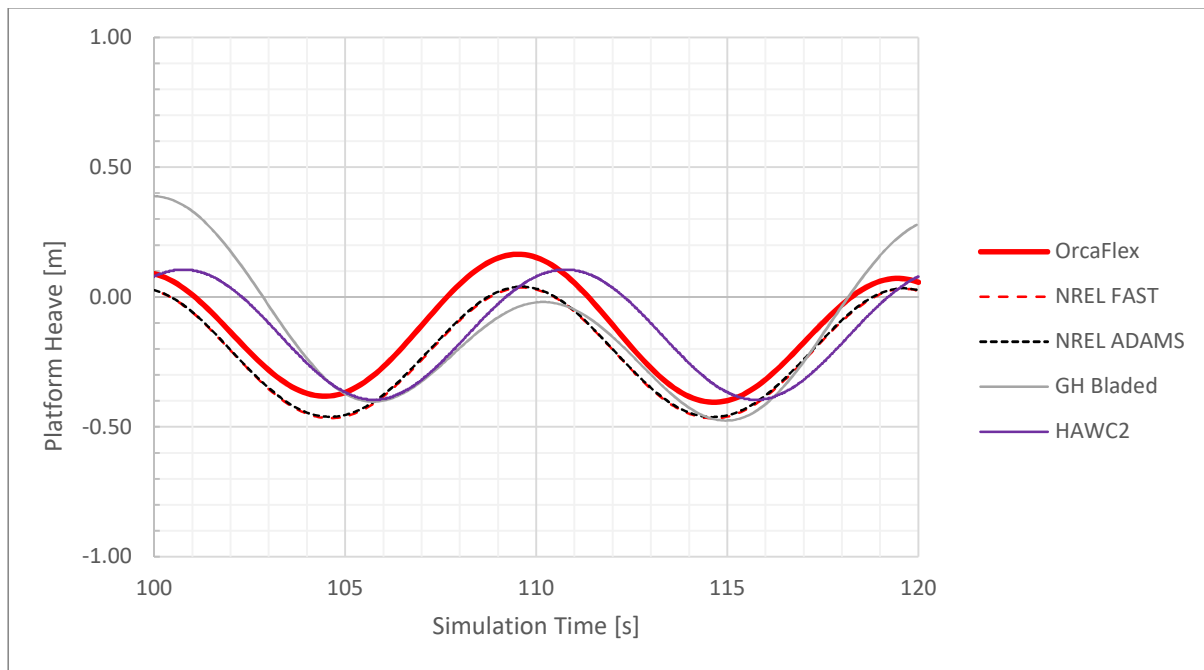
Figure 48 – Spar Platform Heave Results Comparison

Spar Platform Yaw

Lastly, Figure 49 summarises the yaw response of the spar platform. To remain consistent with the other codes, the presented OrcaFlex results account for the influence of the nominal yaw spring stiffness from the mooring system (summarised in Section 4.5.2).

From information provided in [4], the considered main shaft tilt of 5° causes some of the rotor torque to act about the yaw axis of the floating system. As a result, a non-zero mean yaw response was observed in the codes considered as part of the OC3 Phase IV study. Similar behaviour was observed in the OrcaFlex model of the system, where a mean platform yaw response of –0.13° was observed. This result corresponds particularly well with the ADAMS mean response of –0.12°.

The oscillations observed in the responses from the various codes are believed to be caused by a combination of platform pitch motion, in conjunction with rotor inertia. As a result, the observed yaw responses are shown to differ slightly between the codes. Furthermore, inherent differences in the approach taken to augment the mooring yaw spring stiffness may be contributing to the minor inconsistencies between the considered results.
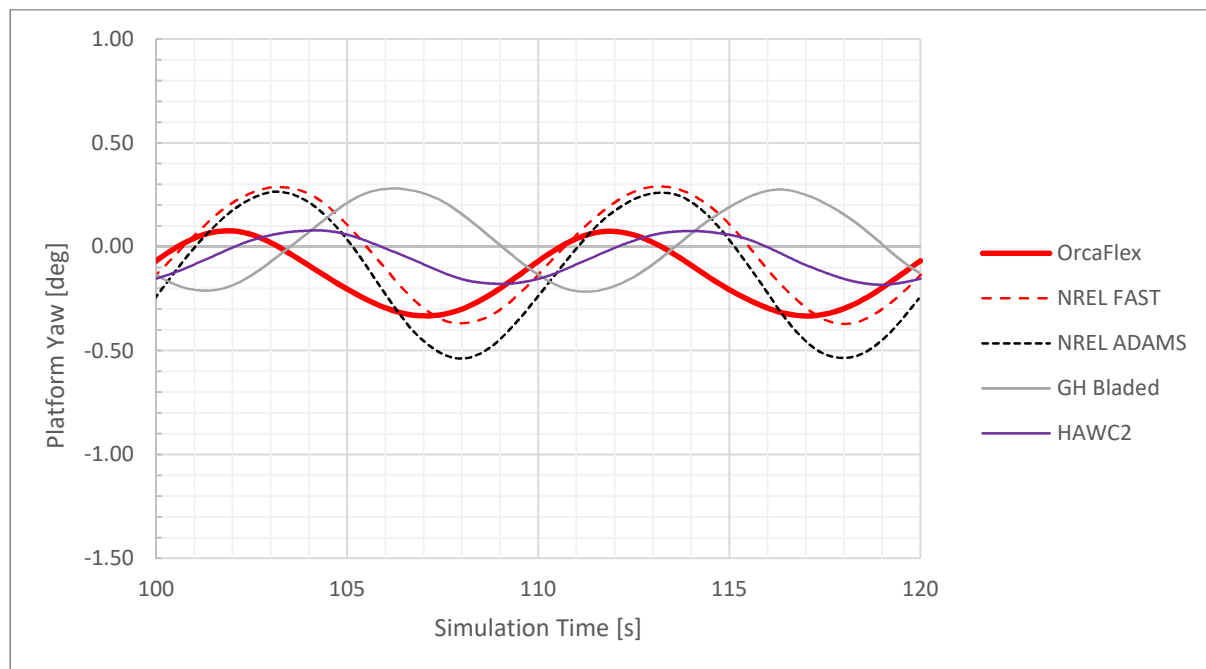
Figure 49 – Spar Platform Yaw Results Comparison

Appendix A – NREL 5-MW Wind Turbine – Blade Data

A.1. NREL Blade Physical Properties

Radius (m)	BlFract	AeroCent	PitchAxis	AeroRef	StrcTwst (°)	BMassDen (kg/m)	FlpStff (N.m²)	EdgStff (N.m²)	EAStff (N)	GJStff (N.m²)	EdgcgOf (m)
1.500	0.000	0.250	0.500	0.500	13.308	678.935	18110000000	18113600000	9729480000	5564400000	0.000
1.700	0.003	0.250	0.500	0.500	13.308	678.935	18110000000	18113600000	9729480000	5564400000	0.000
2.700	0.020	0.250	0.500	0.499	13.308	773.363	19424900000	19558600000	10789500000	5431590000	-0.023
3.700	0.036	0.245	0.495	0.490	13.308	740.550	17455900000	19497800000	10067230000	4993980000	0.003
4.700	0.052	0.233	0.483	0.466	13.308	740.042	15287400000	19788800000	9867780000	4666590000	0.043
5.700	0.068	0.221	0.471	0.441	13.308	592.496	10782400000	14858500000	7607860000	3474710000	0.059
6.700	0.085	0.208	0.458	0.417	13.308	450.275	7229720000	10220600000	5491260000	2323540000	0.065
7.700	0.101	0.196	0.446	0.392	13.308	424.054	6309540000	9144700000	4971300000	1907870000	0.077
8.700	0.117	0.184	0.434	0.368	13.308	400.638	5528360000	8063160000	4493950000	1570360000	0.084
9.700	0.133	0.172	0.422	0.343	13.308	382.062	4980060000	6884440000	4034800000	1158260000	0.102
10.700	0.150	0.159	0.409	0.319	13.308	399.655	4936840000	7009180000	4037290000	1002120000	0.108
11.700	0.166	0.147	0.397	0.294	13.308	426.321	4691660000	7167680000	4169720000	855900000	0.158
12.700	0.182	0.135	0.385	0.270	13.181	416.820	3949460000	7271660000	4082350000	672270000	0.222
13.700	0.198	0.125	0.375	0.250	12.848	406.186	3386520000	7081700000	4085970000	547490000	0.308
14.700	0.215	0.125	0.375	0.250	12.192	381.420	2933740000	6244530000	3668340000	448840000	0.304
15.700	0.231	0.125	0.375	0.250	11.561	352.822	2568960000	5048960000	3147670000	335920000	0.265
16.700	0.247	0.125	0.375	0.250	11.072	349.477	2388650000	4948490000	3011580000	311350000	0.259
17.700	0.263	0.125	0.375	0.250	10.792	346.538	2271990000	4808020000	2882620000	291940000	0.250
19.700	0.296	0.125	0.375	0.250	10.232	339.333	2050050000	4501400000	2613970000	261000000	0.232
21.700	0.328	0.125	0.375	0.250	9.672	330.004	1828250000	4244070000	2357480000	228820000	0.204
23.700	0.361	0.125	0.375	0.250	9.110	321.990	1588710000	3995280000	2146860000	200750000	0.199
25.700	0.393	0.125	0.375	0.250	8.534	313.820	1361930000	3750760000	1944090000	174380000	0.193
27.700	0.426	0.125	0.375	0.250	7.932	294.734	1102380000	3447140000	1632700000	144470000	0.150
29.700	0.459	0.125	0.375	0.250	7.321	287.120	875800000	3139070000	1432400000	119980000	0.154
31.700	0.491	0.125	0.375	0.250	6.711	263.343	681300000	2734240000	1168760000	81190000	0.133
33.700	0.524	0.125	0.375	0.250	6.122	253.207	534720000	2554870000	1047430000	69090000	0.133
35.700	0.556	0.125	0.375	0.250	5.546	241.666	408900000	2334030000	922950000	57450000	0.140
37.700	0.589	0.125	0.375	0.250	4.971	220.638	314540000	1828730000	760820000	45920000	0.140
39.700	0.621	0.125	0.375	0.250	4.401	200.293	238630000	1584100000	648030000	35980000	0.151
41.700	0.654	0.125	0.375	0.250	3.834	179.404	175880000	1323360000	539700000	27440000	0.174
43.700	0.686	0.125	0.375	0.250	3.332	165.094	126010000	1183680000	531150000	20900000	0.249
45.700	0.719	0.125	0.375	0.250	2.890	154.411	107260000	1020160000	460010000	18540000	0.260
47.700	0.751	0.125	0.375	0.250	2.503	138.935	90880000	797810000	375750000	16280000	0.226
49.700	0.784	0.125	0.375	0.250	2.116	129.555	76310000	709610000	328890000	14530000	0.228
51.700	0.816	0.125	0.375	0.250	1.730	107.264	61050000	518190000	244040000	9070000	0.206
53.700	0.849	0.125	0.375	0.250	1.342	98.776	49480000	454870000	211600000	8060000	0.217
55.700	0.881	0.125	0.375	0.250	0.954	90.248	39360000	395120000	181520000	7080000	0.228
56.700	0.898	0.125	0.375	0.250	0.760	83.001	34670000	353720000	160250000	6090000	0.231
57.700	0.914	0.125	0.375	0.250	0.574	72.906	30410000	304730000	109230000	5750000	0.148
58.700	0.930	0.125	0.375	0.250	0.404	68.772	26520000	281420000	100080000	5330000	0.153
59.200	0.938	0.125	0.375	0.250	0.319	66.264	23840000	261710000	92240000	4940000	0.154
59.700	0.946	0.125	0.375	0.250	0.253	59.340	19630000	158810000	63230000	4240000	0.095
60.200	0.954	0.125	0.375	0.250	0.216	55.914	16000000	137880000	53320000	3660000	0.090
60.700	0.963	0.125	0.375	0.250	0.178	52.484	12830000	118790000	44530000	3130000	0.086
61.200	0.971	0.125	0.375	0.250	0.140	49.114	10080000	101630000	36900000	2640000	0.080
61.700	0.979	0.125	0.375	0.250	0.101	45.818	7550000	85070000	29920000	2170000	0.071
62.200	0.987	0.125	0.375	0.250	0.062	41.669	4600000	64260000	21310000	1580000	0.054
62.700	0.995	0.125	0.375	0.250	0.023	11.453	250000	6610000	4850000	250000	0.054
63.000	1.000	0.125	0.375	0.250	0.000	10.319	170000	5010000	3530000	190000	0.052

A.2.   Aerofoil Data: Cylinder 1

Angle of Attack [deg]	Lift	Drag	Moment
-180	0.00	0.50	0.00
0	0.00	0.50	0.00
180	0.00	0.50	0.00

A.3.   Aerofoil Data: Cylinder 2

Angle of Attack [deg]	Lift	Drag	Moment
-180	0.00	0.35	0.00
0	0.00	0.35	0.00
180	0.00	0.35	0.00

A.4. Aerofoil Data: DU40_A17

Angle of Attack [deg]	Lift	Drag	Moment	Angle of Attack [deg]	Lift	Drag	Moment	Angle of Attack [deg]	Lift	Drag	Moment	Angle of Attack [deg]	Lift	Drag	Moment
-180	0	0.0602	0	-21	-0.706	0.2049	0.1215	4.5	0.776	0.0122	-0.0933	25	1.872	0.6141	-0.1664
-175	0.218	0.0699	0.0934	-20	-0.685	0.1861	0.1162	5	0.841	0.0125	-0.0947	26	1.881	0.6593	-0.1724
-170	0.397	0.1107	0.1697	-19	-0.662	0.1687	0.1097	5.5	0.904	0.0129	-0.0957	28	1.894	0.7513	-0.1841
-160	0.642	0.3045	0.2813	-18	-0.635	0.1533	0.1012	6	0.967	0.0135	-0.0967	30	1.904	0.8441	-0.1954
-155	0.715	0.4179	0.3208	-17	-0.605	0.1398	0.0907	6.5	1.027	0.0144	-0.0973	32	1.915	0.9364	-0.2063
-150	0.757	0.5355	0.3516	-16	-0.571	0.1281	0.0784	7	1.084	0.0158	-0.0972	35	1.929	1.0722	-0.222
-145	0.772	0.6535	0.3752	-15	-0.534	0.1183	0.0646	7.5	1.14	0.0174	-0.0972	40	1.903	1.2873	-0.2468
-140	0.762	0.7685	0.3926	-14	-0.494	0.1101	0.0494	8	1.193	0.0198	-0.0968	45	1.82	1.4796	-0.2701
-135	0.731	0.8777	0.4048	-13	-0.452	0.1036	0.033	8.5	1.242	0.0231	-0.0958	50	1.69	1.6401	-0.2921
-130	0.68	0.9788	0.4126	-12	-0.407	0.0986	0.0156	9	1.287	0.0275	-0.0948	55	1.522	1.7609	-0.3127
-125	0.613	1.07	0.4166	-11	-0.36	0.0951	-0.0026	9.5	1.333	0.0323	-0.0942	60	1.323	1.836	-0.3321
-120	0.532	1.1499	0.4176	-10	-0.311	0.0931	-0.0213	10	1.368	0.0393	-0.0926	65	1.106	1.8614	-0.3502
-115	0.439	1.2174	0.4158	-8	-0.208	0.093	-0.06	10.5	1.4	0.0475	-0.0908	70	0.88	1.8347	-0.3672
-110	0.337	1.2716	0.4117	-6	-0.111	0.0689	-0.05	11	1.425	0.058	-0.089	75	0.658	1.7567	-0.383
-105	0.228	1.3118	0.4057	-5.5	-0.09	0.0614	-0.0516	11.5	1.449	0.0691	-0.0877	80	0.449	1.6334	-0.3977
-100	0.114	1.3378	0.3979	-5	-0.072	0.0547	-0.0532	12	1.473	0.0816	-0.087	85	0.267	1.4847	-0.4112
-95	-0.002	1.3492	0.3887	-4.5	-0.065	0.048	-0.0538	12.5	1.494	0.0973	-0.087	90	0.124	1.3879	-0.4234
-90	-0.12	1.346	0.3781	-4	-0.054	0.0411	-0.0544	13	1.513	0.1129	-0.0876	95	0.002	1.3912	-0.4343
-85	-0.236	1.3283	0.3663	-3.5	-0.017	0.0349	-0.0554	13.5	1.538	0.1288	-0.0886	100	-0.118	1.3795	-0.4437
-80	-0.349	1.2964	0.3534	-3	0.003	0.0299	-0.0558	14.5	1.587	0.165	-0.0917	105	-0.235	1.3528	-0.4514
-75	-0.456	1.2507	0.3394	-2.5	0.014	0.0255	-0.0555	15	1.614	0.1845	-0.0939	110	-0.348	1.3114	-0.4573
-70	-0.557	1.1918	0.3244	-2	0.009	0.0198	-0.0534	15.5	1.631	0.2052	-0.0966	115	-0.453	1.2557	-0.461
-65	-0.647	1.1204	0.3084	-1.5	0.004	0.0164	-0.0442	16	1.649	0.225	-0.0996	120	-0.549	1.1864	-0.4623
-60	-0.727	1.0376	0.2914	-1	0.036	0.0147	-0.0469	16.5	1.666	0.2467	-0.1031	125	-0.633	1.1041	-0.4606
-55	-0.792	0.9446	0.2733	-0.5	0.073	0.0137	-0.0522	17	1.681	0.2684	-0.1069	130	-0.702	1.0102	-0.4554
-50	-0.842	0.8429	0.2543	0	0.137	0.0113	-0.0573	17.5	1.699	0.29	-0.111	135	-0.754	0.906	-0.4462
-45	-0.874	0.7345	0.2342	0.5	0.213	0.0114	-0.0644	18	1.719	0.3121	-0.1157	140	-0.787	0.7935	-0.4323
-40	-0.886	0.6215	0.2129	1	0.292	0.0118	-0.0718	19	1.751	0.3554	-0.1242	145	-0.797	0.675	-0.4127
-35	-0.875	0.5067	0.1906	1.5	0.369	0.0122	-0.0783	19.5	1.767	0.3783	-0.1291	150	-0.782	0.5532	-0.3863
-30	-0.839	0.3932	0.167	2	0.444	0.0124	-0.0835	20.5	1.798	0.4212	-0.1384	155	-0.739	0.4318	-0.3521
-25	-0.777	0.2849	0.1422	2.5	0.514	0.0124	-0.0866	21	1.81	0.4415	-0.1416	160	-0.664	0.3147	-0.3085
-24	-0.761	0.2642	0.1371	3	0.58	0.0123	-0.0887	22	1.83	0.483	-0.1479	170	-0.41	0.1144	-0.1858
-23	-0.744	0.244	0.132	3.5	0.645	0.012	-0.09	23	1.847	0.5257	-0.1542	175	-0.226	0.0702	-0.1022
-22	-0.725	0.2242	0.1268	4	0.71	0.0119	-0.0914	24	1.861	0.5694	-0.1603	180	0	0.0602	0

A.5. Aerofoil Data: DU35_A17

Angle of Attack [deg]	Lift	Drag	Moment	Angle of Attack [deg]	Lift	Drag	Moment	Angle of Attack [deg]	Lift	Drag	Moment	Angle of Attack [deg]	Lift	Drag	Moment
-180	0	0.0407	0	-21	-0.714	0.2205	0.1191	5	0.875	0.0108	-0.1076	26	1.539	0.5387	-0.1647
-175	0.223	0.0507	0.0937	-20	-0.693	0.2011	0.1139	5.5	0.941	0.0109	-0.1094	28	1.527	0.6187	-0.177
-170	0.405	0.1055	0.1702	-19	-0.671	0.1822	0.1086	6	1.007	0.011	-0.1109	30	1.522	0.6978	-0.1886
-160	0.658	0.2982	0.2819	-18	-0.648	0.164	0.1032	6.5	1.071	0.0113	-0.1118	32	1.529	0.7747	-0.1994
-155	0.733	0.4121	0.3213	-17	-0.624	0.1465	0.0975	7	1.134	0.0115	-0.1127	35	1.544	0.8869	-0.2148
-150	0.778	0.5308	0.352	-16	-0.601	0.13	0.0898	7.5	1.198	0.0117	-0.1138	40	1.529	1.0671	-0.2392
-145	0.795	0.6503	0.3754	-15	-0.579	0.1145	0.0799	8	1.26	0.012	-0.1144	45	1.471	1.2319	-0.2622
-140	0.787	0.7672	0.3926	-14	-0.559	0.1	0.0682	8.5	1.318	0.0126	-0.1137	50	1.376	1.3747	-0.2839
-135	0.757	0.8785	0.4046	-13	-0.539	0.0867	0.0547	9	1.368	0.0133	-0.1112	55	1.249	1.4899	-0.3043
-130	0.708	0.9819	0.4121	-12	-0.519	0.0744	0.0397	9.5	1.422	0.0143	-0.11	60	1.097	1.5728	-0.3236
-125	0.641	1.0756	0.416	-11	-0.499	0.0633	0.0234	10	1.475	0.0156	-0.1086	65	0.928	1.6202	-0.3417
-120	0.56	1.158	0.4167	-10	-0.48	0.0534	0.006	10.5	1.523	0.0174	-0.1064	70	0.75	1.6302	-0.3586
-115	0.467	1.228	0.4146	-5.54	-0.385	0.0245	-0.08	11	1.57	0.0194	-0.1044	75	0.57	1.6031	-0.3745
-110	0.365	1.2847	0.4104	-5.04	-0.359	0.0225	-0.08	11.5	1.609	0.0227	-0.1013	80	0.396	1.5423	-0.3892
-105	0.255	1.3274	0.4041	-4.54	-0.36	0.0196	-0.08	12	1.642	0.0269	-0.098	85	0.237	1.4598	-0.4028
-100	0.139	1.3557	0.3961	-4.04	-0.355	0.0174	-0.08	12.5	1.675	0.0319	-0.0953	90	0.101	1.4041	-0.4151
-95	0.021	1.3692	0.3867	-3.54	-0.307	0.0162	-0.08	13	1.7	0.0398	-0.0925	95	-0.022	1.4053	-0.4261
-90	-0.098	1.368	0.3759	-3.04	-0.246	0.0144	-0.08	13.5	1.717	0.0488	-0.0896	100	-0.143	1.3914	-0.4357
-85	-0.216	1.3521	0.3639	-3	-0.24	0.024	-0.0623	14	1.712	0.0614	-0.0864	105	-0.261	1.3625	-0.4437
-80	-0.331	1.3218	0.3508	-2.5	-0.163	0.0188	-0.0674	14.5	1.703	0.0786	-0.084	110	-0.374	1.3188	-0.4498
-75	-0.441	1.2773	0.3367	-2	-0.091	0.016	-0.0712	15.5	1.671	0.1173	-0.083	115	-0.48	1.2608	-0.4538
-70	-0.544	1.2193	0.3216	-1.5	-0.019	0.0137	-0.0746	16	1.649	0.1377	-0.0848	120	-0.575	1.1891	-0.4553
-65	-0.638	1.1486	0.3054	-1	0.052	0.0118	-0.0778	16.5	1.621	0.16	-0.088	125	-0.659	1.1046	-0.454
-60	-0.72	1.066	0.2884	-0.5	0.121	0.0104	-0.0806	17	1.598	0.1814	-0.0926	130	-0.727	1.0086	-0.4492
-55	-0.788	0.9728	0.2703	0	0.196	0.0094	-0.0831	17.5	1.571	0.2042	-0.0984	135	-0.778	0.9025	-0.4405
-50	-0.84	0.8705	0.2512	0.5	0.265	0.0096	-0.0863	18	1.549	0.2316	-0.1052	140	-0.809	0.7883	-0.427
-45	-0.875	0.7611	0.2311	1	0.335	0.0098	-0.0895	19	1.544	0.2719	-0.1158	145	-0.818	0.6684	-0.4078
-40	-0.889	0.6466	0.2099	1.5	0.404	0.0099	-0.0924	19.5	1.549	0.2906	-0.1213	150	-0.8	0.5457	-0.3821
-35	-0.88	0.5299	0.1876	2	0.472	0.01	-0.0949	20	1.565	0.3085	-0.1248	155	-0.754	0.4236	-0.3484
-30	-0.846	0.4141	0.1641	2.5	0.54	0.0102	-0.0973	21	1.565	0.3447	-0.1317	160	-0.677	0.3066	-0.3054
-25	-0.784	0.303	0.1396	3	0.608	0.0103	-0.0996	22	1.563	0.382	-0.1385	170	-0.417	0.1085	-0.1842
-24	-0.768	0.2817	0.1345	3.5	0.674	0.0104	-0.1016	23	1.558	0.4203	-0.1452	175	-0.229	0.051	-0.1013
-23	-0.751	0.2608	0.1294	4	0.742	0.0105	-0.1037	24	1.552	0.4593	-0.1518	180	0	0.0407	0
-22	-0.733	0.2404	0.1243	4.5	0.809	0.0107	-0.1057	25	1.546	0.4988	-0.1583				

A.6. Aerofoil Data: DU30_A17

Angle of Attack	Lift	Drag	Moment
-180	0	0.0267	0
-175	0.274	0.037	0.1379
-170	0.547	0.0968	0.2778
-160	0.685	0.2876	0.274
-155	0.766	0.4025	0.3118
-150	0.816	0.5232	0.3411
-145	0.836	0.6454	0.3631
-140	0.832	0.7656	0.3791
-135	0.804	0.8807	0.3899
-130	0.756	0.9882	0.3965
-125	0.69	1.0861	0.3994
-120	0.609	1.173	0.3992
-115	0.515	1.2474	0.3964
-110	0.411	1.3084	0.3915
-105	0.3	1.3552	0.3846
-100	0.182	1.3875	0.3761
-95	0.061	1.4048	0.3663
-90	-0.061	1.407	0.3551
-85	-0.183	1.3941	0.3428
-80	-0.302	1.3664	0.3295
-75	-0.416	1.324	0.3153
-70	-0.523	1.2676	0.3001
-65	-0.622	1.1978	0.2841
-60	-0.708	1.1156	0.2672
-55	-0.781	1.022	0.2494
-50	-0.838	0.9187	0.2308
-45	-0.877	0.8074	0.2113
-40	-0.895	0.6904	0.1909
-35	-0.889	0.5703	0.1696
-30	-0.858	0.4503	0.1475
-25	-0.832	0.3357	0.1224
-24	-0.852	0.3147	0.1156
-23	-0.882	0.2946	0.1081
-22	-0.919	0.2752	0.1
-21	-0.963	0.2566	0.0914
-20	-1.013	0.2388	0.0823
-19	-1.067	0.2218	0.0728
-18	-1.125	0.2056	0.0631
-17	-1.185	0.1901	0.0531
-16	-1.245	0.1754	0.043
-15.25	-1.29	0.1649	0.0353
-14.24	-1.229	0.1461	0.024
-13.24	-1.148	0.1263	0.01
-12.22	-1.052	0.1051	-0.009
-11.22	-0.965	0.0886	-0.023
-10.19	-0.867	0.074	-0.0336
-9.7	-0.822	0.0684	-0.0375
-9.18	-0.769	0.0605	-0.044
-8.18	-0.756	0.027	-0.0578
-7.19	-0.69	0.018	-0.059
-6.65	-0.616	0.0166	-0.0633
-6.13	-0.542	0.0152	-0.0674
-6	-0.525	0.0117	-0.0732
-5.5	-0.451	0.0105	-0.0766
-5	-0.382	0.0097	-0.0797
-4.5	-0.314	0.0092	-0.0825
-4	-0.251	0.0091	-0.0853
-3.5	-0.189	0.0089	-0.0884
-3	-0.12	0.0089	-0.0914
-2.5	-0.051	0.0088	-0.0942
-2	0.017	0.0088	-0.0969
-1.5	0.085	0.0088	-0.0994
-1	0.152	0.0088	-0.1018
-0.5	0.219	0.0088	-0.1041
0	0.288	0.0087	-0.1062
0.5	0.354	0.0087	-0.1086
1	0.421	0.0088	-0.1107
1.5	0.487	0.0089	-0.1129
2	0.554	0.009	-0.1149
2.5	0.619	0.0091	-0.1168
3	0.685	0.0092	-0.1185
3.5	0.749	0.0093	-0.1201
4	0.815	0.0095	-0.1218
4.5	0.879	0.0096	-0.1233
5	0.944	0.0097	-0.1248
5.5	1.008	0.0099	-0.126
6	1.072	0.0101	-0.127
6.5	1.135	0.0103	-0.128
7	1.197	0.0107	-0.1287
7.5	1.256	0.0112	-0.1289
8	1.305	0.0125	-0.127
9	1.39	0.0155	-0.1207
9.5	1.424	0.0171	-0.1158
10	1.458	0.0192	-0.1116
10.5	1.488	0.0219	-0.1073
11	1.512	0.0255	-0.1029
11.5	1.533	0.0307	-0.0983
12	1.549	0.037	-0.0949
12.5	1.558	0.0452	-0.0921
13	1.47	0.063	-0.0899
13.5	1.398	0.0784	-0.0885
14	1.354	0.0931	-0.0885
14.5	1.336	0.1081	-0.0902
15	1.333	0.1239	-0.0928
15.5	1.326	0.1415	-0.0963
16	1.329	0.1592	-0.1006
16.5	1.326	0.1743	-0.1042
17	1.321	0.1903	-0.1084
17.5	1.331	0.2044	-0.1125
18	1.333	0.2186	-0.1169
18.5	1.34	0.2324	-0.1215
19	1.362	0.2455	-0.1263
19.5	1.382	0.2584	-0.1313
20	1.398	0.2689	-0.1352
20.5	1.426	0.2814	-0.1406
21	1.437	0.2943	-0.1462
22	1.418	0.3246	-0.1516
23	1.397	0.3557	-0.157
24	1.376	0.3875	-0.1623
25	1.354	0.4198	-0.1676
26	1.332	0.4524	-0.1728
28	1.293	0.5183	-0.1832
30	1.265	0.5843	-0.1935
32	1.253	0.6492	-0.2039
35	1.264	0.7438	-0.2193
40	1.258	0.897	-0.244
45	1.217	1.0402	-0.2672
50	1.146	1.1686	-0.2891
55	1.049	1.2779	-0.3097
60	0.932	1.3647	-0.329
65	0.799	1.4267	-0.3471
70	0.657	1.4621	-0.3641
75	0.509	1.4708	-0.3799
80	0.362	1.4544	-0.3946
85	0.221	1.4196	-0.4081
90	0.092	1.3938	-0.4204
95	-0.03	1.3943	-0.4313
100	-0.15	1.3798	-0.4408
105	-0.267	1.3504	-0.4486
110	-0.379	1.3063	-0.4546
115	-0.483	1.2481	-0.4584
120	-0.578	1.1763	-0.4597
125	-0.66	1.0919	-0.4582
130	-0.727	0.9962	-0.4532
135	-0.777	0.8906	-0.4441
140	-0.807	0.7771	-0.4303
145	-0.815	0.6581	-0.4109
150	-0.797	0.5364	-0.3848
155	-0.75	0.4157	-0.3508
160	-0.673	0.3	-0.3074
170	-0.547	0.1051	-0.2786
175	-0.274	0.0388	-0.138
180	0	0.0267	0

A.7. Aerofoil Data: DU25_A17

Angle of Attack [deg]	Lift	Drag	Moment	Angle of Attack [deg]	Lift	Drag	Moment	Angle of Attack [deg]	Lift	Drag	Moment	Angle of Attack [deg]	Lift	Drag	Moment
-180	0	0.0202	0	-20	-0.815	0.2237	0.0739	4.5	1.013	0.0076	-0.1456	24	1.251	0.3386	-0.1515
-175	0.368	0.0324	0.1845	-19	-0.833	0.199	0.0618	5	1.062	0.0079	-0.1445	25	1.215	0.3678	-0.1584
-170	0.735	0.0943	0.3701	-18	-0.854	0.1743	0.0488	6	1.161	0.0099	-0.1419	26	1.181	0.3972	-0.1651
-160	0.695	0.2848	0.2679	-17	-0.879	0.1498	0.0351	6.5	1.208	0.0117	-0.1403	28	1.12	0.4563	-0.1781
-155	0.777	0.4001	0.3046	-16	-0.905	0.1256	0.0208	7	1.254	0.0132	-0.1382	30	1.076	0.5149	-0.1904
-150	0.828	0.5215	0.3329	-15	-0.932	0.102	0.006	7.5	1.301	0.0143	-0.1362	32	1.056	0.572	-0.2017
-145	0.85	0.6447	0.354	-14	-0.959	0.0789	-0.0091	8	1.336	0.0153	-0.132	35	1.066	0.6548	-0.2173
-140	0.846	0.766	0.3693	-13	-0.985	0.0567	-0.0243	8.5	1.369	0.0165	-0.1276	40	1.064	0.7901	-0.2418
-135	0.818	0.8823	0.3794	-12.01	-0.953	0.0271	-0.0349	9	1.4	0.0181	-0.1234	45	1.035	0.919	-0.265
-130	0.771	0.9911	0.3854	-11	-0.9	0.0303	-0.0361	9.5	1.428	0.0211	-0.1193	50	0.98	1.0378	-0.2867
-125	0.705	1.0905	0.3878	-9.98	-0.827	0.0287	-0.0464	10	1.442	0.0262	-0.1152	55	0.904	1.1434	-0.3072
-120	0.624	1.1787	0.3872	-8.98	-0.753	0.0271	-0.0534	10.5	1.427	0.0336	-0.1115	60	0.81	1.2333	-0.3265
-115	0.53	1.2545	0.3841	-8.47	-0.691	0.0264	-0.065	11	1.374	0.042	-0.1081	65	0.702	1.3055	-0.3446
-110	0.426	1.3168	0.3788	-7.45	-0.555	0.0114	-0.0782	11.5	1.316	0.0515	-0.1052	70	0.582	1.3587	-0.3616
-105	0.314	1.365	0.3716	-6.42	-0.413	0.0094	-0.0904	12	1.277	0.0601	-0.1026	75	0.456	1.3922	-0.3775
-100	0.195	1.3984	0.3629	-5.4	-0.271	0.0086	-0.1006	12.5	1.25	0.0693	-0.1	80	0.326	1.4063	-0.3921
-95	0.073	1.4169	0.3529	-5	-0.22	0.0073	-0.1107	13	1.246	0.0785	-0.098	85	0.197	1.4042	-0.4057
-90	-0.05	1.4201	0.3416	-4.5	-0.152	0.0071	-0.1135	13.5	1.247	0.0888	-0.0969	90	0.072	1.3985	-0.418
-85	-0.173	1.4081	0.3292	-4	-0.084	0.007	-0.1162	14	1.256	0.1	-0.0968	95	-0.05	1.3973	-0.4289
-80	-0.294	1.3811	0.3159	-3.5	-0.018	0.0069	-0.1186	14.5	1.26	0.1108	-0.0973	100	-0.17	1.381	-0.4385
-75	-0.409	1.3394	0.3017	-3	0.049	0.0068	-0.1209	15	1.271	0.1219	-0.0981	105	-0.287	1.3498	-0.4464
-70	-0.518	1.2833	0.2866	-2.5	0.115	0.0068	-0.1231	15.5	1.281	0.1325	-0.0992	110	-0.399	1.3041	-0.4524
-65	-0.617	1.2138	0.2707	-2	0.181	0.0068	-0.1252	16	1.289	0.1433	-0.1006	115	-0.502	1.2442	-0.4563
-60	-0.706	1.1315	0.2539	-1.5	0.247	0.0067	-0.1272	16.5	1.294	0.1541	-0.1023	120	-0.596	1.1709	-0.4577
-55	-0.78	1.0378	0.2364	-1	0.312	0.0067	-0.1293	17	1.304	0.1649	-0.1042	125	-0.677	1.0852	-0.4563
-50	-0.839	0.9341	0.2181	-0.5	0.377	0.0067	-0.1311	17.5	1.309	0.1754	-0.1064	130	-0.743	0.9883	-0.4514
-45	-0.879	0.8221	0.1991	0	0.444	0.0065	-0.133	18	1.315	0.1845	-0.1082	135	-0.792	0.8818	-0.4425
-40	-0.898	0.7042	0.1792	0.5	0.508	0.0065	-0.1347	18.5	1.32	0.1953	-0.111	140	-0.821	0.7676	-0.4288
-35	-0.893	0.5829	0.1587	1	0.573	0.0066	-0.1364	19	1.33	0.2061	-0.1143	145	-0.826	0.6481	-0.4095
-30	-0.862	0.4616	0.1374	1.5	0.636	0.0067	-0.138	19.5	1.343	0.217	-0.1179	150	-0.806	0.5264	-0.3836
-25	-0.803	0.3441	0.1154	2	0.701	0.0068	-0.1396	20	1.354	0.228	-0.1219	155	-0.758	0.406	-0.3497
-24	-0.792	0.3209	0.1101	2.5	0.765	0.0069	-0.1411	20.5	1.359	0.239	-0.1261	160	-0.679	0.2912	-0.3065
-23	-0.789	0.2972	0.1031	3	0.827	0.007	-0.1424	21	1.36	0.2536	-0.1303	170	-0.735	0.0995	-0.3706
-22	-0.792	0.273	0.0947	3.5	0.89	0.0071	-0.1437	22	1.325	0.2814	-0.1375	175	-0.368	0.0356	-0.1846
-21	-0.801	0.2485	0.0849	4	0.952	0.0073	-0.1448	23	1.288	0.3098	-0.1446	180	0	0.0202	0

A.8. Aerofoil Data: DU21_A17

Angle of Attack [deg]	Lift	Drag	Moment	Angle of Attack [deg]	Lift	Drag	Moment	Angle of Attack [deg]	Lift	Drag	Moment	Angle of Attack [deg]	Lift	Drag	Moment
-180	0	0.0185	0	-19	-0.899	0.172	0.0464	4.5	1.046	0.0079	-0.139	23	1.229	0.2786	-0.1239
-175	0.394	0.0332	0.1978	-18	-0.931	0.1457	0.0286	5	1.095	0.009	-0.1378	24	1.182	0.3077	-0.1305
-160	0.67	0.2809	0.2738	-17	-0.964	0.1197	0.0102	5.5	1.145	0.0103	-0.1369	25	1.136	0.3371	-0.137
-155	0.749	0.3932	0.3118	-16	-0.999	0.094	-0.0088	6	1.192	0.0113	-0.1353	26	1.093	0.3664	-0.1433
-150	0.797	0.5112	0.3413	-15	-1.033	0.0689	-0.0281	6.5	1.239	0.0122	-0.1338	28	1.017	0.4246	-0.1556
-145	0.818	0.6309	0.3636	-14.5	-1.05	0.0567	-0.0378	7	1.283	0.0131	-0.1317	30	0.962	0.4813	-0.1671
-140	0.813	0.7485	0.3799	-12.01	-0.953	0.0271	-0.0349	7.5	1.324	0.0139	-0.1291	32	0.937	0.5356	-0.1778
-135	0.786	0.8612	0.3911	-11	-0.9	0.0303	-0.0361	8	1.358	0.0147	-0.1249	35	0.947	0.6127	-0.1923
-130	0.739	0.9665	0.398	-9.98	-0.827	0.0287	-0.0464	8.5	1.385	0.0158	-0.1213	40	0.95	0.7396	-0.2154
-125	0.675	1.0625	0.4012	-8.12	-0.536	0.0124	-0.0821	9	1.403	0.0181	-0.1177	45	0.928	0.8623	-0.2374
-120	0.596	1.1476	0.4014	-7.62	-0.467	0.0109	-0.0924	9.5	1.401	0.0211	-0.1142	50	0.884	0.9781	-0.2583
-115	0.505	1.2206	0.399	-7.11	-0.393	0.0092	-0.1015	10	1.358	0.0255	-0.1103	55	0.821	1.0846	-0.2782
-110	0.403	1.2805	0.3943	-6.6	-0.323	0.0083	-0.1073	10.5	1.313	0.0301	-0.1066	60	0.74	1.1796	-0.2971
-105	0.294	1.3265	0.3878	-6.5	-0.311	0.0089	-0.1083	11	1.287	0.0347	-0.1032	65	0.646	1.2617	-0.3149
-100	0.179	1.3582	0.3796	-6	-0.245	0.0082	-0.1112	11.5	1.274	0.0401	-0.1002	70	0.54	1.3297	-0.3318
-95	0.06	1.3752	0.37	-5.5	-0.178	0.0074	-0.1146	12	1.272	0.0468	-0.0971	75	0.425	1.3827	-0.3476
-90	-0.06	1.3774	0.3591	-5	-0.113	0.0069	-0.1172	12.5	1.273	0.0545	-0.094	80	0.304	1.4202	-0.3625
-85	-0.179	1.3648	0.3471	-4.5	-0.048	0.0065	-0.1194	13	1.273	0.0633	-0.0909	85	0.179	1.4423	-0.3763
-80	-0.295	1.3376	0.334	-4	0.016	0.0063	-0.1213	13.5	1.273	0.0722	-0.0883	90	0.053	1.4512	-0.389
-75	-0.407	1.2962	0.3199	-3.5	0.08	0.0061	-0.1232	14	1.272	0.0806	-0.0865	95	-0.073	1.448	-0.4004
-70	-0.512	1.2409	0.3049	-3	0.145	0.0058	-0.1252	14.5	1.273	0.09	-0.0854	100	-0.198	1.4294	-0.4105
-65	-0.608	1.1725	0.289	-2.5	0.208	0.0057	-0.1268	15	1.275	0.0987	-0.0849	105	-0.319	1.3954	-0.4191
-60	-0.693	1.0919	0.2722	-2	0.27	0.0057	-0.1282	15.5	1.281	0.1075	-0.0847	110	-0.434	1.3464	-0.426
-55	-0.764	1.0002	0.2545	-1.5	0.333	0.0057	-0.1297	16	1.284	0.117	-0.085	115	-0.541	1.2829	-0.4308
-50	-0.82	0.899	0.2359	-1	0.396	0.0057	-0.131	16.5	1.296	0.127	-0.0858	120	-0.637	1.2057	-0.4333
-45	-0.857	0.79	0.2163	-0.5	0.458	0.0057	-0.1324	17	1.306	0.1368	-0.0869	125	-0.72	1.1157	-0.433
-40	-0.875	0.6754	0.1958	0	0.521	0.0057	-0.1337	17.5	1.308	0.1464	-0.0883	130	-0.787	1.0144	-0.4294
-35	-0.869	0.5579	0.1744	0.5	0.583	0.0057	-0.135	18	1.308	0.1562	-0.0901	135	-0.836	0.9033	-0.4219
-30	-0.838	0.4405	0.152	1	0.645	0.0058	-0.1363	18.5	1.308	0.1664	-0.0922	140	-0.864	0.7845	-0.4098
-25	-0.791	0.3256	0.1262	1.5	0.706	0.0058	-0.1374	19	1.308	0.177	-0.0949	145	-0.869	0.6605	-0.3922
-24	-0.794	0.3013	0.117	2	0.768	0.0059	-0.1385	19.5	1.307	0.1878	-0.098	150	-0.847	0.5346	-0.3682
-23	-0.805	0.2762	0.1059	2.5	0.828	0.0061	-0.1395	20	1.311	0.1987	-0.1017	155	-0.795	0.4103	-0.3364
-22	-0.821	0.2506	0.0931	3	0.888	0.0063	-0.1403	20.5	1.325	0.21	-0.1059	160	-0.711	0.2922	-0.2954
-21	-0.843	0.2246	0.0788	3.5	0.948	0.0066	-0.1406	21	1.324	0.2214	-0.1105	175	-0.394	0.0334	-0.1978
-20	-0.869	0.1983	0.0631	4	0.996	0.0071	-0.1398	22	1.277	0.2499	-0.1172	180	0	0.0185	0

A.9. Aerofoil Data: NACA64

Angle of Attack [deg]	Lift	Drag	Moment	Angle of Attack [deg]	Lift	Drag	Moment	Angle of Attack [deg]	Lift	Drag	Moment	Angle of Attack [deg]	Lift	Drag	Moment
-180	0	0.0198	0	-23	-0.89	0.2556	0.0916	8	1.257	0.0124	-0.1163	30	0.926	0.4294	-0.1668
-175	0.374	0.0341	0.188	-22	-0.911	0.2297	0.0785	8.5	1.293	0.013	-0.1163	32	0.855	0.469	-0.1759
-170	0.749	0.0955	0.377	-21	-0.934	0.204	0.0649	9	1.326	0.0136	-0.116	35	0.8	0.5324	-0.1897
-160	0.659	0.2807	0.2747	-20	-0.958	0.1785	0.0508	9.5	1.356	0.0143	-0.1154	40	0.804	0.6452	-0.2126
-155	0.736	0.3919	0.313	-19	-0.982	0.1534	0.0364	10	1.382	0.015	-0.1149	45	0.793	0.7573	-0.2344
-150	0.783	0.5086	0.3428	-18	-1.005	0.1288	0.0218	10.5	1.4	0.0267	-0.1145	50	0.763	0.8664	-0.2553
-145	0.803	0.6267	0.3654	-17	-1.082	0.1037	0.0129	11	1.415	0.0383	-0.1143	55	0.717	0.9708	-0.2751
-140	0.798	0.7427	0.382	-16	-1.113	0.0786	-0.0028	11.5	1.425	0.0498	-0.1147	60	0.656	1.0693	-0.2939
-135	0.771	0.8537	0.3935	-15	-1.105	0.0535	-0.0251	12	1.434	0.0613	-0.1158	65	0.582	1.1606	-0.3117
-130	0.724	0.9574	0.4007	-14	-1.078	0.0283	-0.0419	12.5	1.443	0.0727	-0.1165	70	0.495	1.2438	-0.3285
-125	0.66	1.0519	0.4042	-13.5	-1.053	0.0158	-0.0521	13	1.451	0.0841	-0.1153	75	0.398	1.3178	-0.3444
-120	0.581	1.1355	0.4047	-13	-1.015	0.0151	-0.061	13.5	1.453	0.0954	-0.1131	80	0.291	1.3809	-0.3593
-115	0.491	1.207	0.4025	-12	-0.904	0.0134	-0.0707	14	1.448	0.1065	-0.1112	85	0.176	1.4304	-0.3731
-110	0.39	1.2656	0.3981	-11	-0.807	0.0121	-0.0722	14.5	1.444	0.1176	-0.1101	90	0.053	1.4565	-0.3858
-105	0.282	1.3104	0.3918	-10	-0.711	0.0111	-0.0734	15	1.445	0.1287	-0.1103	95	-0.074	1.4533	-0.3973
-100	0.169	1.341	0.3838	-9	-0.595	0.0099	-0.0772	15.5	1.447	0.1398	-0.1109	100	-0.199	1.4345	-0.4075
-95	0.052	1.3572	0.3743	-8	-0.478	0.0091	-0.0807	16	1.448	0.1509	-0.1114	105	-0.321	1.4004	-0.4162
-90	-0.067	1.3587	0.3636	-7	-0.375	0.0086	-0.0825	16.5	1.444	0.1619	-0.1111	110	-0.436	1.3512	-0.4231
-85	-0.184	1.3456	0.3517	-6	-0.264	0.0082	-0.0832	17	1.438	0.1728	-0.1097	115	-0.543	1.2874	-0.428
-80	-0.299	1.3181	0.3388	-5	-0.151	0.0079	-0.0841	17.5	1.439	0.1837	-0.1079	120	-0.64	1.2099	-0.4306
-75	-0.409	1.2765	0.3248	-4	-0.017	0.0072	-0.0869	18	1.448	0.1947	-0.108	125	-0.723	1.1196	-0.4304
-70	-0.512	1.2212	0.3099	-3	0.088	0.0064	-0.0912	18.5	1.452	0.2057	-0.109	130	-0.79	1.0179	-0.427
-65	-0.606	1.1532	0.294	-2	0.213	0.0054	-0.0946	19	1.448	0.2165	-0.1086	135	-0.84	0.9064	-0.4196
-60	-0.689	1.0731	0.2772	-1	0.328	0.0052	-0.0971	19.5	1.438	0.2272	-0.1077	140	-0.868	0.7871	-0.4077
-55	-0.759	0.9822	0.2595	0	0.442	0.0052	-0.1014	20	1.428	0.2379	-0.1099	145	-0.872	0.6627	-0.3903
-50	-0.814	0.882	0.2409	1	0.556	0.0052	-0.1076	21	1.401	0.259	-0.1169	150	-0.85	0.5363	-0.3665
-45	-0.85	0.7742	0.2212	2	0.67	0.0053	-0.1126	22	1.359	0.2799	-0.119	155	-0.798	0.4116	-0.3349
-40	-0.866	0.661	0.2006	3	0.784	0.0053	-0.1157	23	1.3	0.3004	-0.1235	160	-0.714	0.2931	-0.2942
-35	-0.86	0.5451	0.1789	4	0.898	0.0054	-0.1199	24	1.22	0.3204	-0.1393	170	-0.749	0.0971	-0.3771
-30	-0.829	0.4295	0.1563	5	1.011	0.0058	-0.124	25	1.168	0.3377	-0.144	175	-0.374	0.0334	-0.1879
-25	-0.853	0.3071	0.1156	6	1.103	0.0091	-0.1234	26	1.116	0.3554	-0.1486	180	0	0.0198	0